DESIGN AND IMPLEMENTATION OF BAND REJECTED ANTENNAS USING ADAPTIVE SURFACE MESHING AND GENETIC ALGORITHMS METHODS

MOHAMMED SAEED BINMELHA

PhD

2013

DESIGN AND IMPLEMENTATION OF BAND REJECTED ANTENNAS USING ADAPTIVE SURFACE MESHING AND GENETIC ALGORITHMS METHODS

Simulation and Measurement of Microstrip Antennas with the Ability of Harmonic Rejection for wireless and Mobile Applications Including the Antenna Design Optimisation Using Genetic Algorithms

MOHAMMED SAEED BINMELHA

B.Sc., MSc

Submitted for the Degree of

Doctor of Philosophy

School of Engineering, Design and Technology
University of Bradford

2013

Abstract

DESIGN AND IMPLEMENTATION OF BAND REJECTED ANTENNAS USING ADAPTIVE SURFACE MESHING AND GENETIC ALGORITHMS METHODS

Simulation and Measurement of Microstrip Antennas with the Ability of Harmonic Rejection for wireless and Mobile Applications Including the Antenna Design Optimisation Using Genetic Algorithms

Keywords

Antennas, Harmonic Suppression, Band Rejected Antennas, Adaptive Surface Meshing, Radiation Patterns, Harmonic Radiations, Genetic Algorithm (GA), Microstrip Patch Antenna, Shorting Wall.

With the advances in wireless communication systems, antennas with different shapes and design have achieved great demand and are desirable for many uses such as personal communication systems, and other applications involving wireless communication. This has resulted in different shapes and types of antenna design in order to achieve different antenna characteristic. One attractive approach to the design of antennas is to suppress or attenuate harmonic contents due to the non-linear operation of the Radio Frequency (RF) front end.

The objectives of this work were to investigate, design and implement antennas for harmonic suppression with the aid of a genetic algorithm (GA). Several microstrip patch antennas were designed to operate at frequencies 1.0, 1.8 and 2.4 GHz respectively. The microstrip patch antenna with stub tuned microstrip lines was also employed at 1.0 and 1.8 GHz to meet the design objectives.

A new sensing patch technique is introduced and applied in order to find the accepted power at harmonic frequencies. The evaluation of the measured power accepted at the antenna feed port was done using an electromagnetic (EM) simulator, Ansoft Designer, in terms of current distribution. A two sensors method is presented on one antenna prototype to estimate the accepted power at three frequencies.

The computational method is based on an integral equation solver using adaptive surface meshing driven by a genetic algorithm. Several examples are demonstrated, including design of coaxially-fed, air-dielectric patch antennas implanted with shorting and folded walls. The characteristics of the antennas in terms of the impedance responses and far field radiation patterns are discussed. The results in terms of the radiation performance are addressed, and compared to measurements. The presented results of these antennas show a good impedance matching at the fundamental frequency with good suppression achieved at the second and third harmonic frequencies.

Acknowledgements

In the name of Allah, the most merciful and beneficent. I am grateful to my Lord who has given me the health, strength and wisdom to complete this work.

I would like to thank the following, who accompanied me during the time when I was working for this degree.

I wish to express my deepest gratitude to my supervisors**, *Prof. Raed A. Abd-Alhameed*** and ***Dr NJ McEwan*.** I am most grateful to them for advice, assistance, support and their continuous encouragement during the difficult starting times, sharing with me the exciting times and for being consistently supportive throughout this work. I will never forget the many opportunities that they gave me in facilities, publications, teaching and travel during the years of my PhD study.

My thanks are also extended to ***Dr O.J. Downing***, ***Dr D Zhou*** and ***Dr CH See*** for their great support and all the other people in the research laboratories, especially Mr MM Abusitta, I.E.T. Elfergani and Mr Imran whose co-operation in connection with the practical aspect of this work cannot be underestimated.

I am grateful to my Government for supporting me all these years and for providing me with financial and moral support for the completion of this degree.

Table of Contents

Acronyms

3D	Three Dimension
LAN	Local Area Network
RF	Radio Frequency
TSAs	Tapered Slot Antennas
GA	Genetic Algorithm
HAS	Harmonic Suppression Antenna
WLAN	Wireless Local Area Network
EMI	Electromagnetic Interference
PBG	Photonic Band Gap
HAS	H-Shaped patch Antenna
MIMO	Multiple Input Multiple Output
Balun	Balanced un balanced
AUT	Antenna Under Test
HFSS	High Frequency Structure Simulator

List of Figures

List of Tables

CHAPTER ONE

1 Introduction

1.1 Background and Motivations

With the advances in wireless communication systems, multiband antennas with different shapes and designs are of great demand and are desirable for many uses such as personal communication systems, small satellite communication terminals and other applications involving wireless communications. This has resulted in different shapes and types of antenna designs to achieve different variations in antenna characteristics [1-2].

One attractive approach of designing antennas is based on fractal geometries that feature two expected common properties which are self-similarity and space filling . However, the lack of closed-form formulae for their design lead the designer in using optimising methods and algorithms. Therefore, numerical techniques remain another option for analysis and synthesis of such antennas. Evolutionary techniques like genetic algorithm (GA) provide a method to overcome this limitation by searching the design space and obtain the effective design parameters to achieve desired performance [2-3].

Genetic Algorithm (GA) is an adaptive search algorithm based on the concepts of natural selection and genetics [1-3]. The GA is used to model processes in natural systems that are required for evolution.

The concept of GA was first established by John Holland in the 1960s. The GA has provided an alternative method to solve complex problems, which has been widely applied in many practical applications [2]. The GA is able to solve real world problems by finding optimal parameters that are difficult to achieve using traditional methods.

GA is now being widely used as an optimisation and efficient tool for search and machine learning. However, prior to the broader application of GA, it was used in pattern identifications [4-5].

In recent years, it has proved to be versatile tool in optimisation, design and control applications. The key principle of GA is that, it applies pressure on a given group with multiple outcomes and managing the result in order to evolve a generic optimum point. It is realised by 'fitness weight selection' process and critical search of the space attained by crossover and mutation of the characteristics available in the sample under observation. Where it is used as an effective optimising mechanism , [2-6].

GA is used as an optimisation medium due to its effectiveness in rigorously searching the entire sample under consideration. There are however other optimisation tools that can be classified as, global techniques with similar characteristic as GA; random walk,

simulated annealing and monte carlo localised techniques – conjugate gradient, quasi newton and simplex methods [6-10].

The above techniques are distinguishable by the process in which they detail their outcome; the results are subject to the initial start condition. By contrast, global techniques are not dependent on conditions at the beginning and puts and weighs some variables on them. GA is effective given the following circumstances:

- The problem has multiple parameters.
- There is likely to be several optimum solutions.
- Non distinguishable objective.

Comparing the two options critically the local techniques give faster convergence than the global techniques. By contrast, in electromagnetic design issues, the convergence rate is relatively less crucial in comparison to optimal results. Amongst the global techniques, GA is considered to be more appropriate to electromagnetic design issues; since it is reliable, robust and readily implemented [3].

In order to put GA in context and fully appreciate its effectiveness, it is essential that all the terms are fully defined. The concept originated from the theory of evolution:

- Generation: particular population or creation that are successfully conceived.
- Parent: members are selected in a stochastic manner from a given population.
- Children: usually derived from parents to form a new generation.

- Fitness: A value that determines the effectiveness of the individual variable.
- Genes: coded variables for optimisation.
- Chromosomes: group of genes in a string format.
- Objective function: numerical value in equation format.
- Search space: area with all likely outcomes.

The GA process can roughly be divided into three parts: initialization, evaluation, and reproduction. The algorithm starts with an initial population of possible solutions. The solutions are encoded as binary or real-valued chromosomes. In the evaluation phase, the performance of each solution in the population is predicted using a simulation tool [2-5].

Then the cost (or fitness) of each solution is evaluated using the proper cost function defined in terms of the design goals. According to the cost, the chromosomes are refined into the next generation through a reproduction process that includes crossover, mutation and geometrical filtering. This series of processes are repeated until the cost is minimized meaning an optimum solution has been found [11].

A harmonic of a wave can be described as an integer multiple of the fundamental frequency signal. The harmonics tend to be periodic at the fundamental frequency and are equally spaced by the size of the fundamental frequency [12-21].

Filters are regarded as essential components in electronic systems to avoid harmonic interference. In practice, the harmonics are suppressed by putting in place low pass or band stop filters. A deeper rejection and compact size can be achieved using a band stop filter that combines shunt open stubs and a spur line [22-23].

Another way of achieving harmonic suppression is to use modified band pass filters. There are three types of band pass filters. The first type of filter is a dual-mode patch, band pass filter. The second type of filter is an open-loop band pass filter. In this case, two open stubs can be added to obtain high suppression in the second harmonic. The third type of filter uses half-wavelength open stubs. In this case, a T-shaped line is used that operates as a band stop filter at the second harmonic [16-19].

The tapered slot antennas (TSAs) are basically printed circuit antennas. These are often found in applications, such as satellite and wireless communications due to their low weight and ease of fabrication. The tapered slot antennas can generate a symmetric beam in the E- and H-planes by selecting the right length, shape and dielectric thickness [16-19].

This research will aim to design a harmonic rejection antenna in order to reduce the harmonic radiations which can interference within the electromagnetic circuitry. The design approach will be to apply GA together with binary-based random search engine and to use method of moments with adaptive service meshing.. Specific design samples will be required for evaluation. The end design will be able to serve as a bandpass filter as well.

1.2 Objectives of the Research

The main goal of this research is to model and design the antenna for harmonic suppression in order to reduce the overall noise levels and interferences by using the theory of harmonic rejection in addition with genetic algorithm to optimise the design parameters. For this pupose a microstrip patch antenna with both fully and partially shorted wall will be designed to operate at 2.4 GHz. Method of moments with adaptive surface patch meshing will be used for antenna modelling and genetic algorithm for design optimization. The microstrip patch antenna with a folded patch will also be used to meet the design objectives.

As the primary criteria of antenna for harmonic suppression is return loss and input impedance, these will be simulated and measured at the fundamental, second and third harmonic frequencies. The radiation patterns for the GA optimised harmonic suppression antennas will also be measured at the fundamental and harmonic frequencies.

1.3 Organization of the Report

Chapter 2 provides a literature review of the harmonic suppression of microstrip patch antennas and active integrated antennas. Published work on various types of antennas are discussed that show good suppression at both second and third harmonics. Published work on antenna designs using GA optimisation is also discussed.

Chapter 3 contains the design of square microstrip antenna operated by 1.8 GHz with harmonic control using inserted micro strip line feed; which can be used for integrating with the device. It is shown that the suppression of the second harmonic resonance of the micro strip antenna can be realised by adding an open circuited tuning stub of proper length at an appropriate position from the micro strip feed line.

Chapter 4 gives a brief view on the harmonics measurement for active patch antenna using sensor patches also the possibility of using this technique to find the power accepted by the antenna at harmonic frequencies is studied. Performance of the sensing patch technique for measuring the power accepted at the antenna feed port of active patch antennas at harmonic frequencies is evaluated using an electromagnetic (EM) simulator Ansoft Designer$^{@}$ [12] in terms of the current distribution.

Chapter 5 discusses genetic algorithm and adaptive meshing program the design of coaxially-fed air-dielectric microstrip harmonic-rejecting patch antennas for 2.4 GHz was investigated, enforcing suppression of the first two harmonic frequencies, using a genetic algorithm. The designs included patch antennas with shorted and folded walls.

Chapter 6 harmonic suppression antennas using generic algorithm the micro strip patch antenna acts as a radiator and also provides circuit functionality by matching circuit and band pass filter. However, in the harmonic radiation is not suppressed it could cause unwanted electromagnetic interference (EMI) in the system. To address this limitation,

shorting pins, slots photonic band gap structures or matching stubs on the antenna feeding line. A microstrip line fed slot antenna was developed for harmonic suppression without using reference antenna and this resulted in complex geometry for 5 GHz operation. However, if the frequency is altered in way, then the complete antenna structure needed to be modified. Matching good impedance at the fundamental design frequency (fo) with an ideal maximum first two harmonic (2fo and 3fo) is considered to be a harmonic suppression antenna (HSA).

Chapter 7 a coplanar edge-fed technique has been proposed and investigated for designing a triangular patch antenna operation at 1.02 GHz with suppression characteristics over harmonic frequency bands . The reflection coefficient was about -1.75 dB at the second harmonic and -2.53 dB at the third harmonic. According to the results obtained, this antenna with its simple harmonic suppression structures is quite effective.

Chapter 8 provides an integrated conclusion to this phases of the work, and indicates How these foundations will be taken forward in future.

1.4 References

[1] C A Balanis, Antenna Theory 2nd edition. New York: Wiley, 1997.

[2] D A Coley An introduction to GA for scientists and engineers; world scientific, Singapore, 1999.

[3] Y. Rahmat-Samii and E Michielssen; Electromagnetic optimisation by GA; John Wiley & sons, Canada 1980.

[4] H H Ammar and Y Tao; fingerprint registration using GA; IEEE symp on applications specific systems and software engineering technology; pp 148-154; 2000.

[5] D E Goldberg; GA in search, optimisation and machine learning; Addison-Wesley publishing co, Canada, 1999.

[6] D E Isbell, "Log periodic dipole arrays." IRE Trans. Antennas Propagation, volume AP-8, pp. 260-267, May 1960.

[7] S N Prasad and S Mahapatra, "A novel MIC slot-line antenna," in 1979 European Microwave Conference, Brighton, England, Sept. 1979, pp. 120-124.

[8] P J Gibson, The Vivaldi aerial, in 1979 European Microwave Conference, Brighton, England, Sept. 1979, pp. 101-105.

[9] K S Yngvesson, D H Schaubert, T L Korzeniowski, E L Kollberg, T Thungren, and J F Johansson, "Endfire tapered slot antennas on dielectric substrates," *IEEE Trans. Antennas Propagat.*, vol. 33, no.12, pp. 1392-1400, December 1985.

[10] W. Sorgel, C. Waldschmidt, and W. Wiesbeck, "Transient responses of a Vivaldi antenna and a logarithmic periodic dipole array for ultra wideband communication," in IEEE Int. Antennas Propagation. Symposium. Dig., Columbus, OH, June 2003, pp. 592-595.

[11] R H Dinger, Engineering design and optimisation with GA; Northcon/98 conference proceedings, pp 114 – 119, October 1998.

[12] Jae-Gon Lee and Jeong-Hae Lee " Suppression of supurious radiations of patch antennas using split-ring resonators (SRRs) " Microwave and optical technology letters, vol. 48, No. 2, pp 283-287, February 2006.

[13] Sin Keng Lee, Yi Qin, and E. Korolkiewicz " Reduction of the second and third harmonics for a rectangular microstrip patch antenna " Microwave and optical technology letters, vol. 40, No. 6, pp 455-460, March 2004.

[14] Yin Qin and Alistair Sambell " Broadband high-efficiency circularly polarised active antenna and array for RF front-end application " *IEEE transactions on microwave and techniques*, vol. 54, No. 7, pp 2910-2916, July 2006.

[15] S. Ver Hoeye, F. Ramirez, and A. Suarez " Nonlinear optimisation tools for the design of high-efficiency microwave oscillators " *IEEE microwave and wireless components letters*, vol.14, No.5, pp 189-191, May 2004.

[16] Dong-Hyuk Choi and Ook Park " Active integrated antenna using T- shaped microstrip- line-fed slot antenna" Microwave and optical technology letters, vol. 46, No. 6, pp 538-540, September 2005.

[17] Hyungrak Kim, Kwang Sun Hwang, Kihun Chang and Young Joong Yoon Suarez " Novel slot antennas for harmonic suppression" *IEEE microwave and wireless components letters*, vol.14, No.6, pp 286-288, June 2004.

[18] Qing-Xin Chu and Meng Hou "An H-shaped harmonic suppression active integrated antenna" International Journal of RF and microwave computer-aided engineering ,pp245-249, September 2005.

[19] Hyungrak Kim and Young Joong Yoon "Microstrip-fed slot antennas with suppressed harmonics " *IEEE transactions on antennas and propagation*, vol. 53, No. 9, pp 2809-2817, September 2005.

[20] Ji-Yong Park, Sang-Min Han and Tatsuo Itoh "A rectenna design with harmonic-rejecting circular-sector antenna" *IEEE antennas and wireless propagation letters*, vol.3, pp 52-54, 2004.

[21] L. Xue and V. Fusco, "Patch fed planar dielectric slab waveguide extended hemielliptical lens antenna," *IEEE Trans. Antennas Propagat.*, vol. 56, no. 3, pp. 661–666, Mar. 2008.

[22] J S Hong and M J Lancaster; Microstrip Filters for RF/Microwave Applications. New York: Wiley, 2001.

[23] R N Bates, "Design of micro strip spur line band stop filters," IEE Journal of Microwave., Optics, Acoustics, vol. 1, no. 6, pp. 209-214, Nov. 1977.

CHAPTER TWO

2 Literature Review

2.1 Harmonic Control for Microstrip Antennas

Microstrip patch antennas are regarded as one of the most widespread antennas used in modern wireless-communication systems, the reason being their compactness, inexpensive and ease of integration with microstrip technology, ease of integration with circuit elements, and can easily be designed to have vertical, horizontal, right-hand circular (RHCP) or left-hand circular (LHCP) polarizations. However, these antennas can introduce a harmful electromagnetic radiation into the system if not properly designed. To overcome this problem, a bandpass filter is put in place between the microstrip antenna and the power amplifier. However, by the addition of this filter the impedance matching of the microstrip antenna can considerably be affected that leads to poor performance of the system. Other solutions proposed by several researchers comprise modification of the patch geometry [1], use of a photonic bandgap (PBG) structure [2], the use of shorting pin and embedded slots at the feeding point [3], and the use of a filter [4-7] for the antenna.

2.1.1 A Selection of Reported Harmonic Suppression of Microstrip Designs

Previous works that have already applied harmonic control to the design of microstrip antennas would be reviewed and presented in this section as follows:

- An approach that applies new harmonic-suppression method for the square microstrip antenna was presented in [8]. The authors' objective was to achieve a suppression of the second and third harmonics by adding loads to the antenna's feeding line. The design involved geometries of two microstrip antennas involving similar parameters to operate at the fundamental frequency of 1.8 GHz. A square radiating patch comprising side length of 40 mm was printed on the same substrate as of the loaded transmission line. The microstrip line had an inset length of 12.8 mm. The gap between the inset microstrip line and the radiating patch was set to 1 mm. The first antenna with two loading cells achieved good suppression of the second harmonic. The second antenna with two large and one small loading cells realized the same performance as the first antenna as well as achieving the suppression of the third harmonic. This paper shows that the fundamental-mode radiation patterns of the second antenna were similar to the reference antenna. Further, an advantage is realised in terms of the suppression of the first two harmonics for the proposed antenna.

- In [9] the method for suppressing the first two harmonics of a rectangular microstrip patch antenna is described. A current density distribution method on a conventional rectangular patch is employed so that the exact positions of shorting pins and slots can be found. The antenna was designed to operate at 2.45 GHz where the patch had length of 38.65 mm and width of 57.7 mm. The simulated results for the rejection of the second harmonic using shorting pins exhibited maximum current density at the fundamental and third harmonic and minimum at the centre of the patch for the second harmonic. The suppression of the third harmonic was realised using little slots where the current density is maximum. The suppression of both second and third harmonics were realised using three shorting pins and two slots. The consequence of shorting pins and slots on the input impedance resulted in reduction from 64 Ω to 2 Ω for the second harmonic and 83 Ω to 2.7 Ω for the third harmonic. The shorting pins and slots had very little effect on the gain of the antenna, which was approximately 8 dB. The paper also showed that the radiation polarization for the rectangular patch was same as the usual designs.

- In [10] the method to suppress the spurious radiation of patch antennas is described with the help of the band-stop characteristic of split-ring resonators. This involved the design of band-stop filter. In order to suppress the first and second spurious modes, four split-ring resonators of different dimensions were used. The rectangular patch antenna was designed with length 13.5 mm and width 16.9 mm in order to operate at 6 GHz. This design shows that the first two

modes were effectively suppressed without affecting the performance of the main mode.

- In [11] a rectenna design is described, which includes a microstrip harmonic-rejecting circular sector antenna operating at 2.4 GHz. This design involved a circular sector angle of 240° and feeding angle of 30° for the circular antenna. This paper shows that the proposed design can effectively suppress the first two harmonics and generate high output power.

- In [12] the microstrip-fed slot antennas with simple structure are described. The design included a novel rectangular slot antenna where the size of this antenna is miniaturized by meandering of the slot. The harmonic suppression was achieved by placing conductor lines attached with ground plane inside the slot. The rectangular slot antenna by meander type slot radiators had sizes of 17.23 mm x 0.7 mm and 6.75 mm x 4.55 mm, respectively. The results showed that the antenna resonate at 5.4 GHz and suppress second and third harmonic at 10.8 GHz and 16.2 GHz frequencies respectively. The second and third harmonic radiations of the proposed rectangular type slot antenna were less than -28 and -33 dB for the normalized peak power of the fundamental frequency, respectively. In case with meander type slot antenna, the second and third harmonic radiations were less than -32 and -35 dB. These antennas showed good operation as radiators and ability to suppress the second and third harmonics effectively.

2.2 Harmonic Suppression for Active Integrated Antennas

The active integrated antenna (AIA) has been attractive area of research more recently, due to their compact size, low cost, and multiple functionalities. The AIA can be regarded as an active microwave circuit where the input or output port is free space. In all cases, the antenna is fully (or closely) integrated with the active device to form a subsystem on the same board and can provide particular circuit functionalities such as resonating, duplexing, filtering as well as radiating, that describes its original role. The AIA's are classified into three types: amplifying-type, oscillating-type and frequency-conversion-type, according to how the active device acts in the antenna [13-20].

2.2.1 A Selection of Reported Harmonic Suppression of AIA Designs

Previous works that have already applied harmonic suppression to the design of AIA would be reviewed and presented in this section as follows:

- In [21] an inset-fed antenna with a shorting pin and slots is presented for harmonic suppression of an AIA. This antenna had a fundamental frequency of 5.8 GHz. The results for the antenna show that the second and third harmonic return losses are suppressed to 6.7 dB and 17.7 dB with respect to the

conventional patch antenna, respectively. This antenna design is particularly appropriate as the harmonic tuning load for a class F amplifier.

- In [22] the integration of an H-shaped microstrip antenna with a bipolar junction transistor (BJT) oscillator is described. This design is aimed to operate at 2.4 GHz. This paper shows that the first two harmonics are reduced by about 10 dBm. The antenna was designed with thickness *h* of 1.0 mm and loss tangent of 0.0002. The antenna dimensions were adjusted to achieve high return losses at the second and third harmonics for suppressing harmonic radiation. The integrated BJT oscillator had a bias voltage of 12 V. The active antenna was measured with Tektronix 2782 spectrum analyzer which showed that the radiation-power was reduced as 10.51 and 8.38 dBm at the second and third harmonic frequencies, respectively. This paper concludes that the proposed design can successfully reduce the electromagnetic radiation.

- In [23] integration of an active antenna using a T-shaped microstrip coupled patch antenna is described. The design is based on feedback-antenna oscillator that uses T-shaped microstrip-coupled patch antenna. This antenna design removes the need of using chip capacitors for blocking the dc current in the radio frequency path resulting in a low-cost solution. The feedback-antenna oscillator was designed with length and width of 16.6 mm to operate at 5.8 GHz. This oscillator antenna design achieved an effective isotropic radiation power of 19.2 mW and reduced cross-polarization levels.

- In [24] the design of a T-shaped microstrip-line-fed slot antenna for 10 GHz is given. This design is based on the feedback-antenna oscillator circuit. The antenna had a slot size of 4.3 mm x 10.8 mm with an optimised T-microstrip line length of 8.8 mm and width of 1.56 mm, which was similar to the width of the 50-Ω microstrip line. This oscillator antenna design achieved an effective isotropic radiation power of 37.79 mW and good cross-polarization levels in both planes. This paper also suggested its potential use in circuits for low-cost transmitting systems.

- In [25-30] the researchers have reported the possibility of integrating microstrip bandpass filter with patch antenna in order to suppress antenna harmonics . This involved compact microstrip pseudo-interdigital, stepped impedance bandpass filter design with enhanced stopband. The purpose of this was to replace microstrip line in inset microstrip-line fed patch antenna. The design of the filter used impedance ratio of 0.72 with the second pass band at $3.85f_o$. The patch antenna was designed using fundamental frequency of 2.4 GHz. The designed filter was then integrated to this patch antenna. The additional transition section consisting of microstrip taper and meander line was used to improve impedance matching. The simulated return-loss results of the integrated antenna-filter showed that both second and third harmonics were fully suppressed. The results also showed that the gain of integrated antenna-filter was 1.3 dB, which was less than conventionally fed antenna.

- In [31-41] the design for new dual-frequency rectifying antenna operating at 2.45 and 5.8 GHz is given. The design included two small ring slot antennas, a low pass filter, and a rectifying circuit. The slot annual ring antenna was used to operate at 2.45 GHz and the slot rectangular ring antenna was used for 5.8 GHz. The slot annual ring antenna used the notched meander line. The slot rectangular ring was inset within the meandered slot annual ring. This rectenna had dimensions of 38.09 mm x 25.54 mm, whose area (regardless of thickness for the substrate) is around 15% of the previous reported designs. Therefore, this makes it the smallest dual-frequency rectenna design. The low pass filter was designed that is based on elliptic-function filter as reported in [40]. This uses two hairpin resonator components to achieve a sharp cut-off frequency response. The length of the filter used was 8.36 mm, which was shorter than $\lambda_g / 10$ at 2.45 GHz. This hairpin filter showed a good suppression of second and third harmonics at both operation frequencies. The rectenna showed good maximum gains and improved RF-to-dc efficiencies at both operating frequencies. This paper suggested that the dual-frequency rectenna design could find its use in applications including microwave power transmissions, embedded sensor, or in combination with other wireless communication components.

- In [42] the AIA based rectenna design is described that uses a new probe-fed U-slot antenna for harmonic suppression. The design uses a u-slot that was located in the centre of the patch. The microstrip patch was fed using a 50-ohm

coaxial probe. The purpose of using the coaxial feed for this antenna was firstly to separate the electric circuit and the antenna by the ground plane, and secondly, to realise the benefit of the layered structure for reduced occupied area. The physical size of this antenna was reduced significantly compared to square patch antenna. The gain of this proposed antenna was 6.96 dBi, which was 2.6 times greater than the gain of a square patch antenna. Due to the u-slot antenna in the rectenna design, the second and third harmonics were suppressed successfully. Therefore, this removed the need for band pass filter as generally required in conventional rectenna [43-49].

- In [50] a novel microstrip antenna for 2.4 GHz with harmonic rejection is described. This design have the same advantages as the earlier reported low cost, low profile, and light weight active integrated antennas [51-53]. The antenna was designed with arc-slot with dimensions W = 9 mm, L = 25 mm, D = 38 mm, K = 17 mm, Theta = 25° on a substrate with thickness of 0.80 mm. The arc-slot was used to lengthen the surface current path. Therefore, the physical size of this novel antenna was reduced by 40% in comparison to the conventional square patch antenna for probe-fed. Advance design system (ADS) 2006a and Agilent Momentum full-wave software were used to optimise antenna's dimensions. The results showed good suppression for both the second and third harmonics. The results also showed that this antenna has linear polarization.

- In [54-57] the design for a 2.4 GHz patch antenna is presented that includes the use of harmonic tuning with Composite Right/Left-handed (CRLH) transmission lines. The width for a 50 Ω transmission line was worked out using ADS transmission line calculator [59]. The integrated patch antenna was designed using simulation called *Sonnet Lite* [58]. The antenna dimensions used in this design were 41.1 mm x 50 mm, and were worked out using cavity (resonant) approach [60]. The results showed that the second and third harmonics could be suppressed using CRLH transmission lines.

- In [61] a wide band harmonic suppression microstrip patch antenna using Koch-shaped defected ground structure (DGS) is described. This proposed antenna design could be applied in active integrated antenna systems. The microstrip circuit of the patch antenna was constructed by Koch patterns on the ground plane of a standard transmission line. The non-uniform distribution was applied to narrow the dimensions of the etched Koch-shaped DGS units [62]. The third iteration order and the iteration factor of 1/3.5 were applied in Koch fractal patterns. The distance between the two adjacent units was set to 12.5 mm. The feed line was fabricated on the substrate with thickness of 0.8 mm. The whole antenna was fabricated on the same substrate as above. The Koch-shaped DGS circuit was adopted as the feed part of the proposed antenna. The source signal was fed directly to the antenna by the 50-microstrip line. The parallel slots were inserted to adjust the impedance matching of the antenna. The length and width of the parallel slots were 11mm and 1.5mm, respectively. The simulated and

measured results demonstrated that the spurious radiations from second to sixth harmonic were suppressed effectively. This paper shows that in comparison with antennas reported in other literatures, the proposed antenna exhibited excellent spurious suppression characteristics.

2.3 Antenna Design Using Genetic Algorithm

The genetic algorithm (GA) can be used to optimize performance of existing antenna designs and in creating new types of antenna designs. The GA gives the possibility of setting down the desired performance of an antenna and let the computer to search the parameters for the proposed design.

The GA has been applied to several different antenna designs for electromagnetic optimisation as reported in [63-99]. The GA technique is extremely useful for many reasons, involving:

- Antenna principles that are based on Maxwell's equations, are very difficult to understand.
- There are numerous high-speed antenna simulators available that requires only seconds to generate correct results.
- There is minimum amount of design information required to produce high-quality results.

2.3.1 A Selection of Reported Antenna Designs Using Genetic Algorithm

Previous works that have already applied GA to the design of various antennas would be reviewed and presented in this section as follows:

- The Crooked Wire antenna is probably the most well-known GA-designed antenna due to its fascinating and non-intuitive shape [100]. Derek Linden designed this antenna as part of his PhD thesis from MIT, with the intention of optimizing the polarization and radiation pattern. Specifically, the search was for a right-hand circularly polarised (RHCP) antenna that radiates over one hemisphere. Each wire component of the antenna was defined by its (X, Y, Z) coordinate for its start and end points. In binary GA, 5 bits were allowed for each axis coordinate, such that there were 323 possible vertices at which the wires could be connected. The antenna was composed of 7 wire segments. The cost function solely optimised the radiation pattern.

  Gene: 5-bits for each axis coordinate, 3 axis coordinates per point, 7 design points

  Chromosome/Individual: 5x3x7 = 105 bits

  Cost Function: Hemispherical Coverage with RHCP—Using NEC2, computes hemispherical radiation pattern at increments of 5° in elevation (θ = -80° to +80°)

and 5 percent in azimuth ($\varphi = 0°$ to $\varphi = 175°$), calculates average gain for RHCP wave for elevation angles above 10°: Score = $\Sigma$for all θ, φ[Gain(θ,φ) – Avg. Gain]^2

Population: 500 individuals

Crossover: 50%

Mutation: Variable, <8%

Generations: 90

Result: The result of this experiment GA antenna clearly has no resemblance to existing antenna designs and concepts yet it functions all the same.

- In [100] the Yagi-Uda antenna consists of an array of elements—a driven dipole, a reflector, and parasistic elements. It is lightweight and inexpensive and has been widely used in high gain and narrowband applications. Because the performance of the Yagi-Uda antenna has been slow to improve, Linden and Altshuler set about optimizing the Yagi-Uda antenna using genetic algorithm. The goal of their first GA optimisation was to increase the gain and improve VSWR for four N-length (N = 14, 17, 18 and 22) Yagi-Uda antenna.

  Gene: The genes were again mapped in binary to represent the lengths of the different elements and spacings between the elements. Each element was constrained to a maximum length of 0.75λ and with a set boom (total length of spacings), each spacing had a minimum of 0.05 λ between the elements.

  Chromosome/Individual: Entire set of element and spacing values.

Cost Function: F= -G + C1 x (VSWR), Where G is the gain, and C1 is 1 when VSWR is greater than 3.0 and .01 when VSWR is less than 3.0. The goal was to *minimize* F.

Population: 50

Crossover: 30%

Mutation: 2%

Generations: N/A

The GA configurations were much different from the typical Yagi antennas with the same boom length. Conventional Yagi antennas have elements whose lengths gradually decrease and spacings gradually increased along the array. The GA Yagis however, the lengths and spacings along the array showed no pattern and appeared to be random. The GA antenna had a higher gain at the design frequency of 432 Mhz. Other GA optimizers were utilized to control gain, sidelobe level, backlobe level, VSWR, and polarization of Yagi antennas. One GA-designed antenna had low sidelobes over a specified region in space and another created a circularly polarised Yagi antenna, both design features that did not previously exist with Yagi antennas.

- In [65] the GA optimisation of broadband patch antenna design is described. This includes a simple patch antenna that was optimised to produce a wider operational bandwidth than classical designs. Specifically, the goal was to produce a patch antenna with a 2:1 VSWR over 20% bandwidth centered at 3 GHz. A 5.0 x 5.0

cm patch was suspended 0.5 cm above the ground plane. The GA optimised the patch by removing square metal subsections from the patch region.

Gene: 1-bit string representing the presence or absence of a subsection of metal in the patch

Chromosome/Individual: $\lambda/2$ square patch, fed by simple wire feed

Cost functions: Minimize S11 magnitude at three frequencies, 2.7 GHz, 3 GHz, and 3.3 GHz. The s-parameter S11 is yet another metric to measure the reflection of energy between two media, like Γ and VSWR. A value of S11 = -10 dB corresponds to a VSWR value of 2. Therefore, S11< -10dB signifies the antenna's impedance bandwidth. Fitness = min (S11n)

Population: 100 Individuals

Crossover: 70%

Mutation: 2%

Generations: 100

Result: the patch antenna had a bandwidth of approximately 6%. After GA optimisation, this bandwidth increased to the desired 20.6%.

- In [96] Choo et. al. uses a similar approach in designing a broadband patch antenna as the Johnson patch antenna described above. Again, they began with a metallic patch, in which sub-patches were represented by either ones (metal) or zeros (no metal). The goal was to broaden the bandwidth of a microstrip antenna around the center frequency of 2 GHz by changing the patch shape. The

implemented cost function was defined as the average S11 values that exceed -10dB within the frequency range of interest. The bandwidth of this design is found to be ~8 % by simulation and measurement where a regular square microstrip antenna (36 x 36 mm) has a bandwidth of only 1.98%. This four-fold increase in bandwidth is a result of creating an unusual ragged-shaped patch antenna that makes no intuitive sense.

- In [101] the goal was to design a dual-band patch antenna for wireless communications operating at 1.9 GHz and 2.4 GHz. The hybrid fitness function combines the VSWR at the desired frequencies as well as the cross-polarised far field (low desired).

  Gene: Like other GA patch antennas, 1-bit string representing the presence or absence of a subsection of metal in the patch.

  Chromosome/Individual: 2D rectangular array of 46 binary metallic elements.

  Population: 260

  Crossover: 70%

  Mutation: 5%

  Generations: 200

  Results: The resulting GA-optimised design has 5.3% and 7% operating bandwidths at 1.9 GHz and 2.4 GHz.

- In [95] the study not only used genetic algorithms to optimize specific antenna designs, but compared the GA-optimised designs to determine which design has better bandwidth performance. The two designs are the bowtie antenna and the reverse bowtie antenna, both over an infinite ground plane.

  Gene: The antenna height H and the flare angle α were the variable genes in this experiment. The reverse bowtie had an additional parameter, the feed height h_f, which is the distance of the feed point above the ground plane.

  Chromosome/Individual: Bowtie or reverse bowtie antenna with specified height H, flare angle α, and feed height h_f in the case of the reverse bowtie.

  Population: For each antenna type, population size was 60.

  Crossover: 50%

  Mutation: 2-4%

  Generations: N/A

  Results: The results showed that the RBT could achieve 80% fractional bandwidth with a significantly smaller size than the regular BT. Fractional bandwidth means that 20% fractional bandwidth around 1 GHz would be 900 MHz – 111 MHz. The GA-optimised antennas were also built and physically tested, of which the measured results matched the simulated results.

  The implications of this paper are more than that the RBT has a better broadband performance than the regular bowtie design. The paper also demonstrates that genetic algorithms are an effective way of evaluating antennas, and specifically the bandwidth of antennas.

- In [102] the GA optimisation for circular microstrip antenna is discussed. The new approach based on GA method [103] was used to optimize circular microstrip antenna. This method was used to determine the optimal parameters of a microstrip antenna, with circular radiant element, fed with coaxial probe. The objective was to find the values of the three parameters: radius a, substrate thickness H and relative permittivity ε_r, so that the antenna satisfies the constraint (a resonant frequency equal to 5 GHz). The DERNERYD [104] model was used as an analysis method. The simulation results of the GA optimisation after 3 seconds were obtained as: a = 1.25 cm, H = 0.35 cm and ε_r = 1.36. The technique used in this paper had the advantage of escaping the local solutions; it produced global optimal results without requiring a great deal of information about the solution domain.

- In [105] the optimisation of E-shaped patch antenna is given. This paper describes that the bandwidth of the antenna can be optimised using fuzzy logic such as fuzzy decision-making. For the fuzzy system, input parameter included population, and output parameters included recombination to generate the next generation. The fuzzy inference system was adopted for the control of the parameters [106]. The antenna bandwidth was increased by adding two slots into the patch. The results showed that this antenna can produce wide bandwidth and can be used for 1.9 and 2.4 GHz. This paper showed that this novel technique is faster in terms of simulation time as compared to conventional genetic algorithm.

- In [107] the techniques of Multiobjective Genetic Algorithm, Multiobjective Simulated Annealing and Divided Range Multiobjective Particle Swarm Optimisation (DRMPSO) are compared in terms of their suitability for designing an antenna tuning unit. The optimisation of harmonic suppression and reflection coefficient of an antenna has been applied in the Pi-Network arrangement to obtain impedance matching. The results show that DRMPSO technique produces the similar standard of optimisation as other techniques and stands out in terms of good algorithm efficiency. This paper also presents significant improvement over the previously reported antenna filter tuning [108-109].

- In [110] the GA optimisation of planar monopole antennas is given. This GA optimised antenna represents an improvement over previously reported notch-band and monopole designs [111-120]. In this design, a matrix-based chromosome was used to explain the shape of the planar monopole element. It was revealed that the pattern symmetry in the notch band could be enhanced by optimizing both impedance matching and radiation pattern characteristics at the same time. This GA optimised antenna exhibited considerably wide attenuation bandwidths than the conventional band-notched planar monopole designs.

- In [121] the microstrip patch antennas with harmonic suppression are designed and optimised, using a GA and applying a novel adaptive meshing program to generate a wire-grid simulation. Two coaxially fed air dielectric patch antenna

designs with shorting walls were investigated. The measured results for the suppression of second and third harmonics were very good and the presented examples showed the capability of the FORTRAN program in antenna design using GA.

- In [122] the new design strategy for miniaturization of antennas is proposed by operation of chromosome-length in GA. Proposed design technique provides a minimum area necessary for keeping antenna characteristics . And, efficient miniaturization of a antenna and removal of many undesirable conductors in a design area is possible. Removing undesirable conductors provides lower-cost designing of antennas. The new design method can become rational design strategy for antennas miniaturization.

- In [123] the novel types of genetic algorithms are used as a global optimisation method to seek the geometry of ultra-wideband slot-line antenna (UWB SLA). The global optimisation method is combined with local optimisation method for accurate results of optimisation. For accurate and wideband computation, time domain method in CST MW Studio is used. The antenna is optimised for two basic parameters: wideband impedance matching and directivity pattern of the antenna. The algorithm exhibits good accuracy of the analysis, fast optimisation and universality of optimisation for similar EM problem.

- In [124] GA is used to design the patch geometry, substrate thickness and permittivity in order to optimize the gain and bandwidth of the antenna. The design parameters and content of fitness function were changed and tested for achieving higher bandwidth properties. The results show that including antenna parameters such as patch geometry, substrate thickness and permittivity in GAO improves the antenna performance than conventional rectangular shape antenna. Using higher thickness values in substrates give comparatively higher bandwidth improvements than reducing return loss value limits.

- In [125] the design of a micro-strip patch antenna is proposed by optimizing its resonant frequency, Bandwidth of operation and Radiation resistance using GA. The disadvantage of micro-strip patch is limited bandwidth (usually 1 to 5%). To overcome this problem the proposed design in this work is an appropriate alternative, which generates an optimised bandwidth in the simulation, as high as 25.52% bandwidth for the resonant frequency of 18 GHz. The design is done for frequency range 3-18 GHz. Therefore, this microstrip antenna is suitable for any application in the microwave frequency band S (3-4 GHz), C (4-6 GHz) and X (8-12 GHz).

- In [126] an optimisation on the input impedance of Koch triangular quasi-fractal antennas using an efficient GA is described. The impedance matching is done by using an inset-fed, which is optimised to minimize the return loss. The excitation of this structure is done using a microstrip line. The antennas are designed using

the Ansoft Design TM software and the new structures that are optimised with GA are simulated, measured and compared with the same patch antenna but with the lengths of the inset-fed (y0) calculated by well-known models available in the literature [127-128]. The return loss value of the GA optimised antenna is below -40 dB at the resonant frequency of 2.4 GHz.

- In [129] a simple dual-frequency microstrip antenna based on the second iteration of modified Koch fractal configuration is presented. Complex structure of fractal shape is built up through replication of a base shape. The aim of this research is to examine new modified fractal element antenna through simulation and optimisation procedure. In the absence of any available closed-form formulae, this scheme uses a real coded genetic algorithm (RCGA) in conjunction with electromagnetic simulation. Parametric definition of conventional Koch shape evolves new geometries of antenna structure, which suggest wide space design [130]. Genetic algorithm efficiently searches the possible combinations of parameters and finds the best structure for the antenna's operation at 5.8 GHz and 2.4 GHz.

2.4 Triangular Patch Antennas

The triangular patch antenna (TPA) has been an attractive area of research recently, due to their small size compared to other shapes like the circular and rectangular patch antennas. The most commonly used shapes of TPA are equilateral TPA (ETPA), right angle isosceles TPA (RAITPA), 30°-60°-90° TPA and 30°-30°-120° TPA. The 30°-60°-90° TPA has the least area among all these triangular shapes [1]. A miniaturized structure is often obtained by applying techniques such as shorting pin or embedding slot onto this triangular shape.

2.4.1 A Selection of Reported Triangular Patch Antenna Designs

Previous works that have used the design of TPA antennas would be reviewed and presented in this section as follows:

- In [131] a triangular patch antenna design with 15°-75°-90° angles is presented. The simulations have been performed using IE3D full-wave simulator on this design to obtain the resonant frequency. It has been established that for the same resonant frequency, this design have the least area among all common triangular shapes. The antenna with reduced size has been simulated with side length of 95 mm and substrate thickness of 1.6 mm for 900 MHz operation. The resonant frequency has been found to be close to the resonant frequency of 30°-60°-90° triangular antenna with the same dimensions, but with significant reduction in area. A 15°-75°-90° TPA has been fabricated and measured to confirm the

simulation results. A 15°-75°-90° TPA with a shorting pin at the tip has been simulated for reflection coefficient and compared to usual 15°-75°-90° TPA without shorting pin. It has been found that a reduction of greater that 75% in the resonant frequency is achieved by shorting the tip of the triangular patch.

- In [132] the design of tri-loaded slotted equilateral triangular antenna is presented. In this paper, a new technique of embedding an equilateral triangular slot in the equilateral triangular patch antenna is used to obtain the antenna size reduction. The antenna was designed with side length of 48 mm and substrate thickness of 1.6 mm. The antenna had an operating resonance frequency of 1915 MHz. A tri-slot with a side length of 33 mm was centered at the null-point of the triangular patch. The antenna had a size reduction of 38% as compared to triangular patch antenna without tri-slot at a fixed frequency. Further 50% size reduction was obtained by vertically splitting the proposed antenna in two equal parts and by optimising the feeding position to ensure the same resonance frequency operation. Therefore, a total of 70% antenna size reduction was achievable with a single band operation.

- In [133] the design of right angle triangular patch antenna with slot is described. The design for reduced antenna size has been achieved by embedding a narrow slot on the proposed antenna and introducing a single feed. The proposed antenna with a truncated tip was designed with substrate thickness of 0.6 mm and was mounted above ground plane at a height of 8 mm. The probe feed method was

used to ensure the feed can be placed at any location in the patch to match with its 50 Ω impedance. This proposed antenna had a resonant frequency of 3.25 GHz and impedance bandwidth of 310 MHz or 9.5% with stable gain and cross polarization characteristics.

- In [134] the design of triangular patch antenna with truncated tip is described. The design for reduced antenna size has been attained by cutting all three tips of the triangular patch antenna and placing a single coaxial feed. The proposed antenna with all three truncated tips was designed with substrate thickness of 1.6 mm and was mounted above ground plane at a height of 6 mm. The coaxial feed method was adopted to ensure the feed can be placed at any location in the patch to match with its 50 Ω impedance. This proposed antenna had a resonant frequency of 3.43 GHz and impedance bandwidth of 380 MHz or 11% with stable gain and cross polarization characteristics. This makes the antenna useful in applications such as modern communication systems where multi-frequency operating modes are required.

- In [135] the design of triangular patch antenna with V-slot is presented. The design for reduced antenna size has been attained by embedding two narrow slots (each of length 29.5 mm) in V shape on the triangular patch antenna and inserting a single feed. The proposed antenna with V-slot was designed with substrate thickness of 0.6 mm and was mounted above ground plane at a height of 6 mm. It was found that the antenna's fundamental resonant frequency can be reduced by

increasing the length of the probe feed. This proposed antenna had a resonant frequency of 3.6 GHz and impedance bandwidth of 330 MHz or 9.2% with antenna gain and return loss observed. This antenna has also shown a good broadside radiation pattern.

- In [136] the design of a short-circuited triangular patch antenna with truncated corner is described. The compact design has been achieved by truncating all the corners of the triangular patch. The antenna design includes insertion of two shorting walls with a V-shaped slot patch, so that the two resonant frequency modes can be excited at the same time. The proposed antenna was designed with substrate thickness of 0.6 mm and was mounted above ground plane at a height of 6.4 mm. The antenna was fed by coaxial transmission line having radius of 0.6 mm. The shape of the patch used was equilateral triangular kind having side length of 60 mm. After corner truncation each side of the patch was reduced to 39.1 mm. This proposed antenna had two resonant frequencies of 2.53 GHz and 3.5 GHz covering the first and second band. The impedance bandwidth of 50 MHz has been achieved for the first band and 310 MHz for the second band. This antenna also had a return loss of below -10 dB over the entire frequency band.

- In [137] the design of right triangular patch antenna (30°-90°-60°) with and without air gap is described. This design has been developed based on previous work of equilateral and right isosceles triangular antennas under different modifications [138, 139]. The proposed antenna was designed with substrate

thickness of 0.159 mm with the backplane conductor to produce a microstrip antenna. The length of the proposed antenna was 51.9 mm and the height used was 30.6 mm. The probe feed method was used to ensure good 50 Ω impedance matching of the antenna. This proposed antenna had a resonant frequency of 3.11 GHz. However, poor radiation efficiencies of around 38% was achieved at this resonant frequency. To improve the design, an air gap between the ground plane and radiating element was applied where the structure had two dielectric layers separated by air gap of 1.5 mm. This enabled the antenna to resonate at two frequencies giving dual band with improved bandwidth. The radiation efficiency at resonance frequency of 3.24 GHz was about 62%, which was much higher as compared to radiation efficiency of antenna design without an air gap. The antenna with air gap design also showed remarkable improvement in terms of gain and directivity values.

- In [140] an equilateral triangular patch antenna design with T-shaped notch is presented. The shape of the patch used was equilateral triangular type having side length 100 mm with height from ground plane of 1.7 mm. The proposed antenna was designed with a centre frequency of 1.8 GHz. This proposed antenna with T-notched exhibited a gain of 9.5 dB at 1.8 GHz, which was higher as compared to the gain of the conventional equilateral triangular antenna without notch. It has been found that higher gain is achievable at the cost of greater T-notch patch area as the ratio of patch surface area.

- In [141] an equilateral triangular patch antenna design with bow-tie aperture coupling is described. In this paper, triangular patch design is achieved by electromagnetically coupling the patch using two orthogonally oriented bow tie shaped apertures. This equilateral triangular patch had a side length of 52 mm. The antenna was designed to transmit and receive the two different types of polarised wide band signals at the same time using a single antenna. The use of a thick dielectric foam gave enhanced improvement in bandwidth. The impedance bandwidth was improved by 7.16 % and the ellipticity bandwidth was improved by 10.14% for the proposed design as compared to the patch of alike geometry with usual rectangular shaped apertures. The use of dielectric foam was beneficial in achieving a low cost and light weight antenna.

- In [142] the design of right triangular patch antenna with and without slits is presented. The antenna was designed having three layer structure in between the ground plane and radiating patch. It was discovered that antenna with no slits present and with an air gap of 1 mm resonated at a single frequency. However, much better bandwidth of 32.8 % was achieved as compared to previous designs. When the two parallel slits in this patch were applied, the proposed antenna exhibited high impedance bandwidth of 33% and showed antenna resonating at two different frequencies. With this antenna, the directivity of up to 7.52 dBi can be achieved. However, further work is needed in experimentation before reaching any conclusion.

- In [143] the design of a short-circuited triangular patch antenna is described. The compact design has been achieved by truncating the corner of the equilateral triangular patch, which is embedded with a V-shaped slot. The antenna design includes insertion of two shorting walls at the opposite edges of a tip-truncated triangular patch with a V-shaped slot, so that the two resonant frequency modes can be excited at the same time. The proposed antenna was designed with substrate thickness of 0.6 mm and was mounted above ground plane at a height of 6.4 mm. The antenna was fed by coaxial probe having radius of 0.6 mm. The shape of the patch used was equilateral triangular kind having side length of 60 mm. This proposed antenna was designed to cover UMTS bands (1.92 - 2.48 GHz). It was found that the centre frequency of the operating frequency band of the proposed antenna can be reduced by 20% than that of the similar-size Planar inverted-F antennas with one shorting wall. The antenna results showed that the 10 dB impedance bandwidth is greater than 25%, and its total antenna height is less than 0.06 free-space wavelengths.

- In [144] the reflection loss of a slotted triangular patch antenna is presented. In this paper, the reflection loss of the equilateral triangular patch at three broadside modes, TM_{10}, TM_{20}, and TM_{21} is shown to be decreased by the insertion of triangular slots that perturb the broadside modes' magnetic field pattern. The resonant frequencies of the triangular patch were calculated using equations as found in [145]. The simulation studies were carried out using antenna patch with side length of 102.5 mm and height of 88.8 mm. The antenna patch had a

substrate thickness of 3 mm and infinite ground plane was assumed. The antenna was fed using coaxial feed. The antenna patch was simulated from 0.5 GHz to 8 GHz. The results showed that the reflection loss at the resonant frequencies for a triangular patch can be decreased by inserting triangular slots nearby the magnetic field nulls. The results suggested that reduced reflection loss can also be attained at higher order resonant frequencies. This method of suitable placement of triangular slots, can be used to further reduce the reflection loss for a particular resonant frequency in a traditional patch antenna. However, further work is required on developing a more accurate location for the triangular slots or using slots of other shapes.

- In [146] the design of an equilateral triangular patch antenna fed by coplanar waveguide is described. This design is based on feeding system that uses electromagnetic coupling to avoid the disadvantages of probe technique. The electromagnetic coupling here is used as microstrip line and coplanar waveguide. This design presents further development to the dual-frequency triangular patch antenna design using microstrip feed line as previously reported in [147]. The proposed antenna was designed using a pair of slits to increase the bandwidth. The antenna was designed with substrate thickness of 1.57 mm. The antenna was operated at the frequency of 4 GHz and had a side length of 26.6 mm. The two slits were inserted at the bottom of the patch antenna symmetrically and parallel to each other with fixed slit height of 12 mm and slit width of 1 mm. The two slits were also separated with a distance g, which was varied. The two resonant frequencies were produced by controlling the distance between the two slits. The

return loss of -25.31 dB at 3.01 GHz and return loss of -23.51 dB at 3.96 GHz was obtained when the distance between the two slits was at 5 mm. The results showed the impedance bandwidth can be increased to 27.26% for the proposed antenna.

- In [148] the design of a triangular patch antenna with a folded shorting wall is presented. The proposed patch antenna was designed with the shape of an isosceles triangle with side lengths 30 mm and 20 mm respectively. The antenna patch was excited by coaxial probe and was placed 6 mm above the ground plane. The folded shorting wall was connected to the edge of the triangular patch and the ground plane. The shorting wall had dimensions of height 3 mm and width of 6 mm. A stable gain of 6.4 dBi was found over a bandwidth of 28.1%. The proposed antenna exhibited 48% area reduction and 34% bandwidth improvement compared to the traditional rectangular patch antenna designs.

- In [149] the design of tuneable equilateral triangular patch antenna with variable air gap is investigated both experimentally and theoretically. The resonant frequencies for different air gap heights were theoretically calculated using equations based on improved cavity model [150]. These results were confirmed with measurements performed for a coaxially-fed antenna. The tunability of the antenna as a function of the air gap height was investigated theoretically giving over 200% tunable range of an equilateral triangular patch antenna having a side length of 50 mm. Bigger patches with high dielectric constant substrate would

offer larger tunable frequency ranges. The computed results for the antennas with no air gap height were compared with a standard spectral domain moment technique analysis as carried out by other earlier reported experiments. A good agreement was shown in all comparisons.

2.5 Conclusions

Several microstrip patch antennas were reviewed for harmonic rejection. The square patch design for 1.8 GHz operation can be used to suppress the first two harmonics by adding loads to the antenna's feeding line. The rectangular patch design using shorting pins and slots has the same radiation polarization as of the conventional patch designs. The rejection of spurious radiation of patch antennas can be achieved using split-ring resonators comprising band-stop filter.

As compared to a conventional square-patch, the circular-sector antenna using inset feeding has high reflection coefficients at the second and the third harmonics.

The active integrated antennas are attractive due to their compact size and low cost. An H-shaped microstrip antenna integrated with a bipolar junction transistor oscillator for 2.4 GHz operation can suppress the first two harmonics. An active antenna integrated using a T-shaped microstrip coupled patch design removes the need of using chip capacitors for blocking the dc current in the radio frequency path resulting in a low-cost

solution. The rectifying antenna (rectenna) design using a new probe-fed U-slot antenna for harmonic suppression gives a reduced antenna physical size as compared to square patch antenna. The rectenna also has higher gain than the square patch antenna.

The genetic algorithm can be used to optimize performance of any antenna design. This method can effectively search the possible combinations of parameters and find the best structure for the antenna at the operating frequency. The genetic algorithms are an effective way of evaluating antennas for bandwidth.

2.6 References

[1] G.R. Buesnel, M.J. Cryan, and P.S. Hall, Harmonic control in active integrated patch oscillators, Electronic Lett 34 (1998), pp 228-229.

[2] Y. Horii and M. Tsutsumi, Harmonic control by photonic bandgap on microstrip patch antenna, *IEEE Microwave Guided Wave Lett*, vol 9, pp. 13-15 January 1999.

[3] B. Kwon, B.M. Lee, Y.J. Yoon, W.Y. Song, and J.G. Yook, A harmonic suppression antenna for an active integrated antenna, IEEE Microwave Wireless Component Lett 13 (2003), pp 54-56.

[4] D.M. Pozar, Microwave engineering, 2nd edition., Wiley, New York, 1998.

[5] F.R. Hsiao,T.W. Chiou, and K.L. Wong, Harmonic control of a square microstrip antenna operated at the 1.8 GHz band, Asia-Pacific Microwave Conf, 2001, Taipei, Taiwan pp. 1052-1055.

[6] P. Vincent, J. Culver, and S. Eason, Meandered line microstrip filter with suppression of harmonic passband response, IEEE Microwave Theory Tech Symp Dig 3 (2003), pp. 1905-1908.

[7] T. Lopetegi, M.A.G. Laso, J. Hernandez, M. Bacaicoa, D. Benito, M.J. Garde, M. Sorolla and M. Guglielmi, New microstrip Wiggly-Line filters with spurious passband suppression, IEEE Trans Microwave Theory Tech 49 (2001), pp. 1593-1598.

[8] Shun-Yun Lin, Kuang-Chih Huang, and Jin-Sen Chen, Harmonic control for an integrated microstrip antenna with loaded transmission line, *Microwave and optical technology letters*, vol. 44, No. 4, pp 379-383, February 2005.

[9] Sin Keng Lee, Yi Qin, and E. Korolkiewicz, Reduction of the second and third harmonics for a rectangular microstrip patch antenna, *Microwave and optical technology letters*, vol. 40, No. 6, pp 455-460, March 2004.

[10] Jae-Gon Lee and Jeong-Hae Lee, Suppression of spurious radiations of patch antennas using split-ring resonators (SRRs), *Microwave and optical technology letters*, vol. 48, No. 2, pp 283-287, February 2006.

[11] Ji-Yong Park, Sang-Min Han and Tatsuo Itoh, A rectenna design with harmonic-rejecting circular-sector antenna, *IEEE antennas and wireless propagation letters*, vol.3, pp 52-54, 2004.

[12] Hyungrak Kim, Kwang Sun Hwang, Kihun Chang and Young Joong Yoon, Novel slot antennas for harmonic suppression, *IEEE microwave and wireless components letters*, vol.14, No.6, pp 286-288, June 2004.

[13] A. Kaya and S. Comlekci, "The design and performance analysis of integrated amplifier patch antenna", *Microwave and optical technology letters*, vol. 50, no. 10, pp. 2732-2736, October 2008.

[14] H. Kim and Y.J. Yoon, "Wideband design of the fully integrated transmitter front-end with high power-added efficiency", *IEEE Transactions on microwave theory and techniques*, vol. 55, no. 5, pp. 916-924, May 2007.

[15] G.-J. Chou and C.-K. C. Tzuang, "Oscillator-type active-integrated antenna: the leaky-mode approach", *IEEE Transactions on microwave theory and techniques*, vol. 44, no. 12, pp. 2265-2272, December 1996.

[16] D.-H. Choi and S.-O. Park, "Active integrated antenna using T-shaped microstrip-line-fed slot antenna", *Microwave and optical technology letters*, vol. 46, no. 6, pp. 538-540, September 2005.

[17] K. Cha, S. Kawasaki, and T. Itoh, "Transponder using self-oscillating mixer and active antenna", IEEE MTT-S Int. Microwave Symp. Digest, pp. 425-428, 1994.

[18] C.M. Montiel, L. Fan and K. Chang, "A novel active antenna with self-mixing and wideband varactor-tuning capabilities for communication and vehicle identification applications", *IEEE Transactions on microwave theory and techniques*, vol. 44, no. 12, part 2, pp. 2421-2430, 1996.

[19] F. Bilotti, F. Urbani, and L. Vegni, "Design of an active integrated antenna for a PCMCIA card", Progress In Electromagnetics Research, Vol. 61, 253-270, 2006.

[20] S. Yang, Q.-Z. Liu, J. Yuan, and S.-G. Zhou, "Fast and optimal design of a k-band transmit-receive active antenna array", Progress In Electromagnetics Research B, Vol. 9, 281-299, 2008.

[21] S. Kwon, B. Moo Lee, Y. Joong Yoon, W. Young Song, and J-Gwan Yook, A harmonic suppression antenna for an active integrated antenna, *IEEE microwave and wireless components letters*, vol.3, No.2, pp 54-56, February 2003.

[22] Qing-Xin Chu and Meng Hou, An H-shaped harmonic suppression active integrated antenna, International Journal of RF and microwave computer-aided engineering, pp245-249, September 2005.

[23] Dong-Hyuk Choi and Seong-Ook Park, Active integrated antenna using a T-shaped microstrip coupled-patch antenna, *Microwave and optical technology letters*, vol. 44, No. 5, pp 434-436, March 2005.

[24] Dong-Hyuk Choi and Seong-Ook Park, Active integrated antenna using T-shaped microstrip-line-fed slot antenna, *Microwave and optical technology letters*, vol. 46, No. 6, pp 538-540, September 2005.

[25] D. Zayniyev, D. Budimir, An integrated antenna-filter with harmonic rejection, 3rd European conference on antennas and propagation, 2009, pp. 393-394.

[26] A. Abbaspour-Tamijani, J. Rizk, and G. Rebeiz, "Integration of filters and microstrip antennas," *Antennas and Propagation Society International Symposium*, 2002, Vol. 2, pp. 874-877.

[27] F. Queudet, I. Pele, B. Froppier , Y. Mahe and S. Toutain, "Integration of pass-band filters in patch antennas," in *European Microwave Conference, 32nd*, 2002, pp 685 - 688.

[28] J. S. Hong and M. J. Lancaster, "Development of new microstrip pseudo-interdigital bandpass filters", *IEEE Microwave and Guided Wave Letters*, Aug. 1995, Vol. 5, Issue 8, pp. 261-263.

[29] M. Sagawa, M. Makimoto, and S. Yamashita, "Geometrical structures and fundamental characteristics of microwave stepped-impedance resonators," *IEEE Trans. Microwave Tech. and Techn*. pp. 1078-1085, July 1997.

[30] S.-Y Lee, "Optimum resonant conditions of stepped impedance resonators", *European Microwave Conf.,* Volume 1, 4-6 Oct. 2005.

[31] Y-J. Ren, M. F. Farooqui, and K. Chang, "A compact dual-frequency rectifying antenna with high orders harmonic rejection," *IEEE Transaction on Antenna and Propag.*, vol. 55, no. 7, pp. 2110–2113, July 2007.

[32] C. H. K. Chin, Q. Xue, and C. H. Chan, "Design of a 5.8-GHz rectenna incorporating a new patch antenna," *IEEE Antennas Wireless Propag. Lett.*, vol. 4, pp. 175–178, 2005.

[33] M. Ali, G. Yang, and R. Dougal, "A new circularly polarised rectenna for wireless power transmission and data communication," *IEEE Antennas Wireless Propag. Lett.*, vol. 4, pp. 205–208, 2005.

[34] B. H. Strassner and K. Chang, "Rectifying antennas (rectennas)," in *Encyclopedia of RF and Microwave Engineering*. Hoboken, NJ:WileyInc., 2005, vol. 5, pp. 4418–4428.

[35] Y. J. Ren and K. Chang, "5.8 GHz circularly polarised dual-diode rectenna and rectenna array for microwave power transmission," *IEEE Trans. Microw. Theory Tech.*, vol. 54, no. 4, pp. 1495–1502, Apr. 2006.

[36] Y. H. Suh and K. Chang, "A high-efficiency dual-frequency rectenna for 2.45- and 5.8-GHz wireless power transmission," *IEEE Trans. Microw. Theory Tech.*, vol. 50, no. 7, pp. 1784–1789, July 2002.

[37] J. Heikkinen and M. Kivikoski, "A novel dual-frequency circularly polarised rectenna," *IEEE Antennas Wireless Propag. Lett.*, vol. 2, pp. 330–333, 2003.

[38] J. Y. Park, S. M. Han, and T. Itoh, "A rectenna design with harmonic-rejecting circular-sector antenna," *IEEE Antennas Wireless Propag. Lett.*, vol. 3, pp. 52-54, 2004.

[39] M. Ali, G. Yang, and R. Dougal, "Miniature circularly polarised rectenna with reduced out-of-band harmonics," *IEEE Antennas Wireless Propag. Lett.*, vol. 5, pp. 107–110, 2006.

[40] L. H. Hsieh and K. Chang, "Compact elliptic-function lowpass filter using microstrip stepped-impedance hairpin resonators," *IEEE Trans. Microw. Theory Tech.*, vol. 51, no. 1, pp. 193–199, Jan. 2003.

[41] J. O. McSpadden, L. Fan, and K. Chang, "Design and experiments of a high-converion-efficiency 5.8-GHz rectenna," *IEEE Trans. Microw. Theory Tech.*, vol. 46, no. 12, pp. 2053–2059, Dec. 1998.

[42] R. Dehbashi, K. Farooraghi, and Z. Atlasbaf, "Active integrated antenna based rectenna using a new probe-fed u-slot antenna with harmonic rejection," *IEEE Antennas and Propagation Letters*, pp. 2225–2228, 2006.

[43] T.-W. Yoo and K. Chang, ''Theoretical and experiment development of 10 and 35 GHz rectennas,'' *IEEE Trans. Microw. Theory Tech.*, vol. 40, no. 6, pp. 1259-1266, Jun. 1992.

[44] N. Shinohara and H. Matsumoto, "Experimental study of large rectenna array for microwave energy transmission," *IEEE Trans. Microwave Theory Tech.*, vol. MTT-46, pp. 261-268, March 1998.

[45] B. Strassner and K. Chang, "5.8-GHz circularly polarised dual-rhombic-loop traveling-wave rectifying antenna for low power-density wireless power transmission applications", *IEEE Trans. Microwave Theory Tech.*, vol. MTT-51, pp. 1548-1553, May 2003.

[46] J. A. Hagerty, F. B. Helmbrecht, W. H. McCalpin, R. Zane, and Z. B. Popovic, "Recycling ambient microwave energy with broad-band rectenna arrays,'' *IEEE Trans. Microw. Theory Tech.*, vol. 52, no. 3, pp. 1014-1024, Mar. 2004.

[47] Y,-H. Suh, C. Wang, and K. Chang, "Circularly polarised truncated-corner square patch microstrip rectenna for wireless power transmission," Electron. Lett., vol. 36, pp. 600-602, March 2000.

[48] S.-M. Han, J. Y. Park, and T. Itoh, "Active Integrated Antenna Based Rectenna Using the Circular Sector Antenna with Harmonic Rejection," 2004 IEEE AP-S Int. Symp., Monterey, USA, June 2004, pp. 2522-3536.

[49] K. Chang, R.A. York, P.S. Hall, and T. Itoh, "Active Integrated Antennas", *IEEE Trans. Microwave Microwave Theory Tech.*, vol. MTT-50, pp. 937-944, March 2002.

[50] E. Hassani Aligudarzi, M. H. Neshati, F. Mohanna, "Novel microstrip antenna for 2.4 GHz with harmonic rejection", International Conference on Microwave Technology and Electromagnetics, pp. 113-114, 2009.

[51] Sohiful Zaniol Murad and Widad Ismail, Design of Active Integrated Antenna for Dual Frequency Image Rejection, American Journal of Applied Sciences (3), pp. 1890-1894, 2006.

[52] K. L.Wong and H. C. Tung, "A compact patch antenna with an inverted U-shaped radiating patch", in Proc. IEEE AP-S Int. Symp., 2001, pp. 728-731.

[53] Qing-Xin Chu, Meng Hou, "An H-shaped harmonic suppression active integrated antenna", 2006 Wiley Periodicals, Inc.

[54] D. Draskovic, D. Zayniyev and D. Budimir, "Microstrip patch antennas with harmonic rejection using composite right-handed transmission lines", *IEEE Antennas and Propagation Society International Symposium*, pp. 365-368, 2007.

[55] C. Caloz, T. Itoh, "Metamaterials for High-Frequency Electronics", Proceedings of the IEEE, Vol. 93, No. 10, Oct. 2005.

[56] A. Dupuy, K. Leong, T. Itoh, "Class-F Power Amplifier Using a Multi-Frequency Composite Right/Left-Handed Transmission Line Harmonic Tuner", Microwave Symposium Digest, 2005 IEEE MTT-S International, June 2005.

[57] G. V. Eleftheriades, A. K. Iyer, and P. C. Kremer, "Planar negative refractive index media using periodically L–C loaded transmission lines," *IEEE Trans. Microwave Theory Tech.*, vol. 50, pp. 2702–2712, Dec. 2002.

[58] Sonnet USA, http://www.sonnetusa.com

[59] Agilent EESof, http://eesof.tm.agilent.com

[60] C. A. Balanis, Antenna Theory 3rd ed. New York: Wiley, 2005.

[61] Z-W. Yu, G-M. Wang, and K. Lu, "Wide band harmonic suppression based on Koch-shaped defected ground structure for a microstrip patch antenna," International conference on microwave and millimetre wave technology (ICMMT), pp. 306–308, 2010.

[62] N. C. Karmakar and M. N. Mollah, "Investigations into nonuniform photonic-bandgap microstripline low-pass filters," *IEEE Trans. Microwave Theory Tech.*, vol. 51, no 2, pp. 564–572, Feb. 2003.

[63] *Electromagnetic Optimisation by Genetic Algorithms.* Y. Rahmat-Samii and E. Michielssen, eds., Wiley, 1999.

[64] J. M. Johnson and Y. Rahmat-Samii, "Genetic algorithm optimisation for aerospace electromagnetic design and analysis," in *Proc. IEEE Aerospace Applications Conf.*, Feb. 1996, pp. 87–102.

[65] J. M. Johnson, Y. Rahmat-Samii, "Genetic algorithms and method of moments (GA/MOM) for the design of integrated antennas," *IEEE Trans. Antennas Propagat.*, vol. 47, pp. 1606–1614, Oct. 1999.

[66] D. P. Jones, K. F. Sabet, J. Cheng, L. P. B. Katehi, K. Sarabandi, and J. F. Harvey, "An accelerated hybrid genetic algorithm for optimisation of electromagnetic structures," in *Proc. IEEE Antennas and Propagation Soc. Int. Symp. Dig.*, July 1999, pp. 426–429.

[67] L. Alatan, M. I. Aksun, K. Leblebicioglu, and M. T. Birand, "Use of computationally efficient method of moments in the optimisation of printed antennas," *IEEE Trans. Antennas Propagat.*, vol. 47, pp. 725–732, Apr. 1999.

[68] R. M. Edwards and G. G. Cook, "Design of printed spiral antennas using a moment method running under a genetic algorithm optimisation routine," in *Proc. IEEE Seminar Practical Electromagnetic Design Synthesis*, Feb. 1999, pp. 61–65.

[69] R. Zentner, Z. Sipus, and J. Bartolic, "Optimum synthesis of broadband circularly polarised microstrip antennas by hybrid genetic algorithm," *Microwave and Optical Technol. Lett.*, vol. 31, no. 3, pp. 197–201, Nov. 2001.

[70] R. L. Haupt and S. E. Haupt, “Optimum population size and mutation rate for a simple real genetic algorithm that optimizes array factors,” *Applied Computational Electromagn. Soc. J.*, vol. 15, no. 2, pp. 94–102, July 2000.

[71] B. Aljibouri, E. G. Lim, H. Evans, and A. Sambell, “Multiobjective genetic algorithm approach for a dual-feed circular polarised patch antenna design,” *Electron. Lett.*, vol. 36, no. 12, pp. 1005–1006, June 2000.

[72] C. Zuffada, T. Cwik, and C. Ditchman, “Synthesis of novel all-dielectric grating filters using genetic algorithms,” *IEEE Trans. Antennas Propagat.*, vol. 46, pp. 657–663, May 1998.

[73] Y. Rahmat-Samii and H. Mosallaei, “GA optimised Luneberg lens antennas; characterizations and measurements,” in *Proc. Int. Symp. Antennas and Propagation*, Aug. 2000, pp. 979–982.

[74] H. Mosallaei and Y. Rahmat-Samii, “Non-uniform Luneburg lens antennas: a design approach based on genetic algorithms,” in *IEEE Antennas and Propagation Soc. Int. Symp. Dig.*, July 1999, pp. 434–437.

[75] “RCS reduction of canonical targets using genetic algorithm synthesized RAM,” *IEEE Trans. Antennas Propagat.*, vol. 48, pp. 1594–1606, Oct. 2000.

[76] “Non-uniform Luneberg and two-shell lens antennas: radiation characteristics and design optimisation,” *IEEE Trans. Antennas Propagat.*, vol. 49, pp. 60–69, Jan. 2001.

[77] A. F. Muscat and C. G. Parini, “Novel compact handset antenna,” in *Proc.11th Int. Conf. Antennas and Propagation,* Apr. 2001, pp. 336–339.

[78] J. Bartolic, Z. Sipus, N. Herscovici, D. Bonefacic, and R. Zentner, “Planar and cylindrical microstrip patch antennas and arrays for wireless communications,” in *Proc. 11th Int. Conf. Antennas and Propagation*, Apr. 2001, pp. 569–573.

[79] J. C. Maloney, M. P. Kesler, L. M. Lust, L. N. Pringle, T. L. Fountain, P. H. Harms, and G. S. Smith, “Switched fragmented aperture antennas,” in *IEEE Antennas and Propagation Soc. Int. Symp. Dig.*, July 2000, pp. 310–313.

[80] D. Lee and S. Lee, “Design of a coaxially fed circularly polarised rectangular microstrip antenna using a genetic algorithm,” *Microwave and Opt. Technol. Lett.*, vol. 26, no. 5, pp. 288–291, Sept. 2000.

[81] E. E. Altshuler, “Design of a vehicular antenna for GPS/Iridium using a genetic algorithm,” *IEEE Trans. Antennas Propagat.*, vol. 48, pp. 968–972, June 2000.

[82] A. Lommi, A. Massa, E. Storti, and A. Trucco, “Sidelobe reduction in sparse linear arrays by genetic algorithms,” *Microwave and Opt. Technol. Lett.*, vol. 32, no. 3, pp. 194–196, Feb. 2002.

[83] C. H. Chen and C. C. Chiu, “Novel radiation pattern by genetic algorithms, in wireless communication,” in *Proc. IEEE Vehicular Technology Conf.*, May 2001, pp. 8–12.

[84] P. Lopez, J. A. Rodriguez, F. Ares, and E. Moreno, “Low-sidelobe patterns from linear and planar arrays with uniform excitations except for phases of a small number of elements,” *Electron. Lett.*, vol. 37, no. 25, pp. 1495–1497, Dec. 2001.

[85] S. Okubo, “A simplification of feed systems of a nonuniformly spaced linear array antenna using genetic algorithm,” *Trans. Soc. Instrument and Control Eng.*, vol. 37, no. 4, pp. 271–280, Apr. 2001.

[86] K. L. Virga and D. Beauvarlet, “The effects of the element factor on low sidelobe circular arc array performance,” in *Proc. IEEE Antennas and Propagation Soc. Int. Symp. Dig.*, July 2000, pp. 1206–1209.

[87] M. M. Dawoud and M. Nuruzzaman, “Null steering in rectangular planar arrays by amplitude control using genetic algorithms,” *Int. J. Electron.*, vol. 87, no. 12, pp. 1473–1484, Dec. 2000.

[88] T. Gunel, “An optimisation approach to the synthesis of rectangular microstrip antenna elements with thick substrates for the specified far-field radiation pattern,” *Int. J. Elect. Commun.*, vol. 54, no. 5, pp. 303–306, 2000.

[89] B. J. Barbisch, D. H. Werner, and P. L. Werner, “A genetic algorithm optimisation procedure for the design of uniformly excited and non-uniformly spaced broadband low sidelobe arrays,” *Appl. Comput. Electromagn. Soc. J.*, vol. 15, no. 2, pp. 34–42, July 2000.

[90] K. N. Sherman, “Phased array shaped multi-beam optimisation for LEO satellite communications using a genetic algorithm,” in *Proc. IEEE Int. Conf. Phased Array Systems and Technology*, May 2000, pp. 501–504.

[91] Y. C. Chung and R. L. Haupt, “Amplitude and phase adaptive nulling with a genetic algorithm,” *J. Electromagn. Waves and Applications*, vol. 14, no. 5, pp. 631–649, 2000.

[92] H. X. Hang and L. D. Yun, “Sidelobe reduction of plane array using genetic algorithm,” *Acta Electronica Sinica*, vol. 27, no. 12, pp. 119–120, Dec. 1999.

[93] S. Lindenmeier and P. Russer, “Automatic optimisation of high gain antenna arrays,” in *Proc. Int. Conf. Microtechnologies,* Sept. 2000, pp. 121–124.

[94] S. D. Rogers, C. M. Butler, and A. Q. Martin, “Realization of a genetic-algorithm-optimised wire antenna with 5:1 bandwidth,” *Radio Sci.,* vol. 36, no. 6, pp. 1315–1325, Nov.–Dec. 2001.

[95] A. Kerkhoff, R. Rogers, and H. Ling, “The use of the genetic algorithm approach in the design of ultra-wideband antennas,” in *Proc. IEEE Radio and Wireless Conf.,* Aug. 2001, pp. 93–96.

[96] H. Choo, A. Hutani, L. C. Trintinalia, and H. Ling, “Shape optimisation of broadband microstrip antennas using genetic algorithm,” *Electron. Lett.,* vol. 36, no. 25, pp. 2057–2058, Dec. 2000.

[97] A. Raychowdhury, B. Gupta, and R. Bhattacharjee, “Bandwidth improvement of microstrip antennas through a genetic-algorithm-based design of a feed network,” *Microwave and Opt. Technol. Lett.,* vol. 27, no. 4, pp. 273–275, Nov. 2000.

[98] J. A. Rodriguez, F. Ares, E. Moreno, and G. Transceschetti, “Genetic algorithm procedure for linear array failure correction,” *Electron. Lett.,* vol. 36, no. 3, pp. 196–198, Feb. 2000.

[99] F. J. Villegas, T. Cwik, Y. Rahmat-Samii, and M. Manteghi, “Parallel genetic algorithm optimisation of a dual-band patch antenna for wireless communications,” in *Proc. Int. Symp. Antennas and Propagation*, June 2002, pp. 334–337.

[100] D. S. Linden, “Automated design and optimisation of wire antennas using genetic algorithms,” *PhD thesis,* MIT, Cambridge, MA, Sept. 1997.

[101] F. Villegas, T. Cwik, Y. Rahmat-Samii, M. Manteghi, “A parallel electromagnetic genetic-algorithm optimisation (EGO) application for patch antenna design,” *IEEE Trans. Antennas Propagat.,* vol. 52, no. 9, September 2004.

[102] L. Merad, F. T. Bendimerad and S. M. Meriah, “Genetic algorithm optimisation for circular microstrip antenna,” ITG, INCA, Berlin On September 17-18-19, 2003.

[103] Goldberg, D. E.: Genetic algorithm search, optimisation and machine learning : Addison-wesley, 1994.

[104] Derneryd, A.G. : Analysis of microstrip disk antenna element. IEEE trans, 1979, Vol. Ap –27, No. 5, S. 660 – 664.

[105] A. A. Lofti Neyestanak, F. H. Kashani, and K, Barkeshli, "E-shaped patch antenna design based on genetic algorithm using decision fuzzy rules," *Iranian Journal of Electrical and Computer Engineering*, vol. 4, no. 1, 2005.

[106] R. Matouek, *Realization of Fuzzy-Adaptive Genetic Algorithms in a Matlab Environment*, Institute of Automation and Computer Science, Brno University of Technology, 2001.

[107] Y. Zhang, W. Q. Malik, "Analogue filter tuning for antenna matching with multiple objective particle swarm optimisation," *IEEE Symposium on Advances in Wires and Wireless Communication*, pp. 196-198, 2005.

[108] M. Thompson, J.K. Fidler, "A Novel Approach for Fast Antenna Tuning using Transporter based Simulated Annealing", Electronic Letters, Vol. 36 No. 7, 2000.

[109] Mark Thompson, Application of Multi Objective Evolutionary Algorithms to Analogue Filter Tuning. EMO 2001, pp. 546-559.

[110] A. J. Kerkhoff and H. Ling, "Design of a band-notched planar monopole antenna using genetic algorithm optimisation," *IEEE Transaction on Antennas and Propagation*, vol. 55, no. 3, pp. 604-610, March 2007.

[111] A. Kerkhoff and H. Ling, "Design of a planar monopole antenna for use with ultra-wideband (UWB) having a band-notched characteristic," in *IEEE AP/S Int. Symp. Dig.*, Columbus, OH, Jun. 2003, vol. 1, pp. 830–833.

[112] H. Schantz, G. Wolenec, and E. Myszka, "Frequency notched uwb antennas," in *Proc. IEEE Conf. UltraWideband Syst. Technol.*,Nov. 2003, pp. 214–218.

[113] A. Kerkhoff and H. Ling, "A parametric study of band-notched UWB planar monopole antennas," in *IEEE AP/S Int. Symp. Dig.*, Monterey, CA, Jun. 2004, vol. 2, pp. 1768–1771.

[114] Y. Kim and D. Kwon, "CPW-fed planar ultra wideband antenna having a frequency band notch function," *Elect. Lett.*, vol. 40, no. 7, pp. 403–405, 2004.

[115] J. Qiu, Z. Du, J. Lu, and K. Gong, "A band-notched UWB antenna," *Microw. Opt. Tech. Lett.*, vol. 45, no. 2, pp. 152–154, 2005.

[116] W. Lee, W. Lim, and J. Yu, "Multiple band-notched planar monopole antenna for multiband wireless system," *IEEE Microw. Wireless Compon. Lett.*, vol. 15, pp. 576–578, Sep. 2005.

[117] S. Rogers, C. Butler, and A. Martin, "Design and realization of GA-optimised wire monopoles and matching network with 20:1 bandwidth," *IEEE Trans. Antennas Propag.*, vol. 51, pp. 493–502, Mar. 2003.

[118] Y. Noh, Y. Kim, and H. Ling, "A broadband on-glass antenna with a mesh-grid structure for automobiles," *Elect. Lett.*, vol. 41, pp. 1148–1149, Oct. 2005.

[119] A. Kerkhoff, R. Rogers, and H. Ling, "Design and analysis of planar monopole antennas using a genetic algorithm approach," *IEEE Trans. Antennas Propag.*, vol. 52, pp. 2709–2718, Oct. 2004.

[120] J. Kim, T. Yoon, J. Kim, and J. Choi, "Design of an ultra wide-band printed monopole antenna using FDTD and genetic algorithm," *IEEE Microw. Wireless Compon. Lett.*, vol. 15, pp. 395–397, Jun. 2005.

[121] D. Zou, R. A. Abd-Alhameed, and P. S. Excel, "Design of antenna for wide harmonic suppression using adaptive meshing and genetic algorithm," *IET 7th International Conference on Computation in Electromagnetics*, pp. 187–188, 2008.

[122] T. Yamamoto, K. Fujimuri, M. Sanagi, S. Nogi, and T. Tsukagoshi, "Efficient antenna miniaturization technique by cut chromosome-length in genetic algorithm," *Asia Pacific Microwave Conference*, pp. 1837–1840, 2009.

[123] Z. Lukes, J. Lacik, and Z. Raida, "Novel ultra-wideband slot-line antenna designed by adaptive real coded genetic algorithm," *International Conference on Electromagnetics in Advanced Applications*, pp. 682–685, 2009.

[124] J. M. J. W. Jayasinghe, D. N. Uduwawala, "Design of broadband patch antennas using genetic algorithm optimisation," *International Conference on Industrial and Information Systems*, pp. 60–65, 2010.

[125] J. Chakraborty, U. Mukherjee, "Microstrip antenna optimisation using genetic algorithm optimisation," *International Conference on Computer and Communication Technology*, pp. 635–640, 2010.

[126] E. Eldervitch C. de Oliveira, A.G. D'Assunção and C.R.M. da Silva, "Optimisation of the input impedance of Koach triangular quasi-fractal antennas using genetic algorithm," *IEEE Conference on Electromagnetic Field Computation*, pp. 1, 2010.

[127] M. Ramesh and Y. KB, "Design Formula for Inset Fed Microstrip Patch Antenna", *Journal of Microwaves and Optoelectronics*, Vol. 3, 2003.

[128] C. Balanis, *Antenna Theory: Analysis and Design*, 2nd ed., Vol. 2. New York: Wiley, 1997.

[129] Z. Adelpour, F. Mohajeri, and M. Sadeghi, "Dual-frequency microstrip patch antenna with modified koch fractal geometry based on genetic algorithm," *Loughborough Antennas and Propagation Conference*, pp. 401-404, 2010.

[130] C. Borja and J. Romeu, "on the behaviour of Koch island fractal boundary microstrip patch antenna," *IEEE Trans. on Antennas and Propag.*, vol. 15, no. 6. June 2003.

[131] M. M. Olaimat and N. I. Dib, "A Study of 15°-75°-90° Angles Triangular Patch Antenna," *Progress In Electromagnetics Research Letters.*, vol. 21, pp. 1-9, 2011.

[132] M.S. El-Sallamy, M.Y. Omar, D. Abdelaziz, "Tri-Slot Loaded Equilateral Triangular Microstrip Antenna for Compact And Dual-Frequency Operation," National Radio Science Conference, pp. 1-6, 2009.

[133] Y. Bhomia, A. Kajla, and D. Yadav, "Slotted right angle triangular microstrip patch antenna," *International Journal of Electronic Engineering Research*, vol. 2, no. 3, pp. 393-398, 2010.

[134] A. Chaturvedi, Y. Bhomia, D. Yadav, "Truncated tip triangular microstrip patch antenna," International Symposium on Antennas Propagation and EM Theory (ISAPE), pp. 212-214, 2010.

[135] Y. Bhomia, A. Kajla, and D. Yadav, "V-slotted triangular microstrip patch antenna," *International Journal of Electronics Engineering*, vol. 2, pp. 21-23, 2010.

[136] N. Singh, D.P. Yadav, S. Singh, R.K. Sarin, "Compact corner truncated triangular patch antenna for WiMax application," Mediterranean Microwave Symposium (MMS), pp. 163-165, 2010.

[137] A. Kimothi, V. Tiwari, V.K. Saxena, J.S. Saini, D. Bhatnagar, "Radiations from a right triangular patch antenna with and without air gap," International Conference on Recent Advances in Microwave Theory and Applications, pp.154-156, 2008.

[138] E. G. Lim, E. Korolkiewicz, S. Scott, A. Sambell, and B. Aljibouri , "An Efficient Formula for the Input Impedance of a Microstrip Right-Angled

Isosceles Triangular Patch Antenna" *IEEE Antennas And Wireless Propagation Letters*, vol. 1, pp. 18-21, 2002.

[139] Wei Chen, Kai-Fong Lee, Jashvant S. Dahele, "Theoretical and Experimental Studies of the Resonant Frequencies of Right Triangular Microstrip Antennas" *IEEE Trans AP*, vol. 40, no. 10, 1992.

[140] P. Tilanthe, P.C. Sharma, "An equilateral triangular patch antenna with T-shaped notch for enhanced gain" Fourth International Conference on Wireless Communication and Sensor Networks, pp. 179-180, 2008.

[141] A. Kumar Sharma, C.K. Kumar, A. Mittal, "A Triangular Patch Antenna with Bow Tie Aperture Coupling for Improved Ellipticity Bandwidth" 38th European Microwave Conference, pp. 397-400, 2008.

[142] V. Sharma, D. Saxena, K.B. Sharma, "Design of broad band dual frequency right triangular microstrip antenna with slits" IEEE Applied Electromagnetics Conference, pp. 1-4, 2007.

[143] Jeen-Sheen Row and Yen-Yu Liou, "Broadband Short-Circuited Triangular Patch Antenna" IEEE Transactions on Antennas and Propagation, vol. 54, no. 7, pp. 2137-2141, 2006.

[144] Varun Jeoti, Chin Ooi Kua and Lee Sheng Chyan, "Slotted Triangular Patch Antenna for Reduced Reflection Loss" International RF and Microwave Conference, pp. 187-191, 2006.

[145] Chen, W., K. F. Lee and J. S. Dahele, "Theoretical and Experimental Studies of the Resonant Frequencies of the Equilateral Triangular Microstrip Antenna," IEEE Trans. On Antennas and Propagation, Vol. AP-40, 1992, pp. 1253-1256.

[146] Indra Surjati, Eko Tjipto Rahardjo, Djoko Hartanto, "Increasing Bandwidth Dual Frequency Triangular Microstrip Antenna Feed By Coplanar Waveguide," Asia-Pacific Conference on Communications, pp. 1-4, 2006.

[147] Indra Surjati, "Dual frequency operation triangular microstrip antenna using a pair of slit," *11th Asia Pacific Conference on Communications*, Perth, Western Australia, 2005.

[148] Yuan Li, R. Chair, K. M. Luk, and K. F. Lee, "Broadband Triangular Patch Antenna With a Folded Shorting Wall," IEEE Antennas and Wireless Propagation Letters, vol. 3, pp. 189-192, 2004.

[149] Guha, D. and J. Y. Siddiqui, "Resonant frequency of equilateral triangular microstrip patch antenna with and without air gaps,"*IEEE Trans. Antennas Propagat.*, Vol. 52, No. 8, 2174-2177, Aug. 2004.

[150] D. Guha, "Resonant frequency of circular microstrip antennas with and without airgaps," *IEEE Trans. Antennas Propagat.*, vol. 49, pp. 55–59, Jan. 2001.

[151] Karaboga, D., K. Guney, A. Kaplan, and A. Akdagli, "A new effective side length expression obtained using a modified tabu search algorithm for the resonant frequency of a triangular microstrip antenna," *Int. J. RF and Microwave CAE*, Vol. 8, No. 1, 4-10, Dec. 1998.

[152] Olaimat, M., "Design and analysis of triangular microstrip patch antennas for wireless communication systems," Master Thesis, Jordan University of Science and Technology, 2010.

[153] Dey, S. and R. Mittra, "Compact microstrip patch antenna,"*Microwave and Optical Technology Letters*, Vol. 13, No. 1, pp. 12-14, Sep. 1996.

[154] Wong, K.-L. and S.-C. Pan, "Compact triangular microstrip antenna," *Electronics Letters*, Vol. 33, No. 6, pp. 433-434, Mar. 1997.

CHAPTER THREE

3 Square Microstrip Antenna Operated by 1.8 GHz with Harmonic Control

3.1 Introduction

In modern wireless networks; it would be feasible to incorporate built in active micro strip antennas in diverse applications such as electronic tag, wireless local area network and electronic point of sales terminals. In these applications, not only the microstrip antenna is functioning as a radiator, it also serves as a resonator for the power transformers and amplifies in the active circuits [1-8].

In such a set up, unless attempt is made to suppress harmonic resonance, it is likely that unwanted electromagnetic interference (EMI) would occur. To overcome this; bandpass filter should be installed between micro strip antenna and the power amplifier. Nevertheless, the added filter can have an effect on the impedance matching of the microstrip antenna operated at the fundamental frequency. Furthermore, by operating at higher frequencies, the interconnects added as a result of the supplementary components will not be effective and the system output would equally be compromised. There are however other methods such as modifying the patch geometry [1-3] or alternatively

using photonic bandgap (PBG) ground plane [4-5] for the micro strip antenna has also been illustrated. By altering the patch geometry, the specifications of using a circular sector radiating patch at the patch's centre line [2] or radiating edge [3] with several shorting pins are identified. By using PBG ground plane, which restricts the electromagnetic wave propagation within the designed stopband, the suppression of the second and third harmonic resonances of the microstrip antenna has been presented in [9-16]. The embedded PBG revolves within the antenna's ground plane causing the radiation patterns of the antenna at the fundamental frequency to become two directional.

3.2 Antenna Design Concept

This design illustrates the basic harmonic control system for micro strip antenna; using inserted micro strip line feed that can be used for integrating with the device. It is shown that the suppression of the second harmonic resonance of the micro strip antenna can be realised by adding an open circuited tuning stub of proper length at an appropriate position from the micro strip feed line. Additional details are presented below and experimental results are given and discussed.

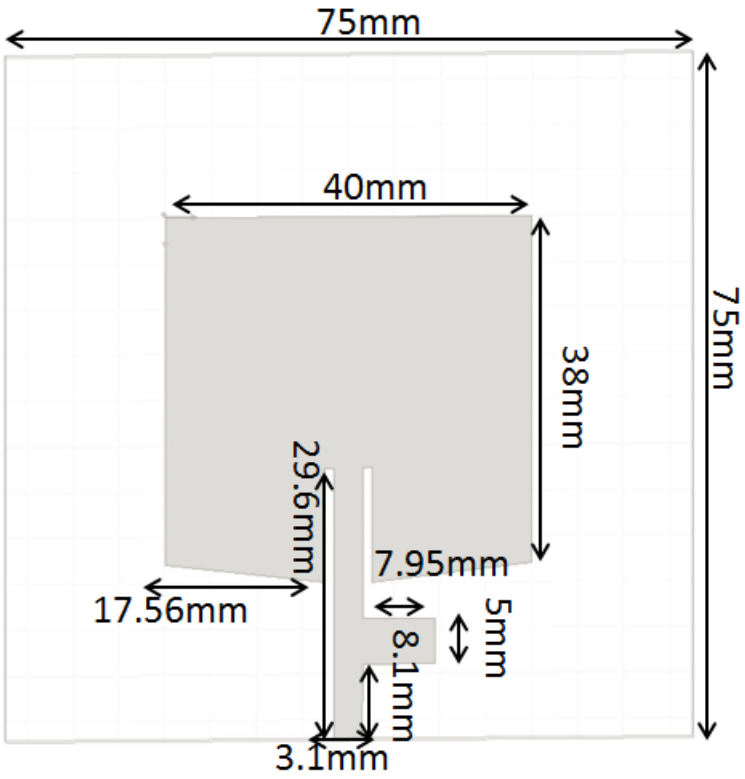

Figure 3:1: The geometry of the square microstrip antenna fed by 50 Ω inset microstrip-line and the proposed 50 Ω inset microstrip-line (a tuning stub to the ground dielectric substrate is not shown).

3.3 Antenna specification

The geometries of the regular and suggested inset microstrip-line fed are shown in Figure 3.1. The square radiating patch has a side length of *L* and is engraved on a microwave substrate of thickness *h* and relative permittivity of *e*. The inset microstrip-

line is a 50 Ω characteristics impedance and with a width of *w f*. The inset length of the microstrip-line is *ln* and the gap between the inset microstrip-line and the patch is represented as *g*, which is confined to only 1mm. The open-circuited tuning stub has a length of *l*, which is measure to 0.125 guided wavelengths at the fundamental resonant frequency (*f01*) and is placed at *l1* from the feed point.

The distance between the tuning stub and the microstrip line is represented by *l2* which is expected to be 0.125 guided wave length at the fundamental resonant frequency. As the antenna is designed to operate at the fundamental resonant frequency, the likely second harmonic (*2f01*) signal into the antenna can be impaired and blocked. It is as a result of the tuning stub length of 0.25 – guided wavelength at the frequency 2(*f01*). Therefore the impedance at point (b) is seen in the tuning stub zero or short-circuited and as a result the impedance at point (a) is visible in to the microstrip antenna's infinite or open circuited. This suggests that the likely second harmonic radiation of the proposed antenna is suppressed and equally the undesirable EMI is resolved.

3.4 Simulated Antenna And measurement Results

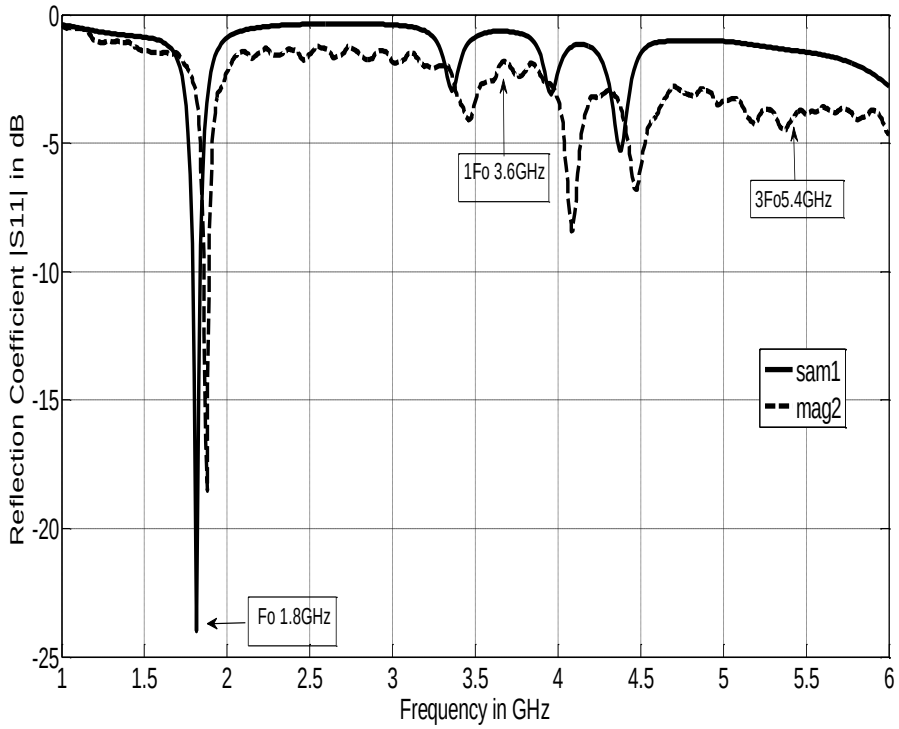

Figure 3:2: Reflection Coefficient |S11| versus the operating frequency.

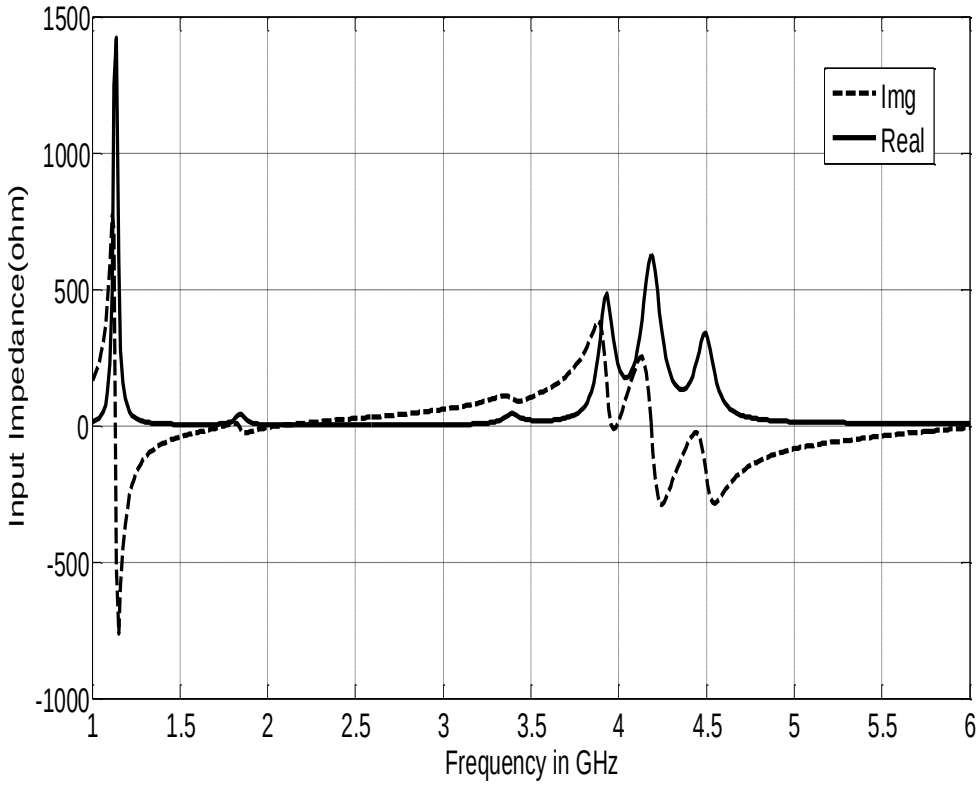

Figure 3:3 : Simulated input impedance for the proposed antenna (e_r = 3.1, h = 1.6mm, l = 40mm, l1 = 12.5mm, l2 29.6mm, g = 1mm, w = 5mm, ground-plane size = 75 x 75 mm square).

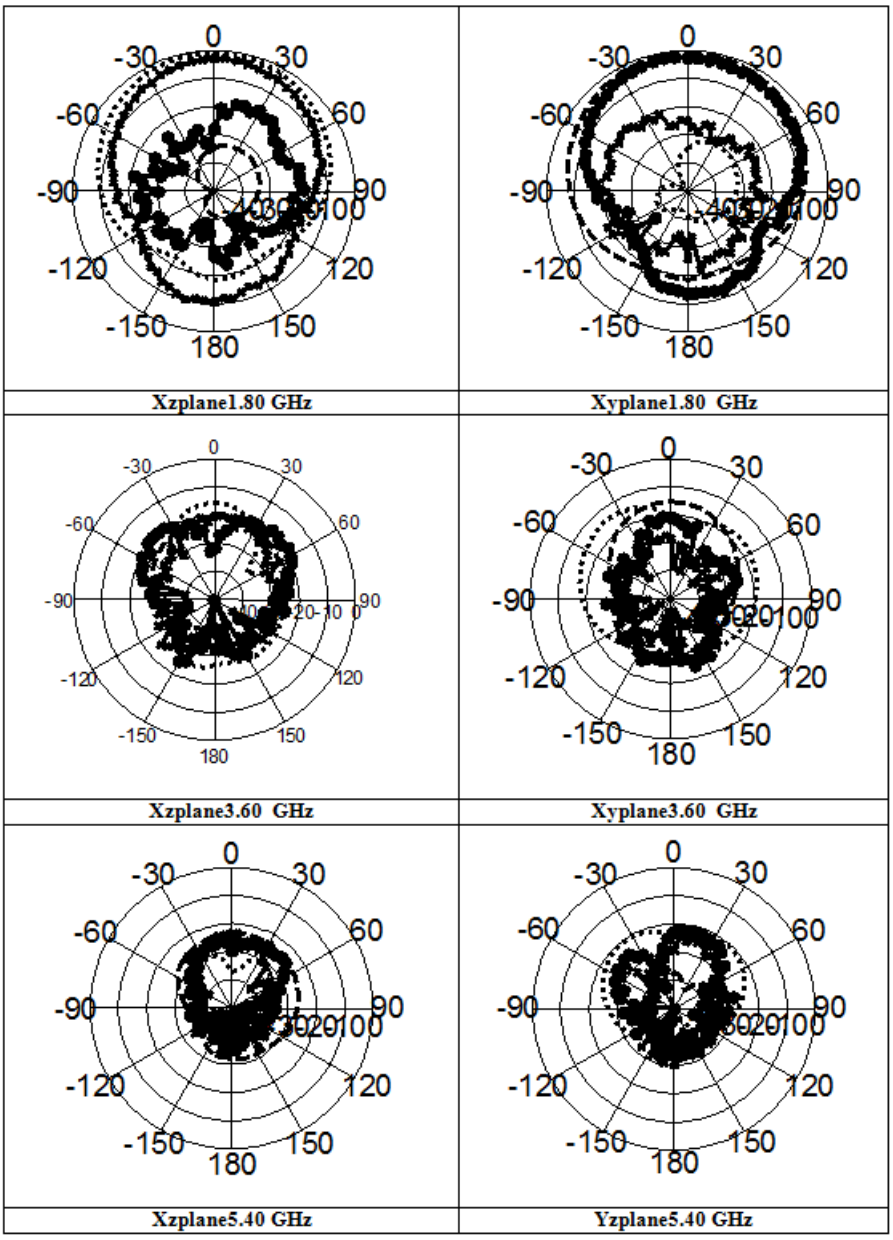

Figure 3:4: **Measured and simulated radiation patterns for 1.8 GHz, 3.6 GHz and 5.4 GHz over: (top) z-x plane; (bottom) z-y plane; (‘x x x ’measured E_θ, (‘- - - - ’simulated E_θ, ‘o o o’ measured E_ϕ, ‘——’ simulated E_ϕ).**

.

3.5 Results and Conclusions

The existing and proposed microstrip antenna is represented in Figure 3.1. It is designed to operate at TM01 mode, the fundamental resonant mode at around 1.8 GHz. Therefore, the square radiating patch is measures 40mm (l) and the FR4 dielectric substrate is h = 1.6mm; e_r = 3.1 and L4 = 17.56mm.

Figure 3.2 gives the measured real input impedance against frequency. At the second harmonic resonant frequency ($2f_{01}$) is not zero which makes it possible to generate the second harmonic radiation. The measured imaginary impedance of the proposed antenna is illustrated in Figure 3.3. It is evident that the real part of the input impedance at ($2f_{01}$) is down to zero, thus the increase in the second harmonic resonance is suppressed.

The measured return loss against frequency for the designed antenna is given in Figure 3.4 and compared with other antennas described in references. The proposed antenna with w = 5mm shown in the diagram is compared to other antennas. A strong excitation of the fundamental resonant mode is apparent and it is likely that excitation of high order modes (TM02 and TM21 modes) close to $2f_{01}$ are suppressed. The suppression of the third harmonic resonance caused by the addition of two or more stubs lengths to the inset microstrip line at appropriate locations is given in Figure 3.3.

The results show that the good suppression at the second and third harmonic frequencies can be achieved using a suitably designed square patch antenna fed by 50 Ω inset microstrip-line and by adding more stub lengths to the feeding point.

3.6 References

[1] F. R. Hsiao, T. W. Chiou and K. L. Wong, "Harmonic control of a square microstrip antenna operated at the 1.8 GHz band", Proceedings of APMC2001, Taipei, Taiwan, pp. 1052-1055, 2001.

[2] V. Radistic, Y Qian and T Itoh: Class F power amplifier integrated with circular sector micro strip antenna, 1997 IEEE MTT- SDig, PP 687 – 690

[3] V. Radistic, S T Chew, Y Qian and T Itoh: High efficiency power amplifier integrated with antenna IEEE Microwave Guided Wave Lett, vol 7, pp 39 – 41, February 1997.

[4] G R Buenel, M J Cryan and P S Hall, Harmonic control in active integrated patch oscillators, Electron Lett, vol 34,pp 228 – 229 February 1998.

[5] Y Horii and M Tsutsumi, Harmonic control by photonic bandgap on microstrip patch antenna, IEEE Microwave Guided Wave Lett, vol 9, pp13 – 15 January 1999.

[6] A. Kaya and S. Comlekci, "The design and performance analysis of integrated amplifier patch antenna", Microwave and optical technology letters, vol. 50, no. 10, pp. 2732-2736, October 2008.

[7] H. Kim and Y.J. Yoon, "Wideband design of the fully integrated transmitter front-end with high power-added efficiency", IEEE Transactions on microwave theory and techniques, vol. 55, no. 5, pp. 916-924, May 2007.

[8] A. Dupuy, K. Leong, T. Itoh, "Class-F Power Amplifier Using a Multi-Frequency Composite Right/Left-Handed Transmission Line Harmonic Tuner", Microwave Symposium Digest, 2005 IEEE MTT-S International, June 2005.

[9] W. Whittow, C. Panagamuwa, R. Edwards, J. Vardaxoglou and P. McEvoy, "A study of head worn jewellery, mobile phone RF energy and the effect of differing issue types on rates of absorption," 2006.

[10] E. Reusens, W. Joseph, G. Vermeeren and L. Martens, "On-body measurements and characterization of wireless communication channel for arm and torso of human," in *IFMBE PROCEEDINGS*, 2007, pp. 264.

[11] A. Fort, J. Ryckaert, C. Desset, P. De Doncker, P. Wambacq and L. Van Biesen, "Ultra-wideband channel model for communication around the human body," *IEEE J. Select. Areas Commun.*, vol. 24, pp. 927, 2006.

[12] H. Ghannoum, C. Roblin and X. Begaud, *Investigation of the UWB on- Body Propagation Channel*, 2005.

[13] A. Fort, C. Desset, J. Ryckaert, P. De Doncker, L. Van Biesen and P. Wambacq, "Characterization of the ultra wideband body area propagation channel," in *2005 IEEE International Conference on Ultra-Wideband, 2005. ICU 2005*, 2005, pp.6.

[14] A. Alomainy, Y. Hao, X. Hu, C. Parini and P. Hall, "UWB on-body radio propagation and system modelling for wireless body-centric networks," *IEE Proceedings-Communications*, vol. 153, pp. 107-114, 2006.

[15] Y. Koyanagi, H. Kawai, K. Ogawa and K. Ito, "Consideration of the local SAR and radiation characteristics of a helical antenna using a cylindroids whole body phantom at 150 MHz," *Electronics and Communications in Japan (Part I: Communications)*, vol. 87, 2004.

[16] N. C. Karmakar and M. N. Mollah, "Investigations into non-uniform photonic-bandgap microstripline low-pass filters," *IEEE Trans. Microwave Theory Tech.*, vol. 51, no 2, pp. 564–572, Feb. 2003.

CHAPTER FOUR

4 Harmonics Measurement on Active Patch Antenna Using Sensor Patches

4.1 Introduction

More recently, the active integrated antenna (AIA) has been an attractive area of research, due to its compact size, low weight, low cost, and multiple functionalities. In all cases, the antenna is fully (or closely) integrated with the active device to form a subsystem on the same board and can offer particular circuit functions such as duplexing, resonating, filtering as well as radiating, that describes its original role. AIAs are classified into three types: amplifying-type, oscillating-type and frequency-conversion-type, according to how the active device acts in the antenna [1-12].

In general, radiated power by the active integrated antenna at the targeted design frequency and its harmonics can be measured using Friis transmission equation in the anechoic chamber [13]. In addition, a simple measurement technique for measuring the power accepted by the active patch antenna, using a sensing patch feeding the network or spectrum analyzer, was first proposed in [14]. The technique eliminates many uncertainties and errors, such as cable losses, effects of the pattern, effects of nearby

scatterers, and gain estimation errors, and even makes it unnecessary to operate in the far field. This technique was originally developed for the measurement of amplifying-type active patch antennas at their fundamental design frequency. It was subsequently applied to measurements on oscillating-type antennas [15].

This work introduces the possibility of using this technique to find the power accepted by the antenna at harmonic frequencies. Performance of the sensing patch technique for measuring the power accepted at the antenna feed port of active patch antennas at harmonic frequencies is evaluated using an electromagnetic (EM) simulator Ansoft Designer [16] in terms of the current distribution. A prototype antenna, including two sensors at appropriate locations around the patch, is fabricated and tested at three designated frequencies to estimate the accepted power by the antenna, including determination of the sensor calibration factor. It is shown, based on experimental results, that the original technique can also be employed to measure the second harmonic power; measurement of the third harmonic power is also possible if another sensing patch is added in an appropriate position.

4.2 Antenna Design Geometry

An inset microstrip-fed patch antenna, resonating at 2.44 GHz, was chosen for the test, since this type of antenna is convenient for the design of active oscillator antennas. The important dimensions of this antenna are illustrated in Figure 4.1.

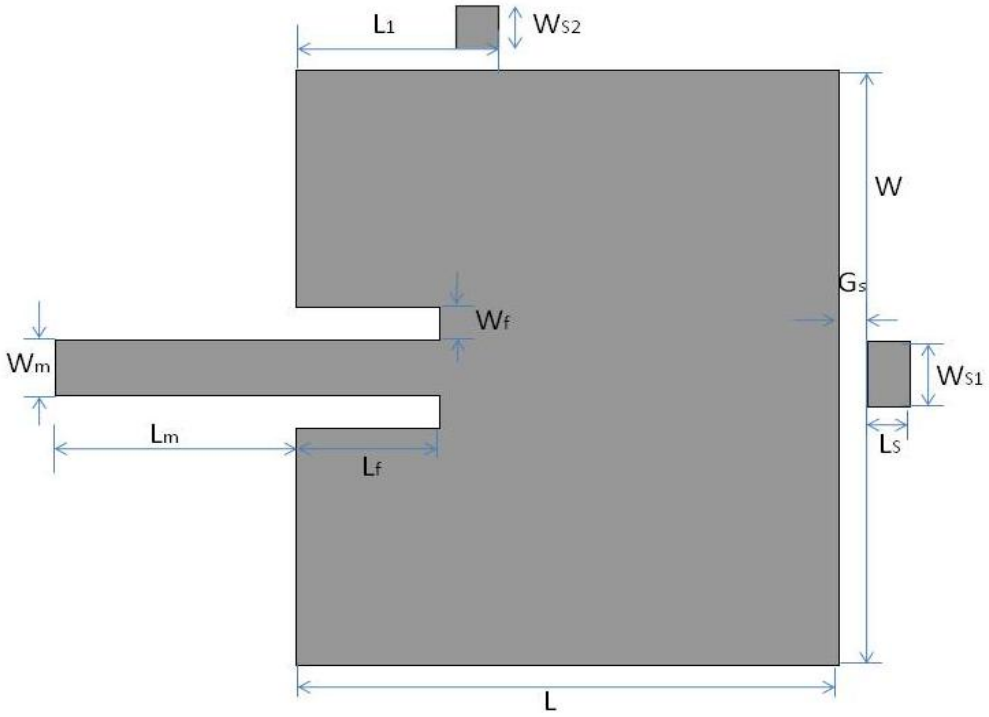

Figure 4:1:Important dimensions of the patch antenna studied (W=38.15, L=45.96, L_1=18.32, W_m=4.24, L_m=17, W_f=2.54, L_f=10.02, G_s=2, W_{s1}=5, W_{s2}=3 and L_s=3; all dimensions are in millimetres).

The performance of the sensing patch method at the fundamental, 2nd and 3rd harmonic frequencies was evaluated with this antenna. The current distribution on the patch at harmonic frequencies was first studied to find the proper position for the sensing patch. Figure 4.2, Figure 4.3 and Figure 4.4 show the corresponding harmonic current distributions on the patch.

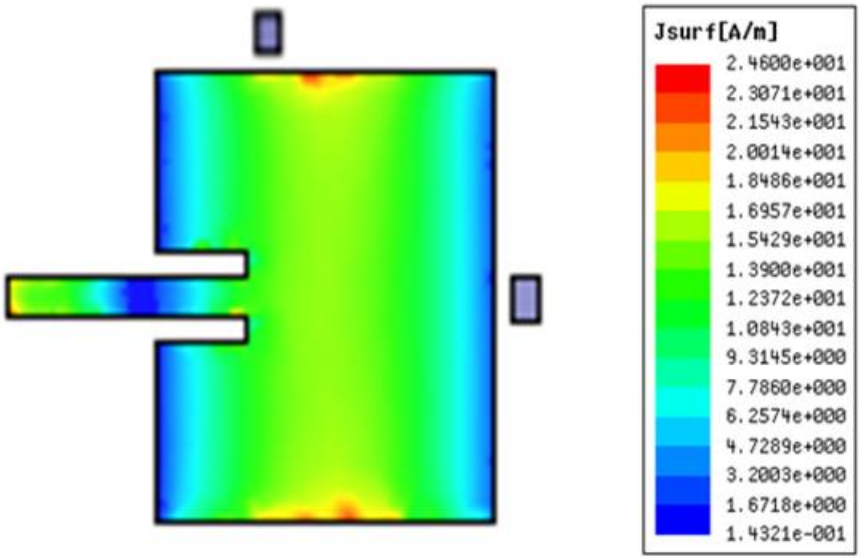

Figure 4:2: Current distribution on the patch antenna at fundamental frequency

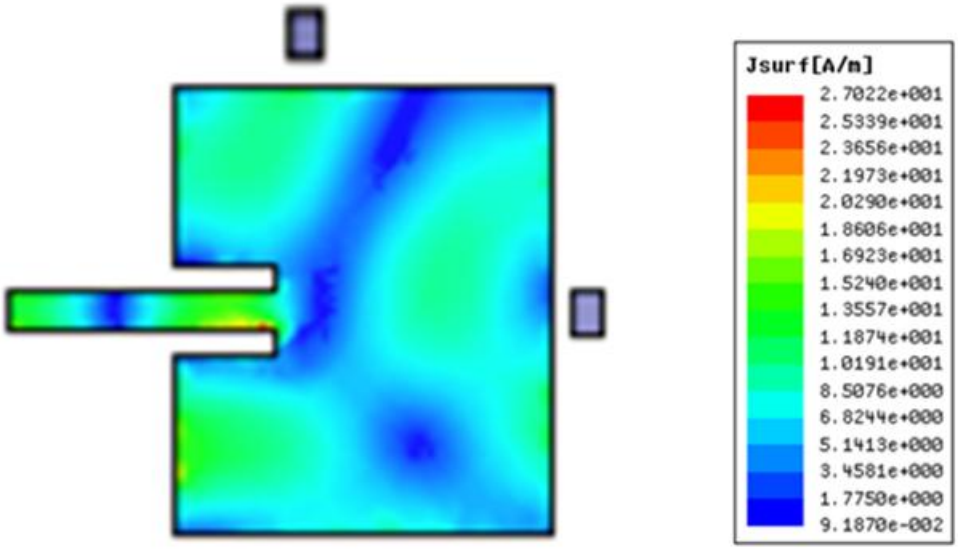

Figure 4:3: Current distribution on the patch antenna at 2nd harmonic frequency.

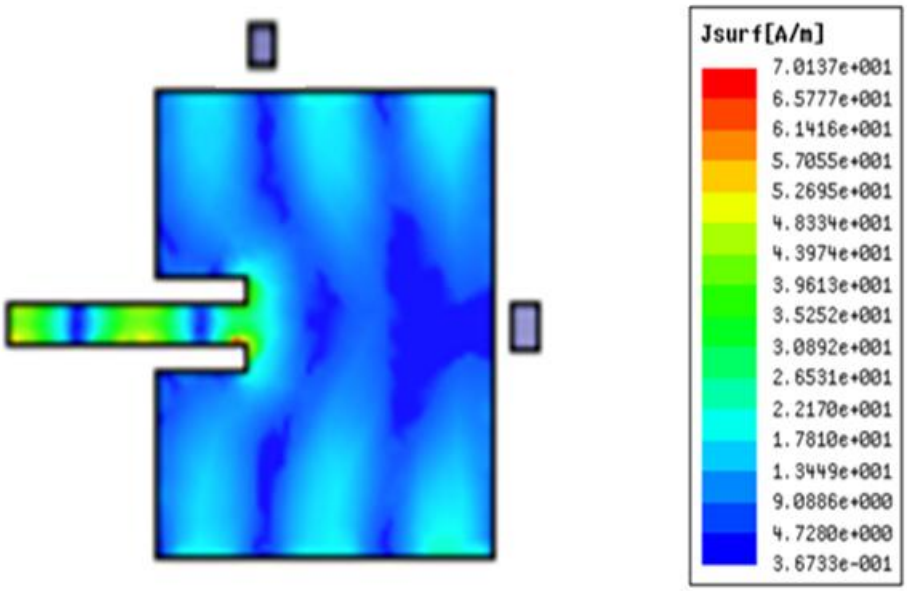

Figure 4:4: Current distribution on the patch antenna at 3rd harmonic frequency.

The position of the sensing patch is optimally set adjacent to a point of maximum voltage, which corresponds to a point of minimum current distribution on the patch. Thus, the position of the sensing patch can be set next to the middle of the end edge of the patch for the 2nd harmonic and one-third of the way along one side of the patch for the 3rd harmonic. It was found that the presence of the sensing patch has very little effect (about ±0.2 dB) on the return loss at the input port of the main patch at the fundamental operating frequency and the first two harmonics as shown in Figure 4.4.

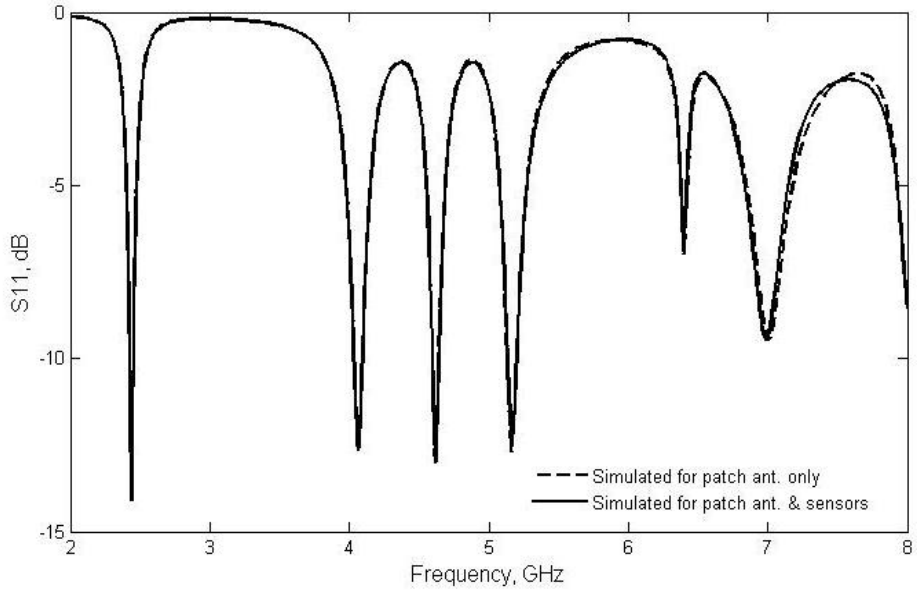

Figure 4:5: Simulated antennas return loss with and without the sensor patch.

The antenna with two sensing patches was mounted on 1.524 mm thick Duroid substrate material with relative permittivity of 2.55 and loss tangent of 0.0018. The sizes of the sensing patches used for the 2nd and 3rd harmonic frequencies were 3 mm x 5 mm and 3 mm x 3 mm, respectively. A spacing distance of 2 mm between the sensing patches and the antenna patch (see Figure 4.5) was found acceptable for sufficient coupling and had no noticeable effect on the antenna input return loss. It has to be noted that the sensing patch at the 2nd harmonic has the same location as at the fundamental. The sensing patch was linked to ground via a 50 Ω chip resistor. The inclusion of the 50 Ω resistor creates a relatively well-matched source for the attached cable. A 50 Ω coaxial probe was mounted at the rear of the circuit board and connected to the resistor load: this fed the sensor output to a traceably-calibrated network analyzer.

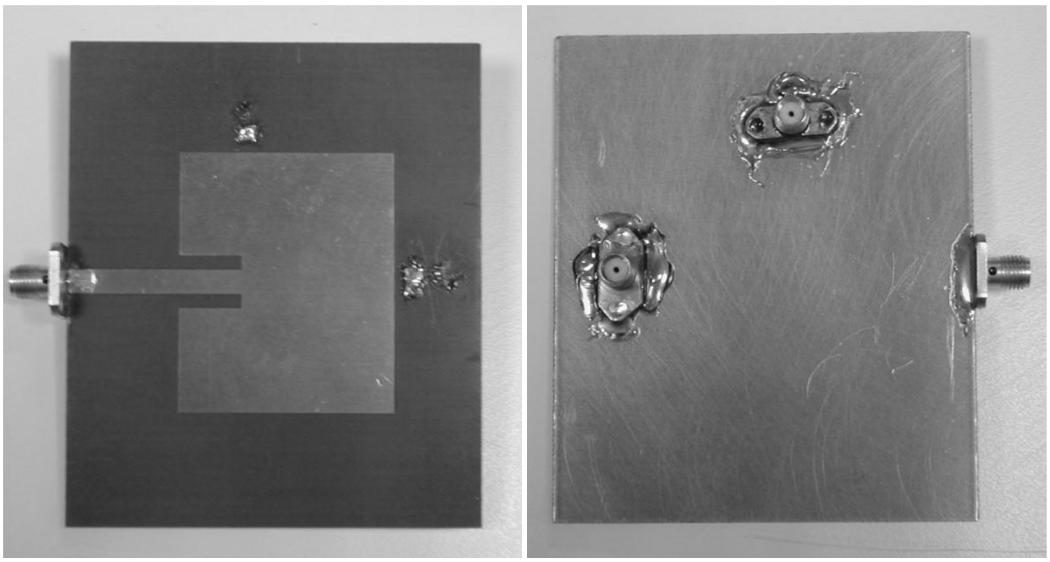

Figure 4:6: Fabricated antenna showing sensor locations: (left) Top view, (right) Underside.

The sensing patch for the 2nd harmonic was first tested. According to the work presented in [14], the performance of the sensing patch for harmonics can be evaluated using the calibration factor $|S_{21}'|$, which relates the sensor's output power to the power accepted by the radiator from RF circuitry (e.g. a RF power amplifier or oscillator), as follows:

$$\left|S_{21}'\right|^2 = |S_{21}|^2 \Big/ \left(1 - \left|S_{11}{}^2\right|\right) \tag{1}$$

where $[S] = \begin{bmatrix} S_{11} & S_{12} \\ S_{21} & S_{22} \end{bmatrix}$

The scattering parameters [*S*] in Eqn. 1 were obtained by measuring two-port S-parameters between the antenna input feed line and the sensor's output from 2 GHz to 8 GHz using a traceably-calibrated network analyzer (HP 8510C). The variations of the

measured [S]'s extended over the fundamental frequency and the first two harmonics are presented in Figure 4.6; the corresponding calibration factor from the measured antenna data was computed using Eqn. (1). The measured return loss and computed calibration factors are presented in Table 1 at 2.44, 4.88, and 7.32 GHz, respectively.

In order to evaluate the sensor's calibration factor for harmonics, a 0 dBm RF signal was injected into the main patch from a sweep oscillator HP 8350B at the fundamental and harmonic frequencies. The measurement setup is illustrated in (Figure 4.6, Figure 4.7 and Figure 4.8). The Return Loss (R.L.) of the antenna tested was optimised at its fundamental frequency into an impedance of 50 Ω, as shown in Table 4.1.

Table 4.1: 2nd harmonic sensor measurement results for the fundamental and harmonics.

Freq (GHz)	S_{11} (dB)	$\|S_{21}'\|^2$ (dB)	L_{cable} (dB)	$P_{reading}$ (dBm)	$P_{accepted}$ (dBm)	$P_{accepted}'$ (dBm)
2.44	-24.86	-23.20	1.33	-25.33	-0.0144	-0.8
4.88	-1.75	-20.42	2.67	-28.5	-4.796	-5.412
7.32	-4.241	-23.45	4	-27	-2.052	0.45

4.3 Measured two-port S-parameters

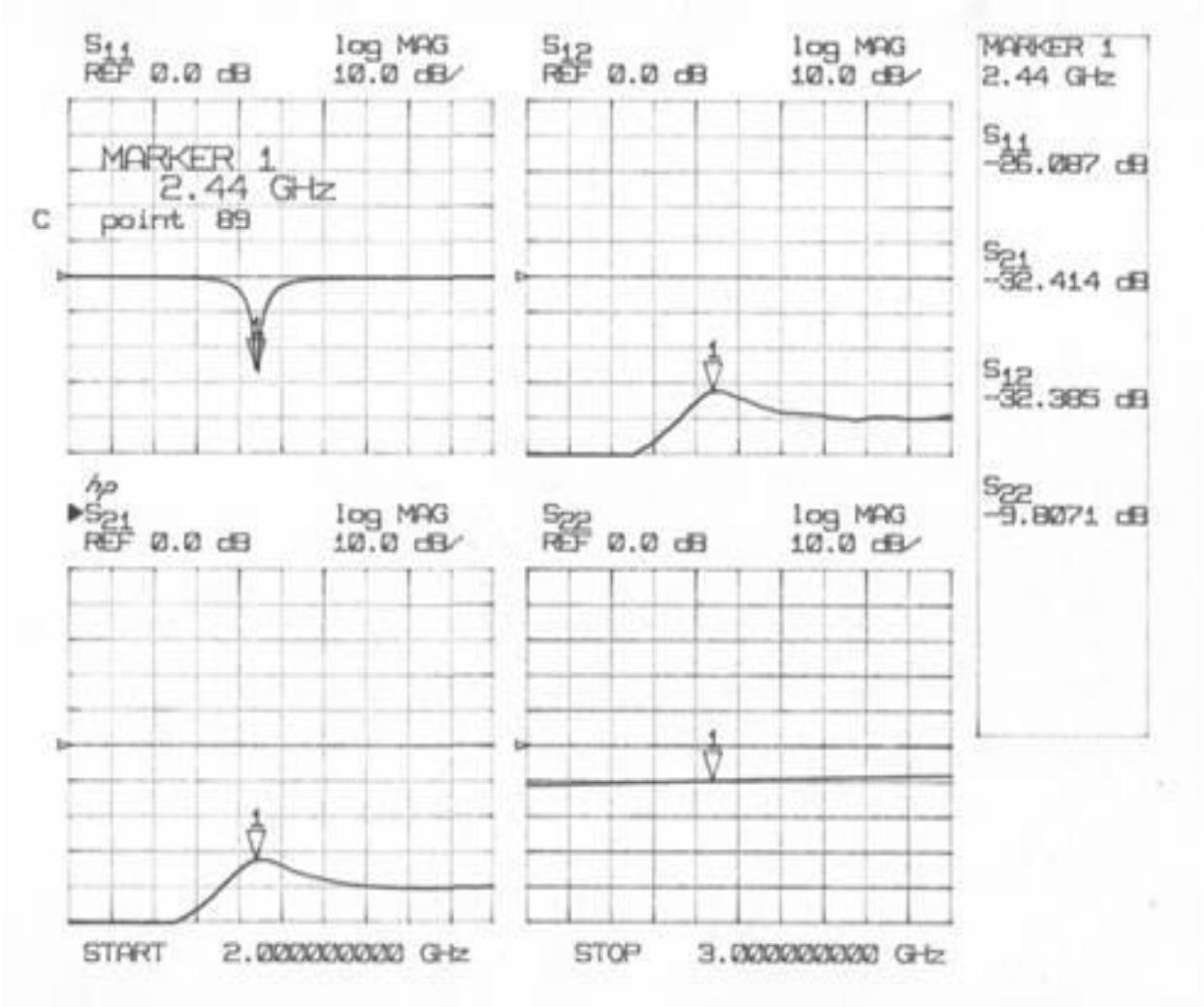

Figure 4:7: Measured two-port S-parameters between the antenna input port and the sensor's output port at fundamental frequency.

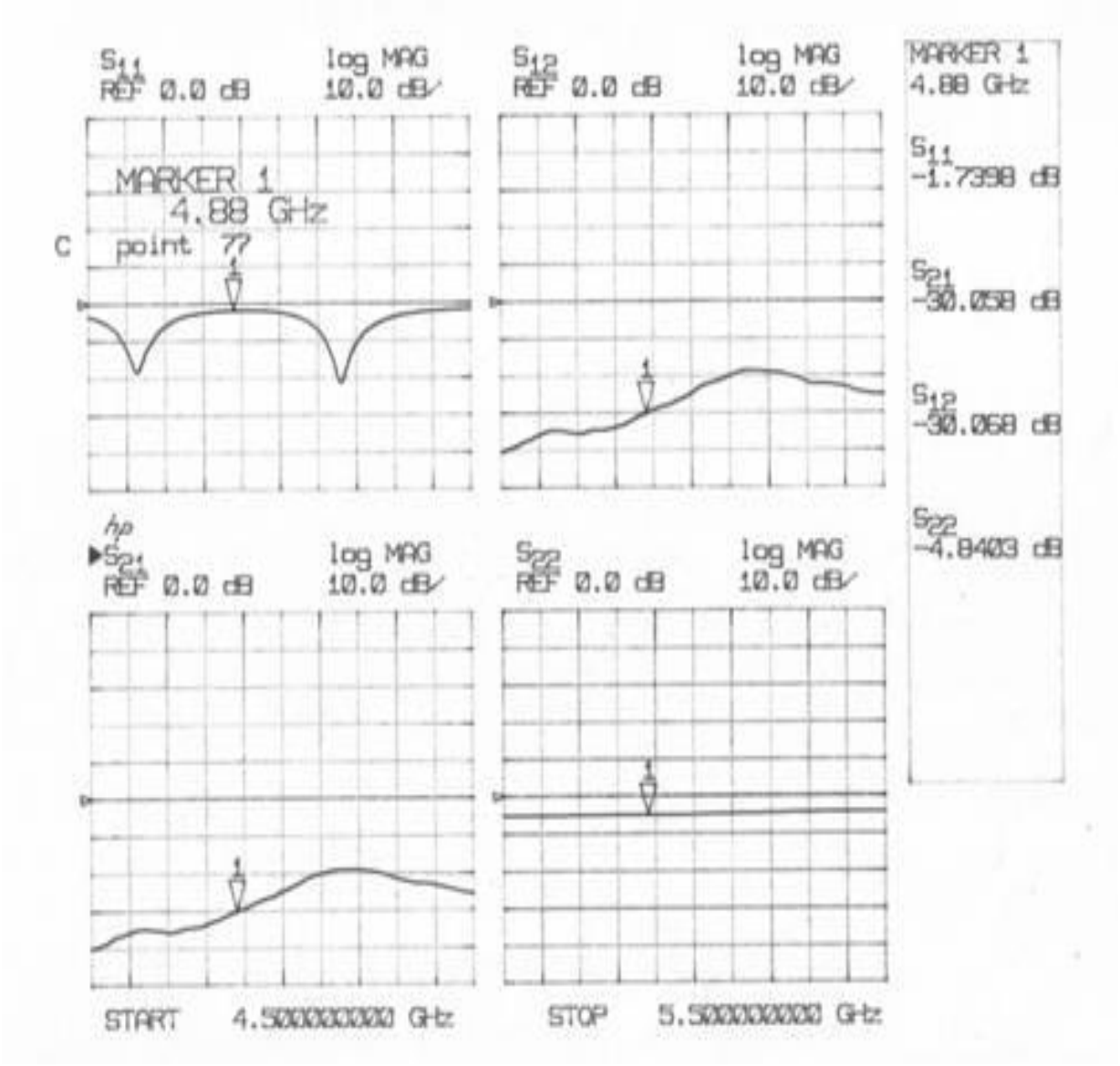

Figure 4:8: Measured two-port S-parameters between the antenna input port and the sensor's output port at the 2nd harmonic frequency.

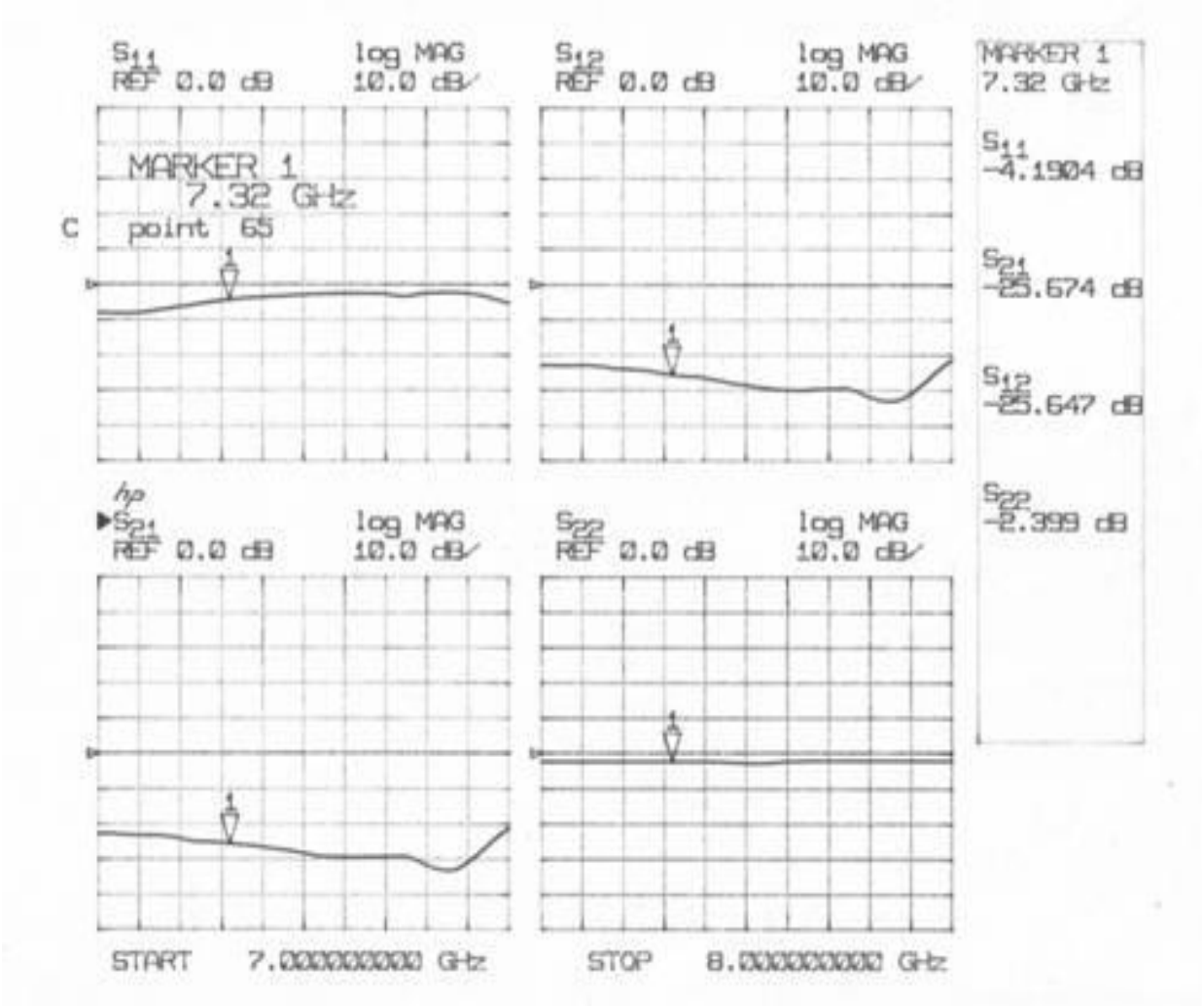

Figure 4:9: Measured two-port S-parameters between the antenna input port and the sensor's output port at the 3rd harmonic frequency.

However, at harmonic frequencies, the input impedance of the antenna was greatly different from 50 Ω. Thus, the power accepted by the antenna ($P_{accepted}$) is given by:

$$P_{accepted} = P_{incident}\left(1 - |\Gamma|^2\right) \tag{2}$$

where Γ is the reflection coefficient at the input of the antenna and $|\Gamma|^2 = P_{reflected}/P_{incident}$. $P_{reflected}$ is the power reflected at the antenna input, and $P_{incident}$ is the power outgoing from the signal generator (in this case, $P_{incident}$ = 0 dBm at all frequencies). The power from the sensor's output ($P_{reading}$) was observed using a spectrum analyzer (HP 8563A). Care was taken to find the loss in the cable (L_{cable}) before measuring the output power from the sensor. The estimated power accepted by the antenna ($P_{accepted}'$) can be found as:

$$P_{accepted}' = P_{reading} - \left|S_{21}'\right|^2 - L_{cable} \tag{3}$$

A summary of measured parameters for the 2nd harmonic sensor is presented in Table 4.1. The technique shows that the power accepted by the antenna at the fundamental and 2nd harmonic frequencies can be achieved using the same sensing patch. It can be seen from Table 4.1 that the accuracy of this technique is around 0.7 dB (i.e., the maximum difference between the $P_{accepted}$ and $P_{accepted}'$ at the fundamental and 2nd harmonic). It should be noted that the power accepted at the 3rd harmonic frequency varies greatly in the measurement and this is because the sensor at this position is weakly coupled to the maximum voltage of the 3rd harmonic.

Similarly, for the 3rd harmonic sensor, the same process was used as with the 2nd harmonic sensor. A summary of measured parameters for the 3rd harmonic sensor is presented in Table 4.2

Table 4.2: 3rd harmonic sensor measurement results for the fundamental and harmonics.

Freq (GHz)	S_{11} (dB)	$\|S_{21}'\|^2$ (dB)	L_{cable} (dB)	$P_{reading}$ (dBm)	$P_{accepted}$ (dBm)	$P_{accepted}'$ (dBm)
2.44	-26.09	-32.403	1.33	-33	-0.0109	0.733
4.88	-1.74	-25.25	2.6	-33	-4.814	-5.155
7.32	-4.19	-23.59	4	-30.67	-2.084	-3.08

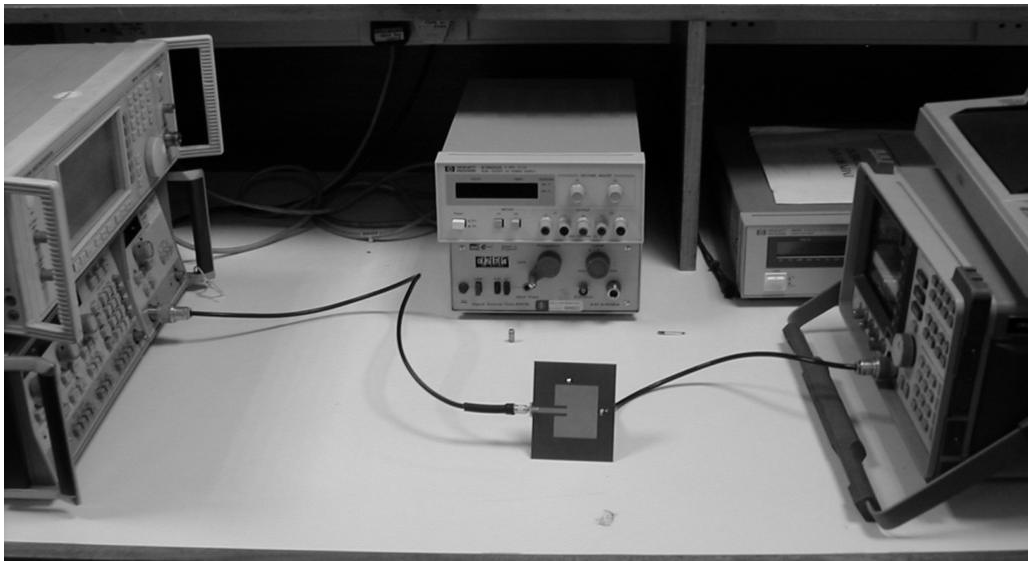

Figure 4:10: Photograph of measurement setup in this study.

It is shown that the technique is still valid within 1dB accuracy for 3rd harmonic power measurement. In addition, this sensor can also be applied for the 2nd harmonic power measurement, with very good accuracy. This is because the current distribution at the 2nd harmonic frequency near to the location of the 3rd harmonic sensor is close to minimum, and this can be easily seen from Figure 4.5. It is notable that the power accepted at the fundamental frequency varies greatly in the measurements. In addition, care should be taken on means of improving the port impedance matching at the sensor patch port in order to eliminate measurement errors and improve measurement accuracy at fundamental and harmonic levels using this proposed technique. This challenging problem including the antenna operation over a wide frequency band is left to future work.

4.4 Conclusions

The measurement of the power accepted by a microstrip patch antenna, using the sensing patch measurement technique, has been demonstrated at both fundamental and first two harmonic frequencies. The results of the present work are shown to be acceptable and agreed with direct measurements. The proposed technique is shown to achieve good accuracy of 0.7 dB and 1 dB for the 2nd and 3rd harmonic measurements respectively.

4.5 References

[1] A. Kaya and S. Comlekci, "The design and performance analysis of integrated amplifier patch antenna", Microwave and optical technology letters, vol. 50, no. 10, pp. 2732-2736, October 2008.

[2] H. Kim and Y.J. Yoon, "Wideband design of the fully integrated transmitter front-end with high power-added efficiency", IEEE Transactions on microwave theory and techniques, vol. 55, no. 5, pp. 916-924, May 2007.

[3] G.-J. Chou and C.-K. C. Tzuang, "Oscillator-type active-integrated antenna: the leaky-mode approach", IEEE Transactions on microwave theory and techniques, vol. 44, no. 12, pp. 2265-2272, December 1996.

[4] S. Yang, Q.-Z. Liu, J. Yuan, and S.-G. Zhou, "Fast and optimal design of a k-band transmit-receive active antenna array", Progress In Electromagnetics Research B, Vol. 9, 281-299, 2008.

[5] A. Dupuy, K. Leong, T. Itoh, "Class-F Power Amplifier Using a Multi-Frequency Composite Right/Left-Handed Transmission Line Harmonic Tuner", Microwave Symposium Digest, 2005 IEEE MTT-S International, June 2005.

[6] V. Radistic, Y Qian and T Itoh: Class F power amplifier integrated with circular sector micro strip antenna, 1997 IEEE MTT- SDig, PP 687 – 690

[7] V. Radistic, S T Chew, Y Qian and T Itoh: High efficiency power amplifier integrated with antenna IEEE Microwave Guided Wave Lett, vol 7, pp 39-41, February 1997.

[8] G R Buenel, M J Cryan and P S Hall, Harmonic control in active integrated patch oscillators, Electron Lett, vol 34,pp 228 – 229 February 1998.

[9] Shun-Yun Lin, Kuang-Chih Huang, and Jin-Sen Chen, Harmonic control for an integrated microstrip antenna with loaded transmission line, Microwave and optical technology letters, vol. 44, No. 4, pp 379-383, February 2005.

[10] D. Zayniyev, D. Budimir, An integrated antenna-filter with harmonic rejection, 3rd European conference on antennas and propagation, 2009, pp. 393-394.

[11] K. Chang, R.A. York, P.S. Hall, and T. Itoh, "Active Integrated Antennas", *IEEE Trans. Microwave Microwave Theory Tech.*, vol. MTT-50, pp. 937-944, March 2002.

[12] Sohiful Zaniol Murad and Widad Ismail, Design of Active Integrated Antenna for Dual Frequency Image Rejection, American Journal of Applied Sciences (3), pp. 1890-1894, 2006.

[13] C.A. Balanis, "Antenna Theory: analysis and design", Third edition, John Wiley & Sons Inc., pp. 94-96, 2005.

[14] E.A. Elkhazmi, N.J. McEwan, and N.T. Ali, "A Power and Efficiency Measurement Technique for Active Patch Antennas", IEEE Trans. Microwave Theory and Techniques, Vol. 48, No. 5, pp. 868-870, May 2000.

[15] R.A. Abd-Alhameed, P.S. Excell, and E. Elkhazmi, 'Design of Integrated-Oscillator Active Microstrip Antenna for 2.45GHz', XXVIIth General Assembly of URSI, Maastricht, Paper No. 1181, August 2002.

[16] Ansoft Designer, Version 1.0, Ansoft Corporation, USA.

CHAPTER FIVE

5 Genetic Algorithm And Adaptive Meshing Program

5.1 Introduction

Active transmitting antennas often suffer from significant non-linearity; the driving transistor drain (or collector) produces time-harmonic currents which feed directly into the radiator, resulting in unwanted radiated power [1]. In active antenna design these unwanted harmonic currents can be terminated (or substantially eliminated) using the radiator itself, in which case the active circuit does not require any additional complexity for harmonic tuning, thus contributing to the desired compactness of the design.

Harmonic suppression antennas (HSAs) are used to suppress power radiation at harmonic frequencies from active integrated antennas. An antenna that presents a good impedance matching at the fundamental design frequency (f_o) and maximised reflection at harmonic frequencies is said to be a harmonic suppression antenna. In addition, the input impedance of any HSA design has to have minimised resistance at the harmonic frequencies and hence will be largely reactive [2]. Several techniques have been

proposed to control such harmonics, such as shorting pins, slots or photonic bandgap structures [3, 4]. In [5], the modified rectangular patch antenna with a series of shorting pins added to the patch centre line was applied to shape the radiated second harmonic from the active amplifying-type antenna, in order to increase the transmitter efficiency. Unfortunately, the proposed design does not give the termination for the third harmonic. A circular sector patch antenna with 120° cut out was investigated and proved to provide additional harmonic termination for the third harmonic, also claiming a further enhancement in the transmitter efficiency [2]. Further, an H-shaped patch antenna was designed and applied in oscillator-type active integrated antennas for the purpose of eliminating the unwanted harmonic radiation [6, 7].

Generally, most of the published designs for modified patch HSA have been based on a specific reference antenna, suggesting that the proposed techniques for rejecting harmonic radiation have specific constraints imposed onto them. For example, in [8] a microstrip-line fed slot antenna was developed for harmonic suppression without using a reference antenna. This was achieved with a rather complex geometry for 5 GHz operation. This process does not usefully generalise, so that if a new operating frequency is required, then the whole structure must be redesigned. Thus there exists a clear motivation to develop a coherent design strategy for microstrip HSA in active integrated applications. In this design we adopt a computational technique using adaptive surface meshing driven by a genetic algorithm.

5.2 Genetic Algorithm and Adaptive Meshing Program

Genetic algorithms (GA) are stochastic search procedures modelled on natural genetics, selection and evolution. They are adapted from Darwinian concepts of natural evolution, thus making them plausibly thorough in seeking an optimal design [9]. After its first introduction in the 1960s by J. Holland, GA has become an efficient tool for search, optimisation and machine learning; however in the pre–GA era, similar concepts had been looming and applied in game playing and pattern recognition [10]. Over the recent years, it has proven to be a promising technique for different optimisations, designs and control applications.

An approach to the use of GA in collaboration with an electromagnetic simulator has been presented for antenna designs and has become ever more accepted more recently [11]. For example, GA has been used to design wire antennas [12, 13] and microstrip antennas [14]. Other uses have also been developed such as wideband antenna designs based on the fundamental requirement for near field imaging tools such as are needed for microwave breast cancer detection: this was reported using GA as the main optimisation tool [15]. Another application applied to beam-control of an antenna array was also derived through the use of a genetic algorithm, based on adjusting the required reactance values to obtain the optimum solution [16]. In addition, GA can enhance antenna designs for multiple input multiple output (MIMO) systems, which dramatically increase channel capacity in wireless communication systems [17-20]. The GA-

optimised MIMO antenna designs provide substantial size reduction, reduced power consumption [19] and cost minimisation [18] in such systems.

The advantage of using GA methods is that they give high-speed, high accuracy and reliable solutions for the antenna structures. A genetic algorithm driver [21], which was written in Fortran, was employed in this work in combination with the authors' Fortran source code [22]. Several antenna designs, derived using GA in previous work by the authors [23-25], have shown GA method to be an efficient optimiser tool that can be used to search and find rapid solutions for complex antenna geometries.

An adaptive meshing program was also written in Fortran by the present author and added as a subroutine to the GA driver, with the main purpose of simulating air-dielectric planar microstrip patch antenna designs: this used a surface patch model in cooperation with a GA. The program is also able to support the design of any 3D antenna geometry structure, including moderate amounts of dielectric materials. The present work is an extended version of preliminary work reported in [26].

An antenna under GA optimisation needs to be defined by a number of parameters that can define its configuration. For the electromagnetic surface patch model used, the antenna geometry is divided into optimum numbers of trilateral and quadrilateral polygons, each polygon node being specified by its x, y and z co-ordinates, subject to the defined antenna parameters. These polygonal surfaces are then optimally subdivided into a set of rectangular and triangular surface patches, constrained to be

small compared with the operating wavelength, and then an appropriate basis functions are adaptively generated over these patches using a designated algorithm as shown in Figure 5.1 and the following subsection.

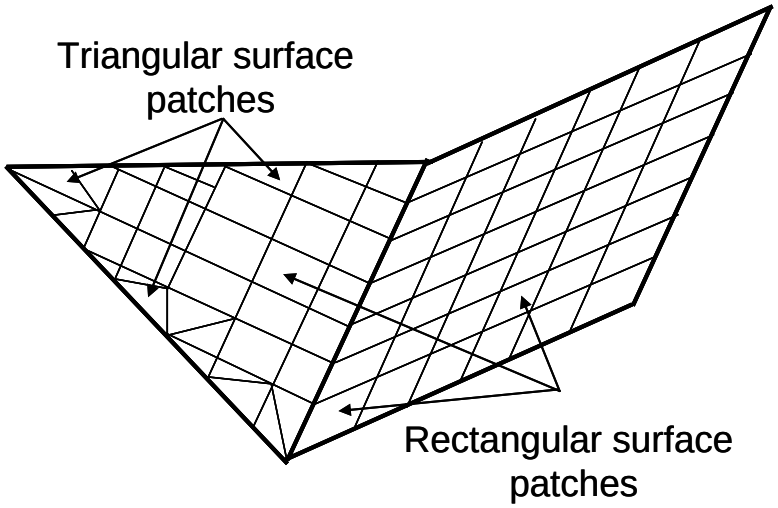

Figure 5:1: The adaptive surface patch meshing used for antenna modelling.

5.2.1 The GA Driver

Review procedure was attempted and was observed that various versions of Genetic Algorithms drivers are available for optimisation process such as the ones implemented in C, MATLAB and FORTRAN 77. From review and experience on home programmes (From Antenna and Advanced Electromagnetics Research Group University of Bradford) , FORTRAN 77 seemed more friendly and easier to manipulate for the present research work. The FORTRAN 77 version of the GA driver, written by David L. Carroll of the CU Aerospace USA [21], uses the randomized approach to initialize its start individuals and the tournament selection with shuffling techniques in choosing

random pairs for mating. Binary coding also enabled the uniform and non-uniform process of single point crossovers.

The GA driver can be controlled and adjusted through an associated input data file as shown in the Fig. 5.2. This figure illustrates a set of parameters, these include: GA driver elements and the variables that need to be optimised and used through the electromagnetics computational codes. The functions of samples of these parameters have been highlighted in the data file of Figure 6.3. These variables are the most important and influential to the GA driver in the antenna design and should be adaptively adjusted according to the various design types or objectives, in order to maximize the GA driver performance in searching for optimum solutions of antenna designs.

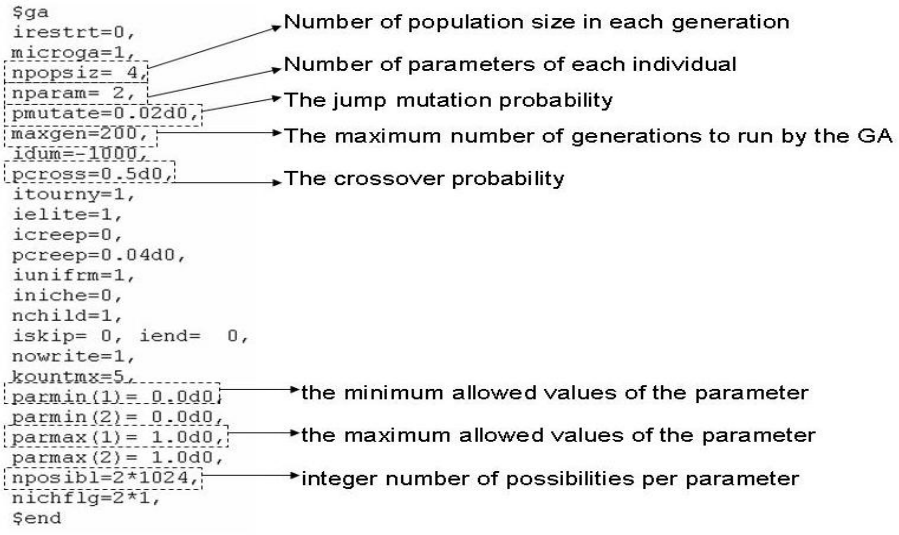

Figure 5:2: A sample of GA driver input file

5.2.2 Implementation of antenna designs using GA driver

The FORTRAN source code in [22] was adopted inside the GA fitness function to perform the required calculations for the cost functions. The source code was modified to accept the input data file generated by the GA code within the fitness calling function. These modifications are found very helpful to reduce the execution processing time and manipulate the output data files between the sources codes.

It should be noted that before the optimisation process is initiated, the target objectives and number of parameters required for the whole process to achieve the optimum desired goal were estimated. These include the most important antenna parameters that are directly measured by the fitness function. Sometimes a relationship was required to define a threshold for the GA which enables it to evaluate the designed antenna performance and terminate where necessary. Usually, this is a complex procedure to be applied; however, one can apply a certain constraints inside the cost function to support the data processing when nearly reaching the optimal design requirements. The cost function is usually included in the algorithm and it measures the fitness of the individuals produced in each generation of the algorithm.

A flow chart to represent the easiest way in which the GA optimizer coordinates its functions is represented in Fig. 5.3. The algorithm randomly initiates its population and converts the parameters of the initiated individuals to the electromagnetic code to developed the meshing process and execute the MOM to compute the induced currents and radiation performances and return back the targeted variables to the cost function.

The process will continue till the maximum value of the fitness function is obtained for convergence, otherwise the whole process is repeated until optimal results are produced.

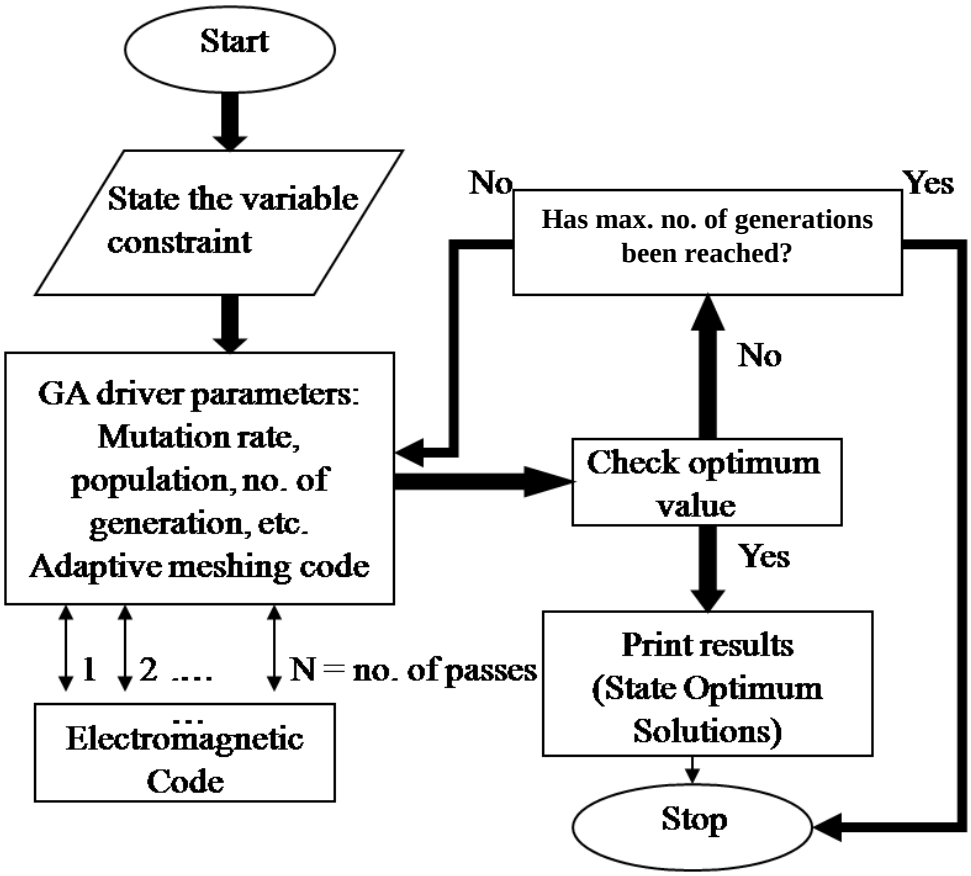

Figure 5:3: Flow chart of the genetic algorithm adopted in this study.

5.2.3 Method of Moment Formulation

In The approach for MOM it is assumed that the surface current is allowed to have components both parallel to, and transverse to the surface patch segments. This leads to an equation of the form:

$$\sum_j I_j . L(\mathbf{J}_j) = (\mathbf{E}_i) \tag{5.1}$$

where I_j is a basis function for the surface current $\mathbf{J}_j$, $\mathbf{E}_i$ is the incident electric field strength and L is the integro-differential operator given by:

$$L(\mathbf{J}) = (j\omega\mathbf{A} + \nabla\phi)_{\tan} \tag{5.2}$$

where A and ϕ are the vector and scalar potentials. If a set of testing functions $\mathbf{W}_m$ is defined, equation (5.1) may be rewritten as:

$$\sum_j I_j \left\langle \mathbf{W}_m, L(\mathbf{J}_j) \right\rangle = \left\langle \mathbf{W}_m, \mathbf{E}_i \right\rangle \qquad for \quad j = 1,2,..N \tag{5.3}$$

where

$$\left\langle \mathbf{W}_m, L(\mathbf{J}_j) \right\rangle = \iint_s \iint_{s'} (\mathbf{W}_m . L(\mathbf{J}_j)) ds' ds = Z_{mj} \tag{5.4}$$

$$\left\langle \mathbf{W}_m, \mathbf{E}_i \right\rangle = \iint_{s'} (\mathbf{W}_m . \mathbf{E}_i) ds = V_m \tag{5.5}$$

where ds' and ds are the differential areas on the patch surface for the source and the observation points respectively, m = 1, 2, ...N is the index of the testing function and Z and V are the conventional abbreviations for the interaction matrix and excitation vector terms in the Method of Moments. The impedance matrix elements Z_{mj} can be written using the closed surface integral identity [27] as follows:

$$Z_{mj} = j\omega\mu \iint_s \iint_{s'} \left(\mathbf{J}_j . \mathbf{W}_m - \frac{1}{k^2} (\nabla . \mathbf{J}_j)(\nabla . \mathbf{W}_m) \right) g(R) ds' ds \tag{5.6}$$

where $g(R)$ is the free-space Green function [28-29] and is given by the expression:

$$g(R) = \frac{e^{-jkR}}{4\pi R} \tag{5.7}$$

R is the distance between the observation and source points on the patch surface. Singular integral occurs when $R = 0$ (i.e., $g(R) \rightarrow \infty$).

Any arbitrary surface shape can be modelled by a number of surface patches to represent a discretised version of a complex current distribution. The currents were represented by overlapping surface dipoles, where the current basis functions are generally continuous and may have continuous derivatives. The Electric Field Integral Equation was applied to evaluate the current distribution. For the problem shown in Fig. 5.1, the rectangular and triangular patches were used as discretising elements of the geometry. The self and mutual impedances of these surface dipoles were obtained from:

$$Z_{rr} = j\omega\mu \iint_{s'} \iint_{s} (\hat{a}_{p'}.\hat{a}_p f(p') f(p') - \tfrac{1}{k^2} f'(p') f'(p)) \, G(R) ds ds' \tag{5.8}$$

$$Z_{tt} = j\omega\mu \iint_{s'} \iint_{s} (\pm \mathbf{f}(u').\mathbf{f}(u) \pm \tfrac{1}{k^2} \nabla.\mathbf{f}(u') \nabla.\mathbf{f}'(u)) \, G(R) ds ds' \tag{5.9}$$

$$Z_{rt} = j\omega\mu \iint_{s'} \iint_{s} (\pm \hat{a}_p.\mathbf{f}(u') f(p) \pm \tfrac{1}{k^2} \nabla.\mathbf{f}(u') f'(p)) \, G(R) ds ds' \tag{5.10}$$

where Z_{rr} and Z_{tt} are the self-impedances of the current basis functions on rectangular and triangular patches respectively. $Z_{rt} = Z_{tr}$ is the mutual impedances between the current basis functions on the triangular patches. *f(p)* is the current basis function for the rectangular patch, whereas the $\boldsymbol{f}$(u) is the vector basis function of the triangular basis

function. $f'(u)$ and $f'(p)$ are the derivatives of $f(u)$ and $f(p)$ respectively. $\hat{\phi}_p$ is the unit vector that specify the current basis function direction for the rectangular patch. $k = 2\pi/\lambda$ is the propagation constant, and λ is the operating wavelength. $G(R)$ is the free space Green function. Similarly, the source code also includes the self and mutual impedances over wire segments and attachment patch modes that are not shown here. It should also be noted that weighting functions are a copy of the basis functions.

5.3 Conclusions

The description of the numerical method employing the genetic algorithm and the electromagnetics codes has been presented. Set of the most appropriate parameters included in the GA and incorporated with the electromagnetics solver was demonstrated. A computational technique using adaptive surface meshing driven by GA has been written in Fortran and has been examined in the next chapter which can support the design of 3D antenna geometry structures such as the design of coaxially-fed, air-dielectric, microstrip, harmonic-rejecting patch antennas for 2.4 GHz was investigated, enforcing suppression of the first two harmonic frequencies.

5.4 References

[1] E. Elkhazmi, N.J. McEwan and J. Moustafa, “Control of harmonic radiation from an active microstrip patch anrtenna”, Journees Internationale de Nice sur les Antennes, pp. 313-316, November 1996.

[2] V. Radisic, Y. Qian, and T. Itoh, “Class F power amplifier integrated with circular sector microstrip antenna,” IEEE MTT-S Symposium Digest, pp. 687-690, 1997.

[3] H. Kim, K.S. Hwang, K. Chang and Y.J. Yoon, “Novel slot antennas for harmonic suppression”, IEEE Antennas and Wireless Components Letters, Vol. 14, No. 6, pp. 286-288, 2004.

[4] Y.J. Sung and Y.-S. Kim, “An improved design of microstrip patch antennas using photonic bandgap structure”, IEEE Transactions on Antennas and Propagation, Vol 53, No. 5, pp. 1799-1804, 2005.

[5] V. Radisic, S.T. Chew, Y. Qian, and Tatsuo Itoh, “High efficiency power amplifier integrated with antenna”, IEEE Microwaves and Guided Wave Letters, Vol. 7, No. 2, pp. 39-41, February 1997.

[6] A.F. Sheta, “A novel H-shaped patch antenna”, Microwave and Optical Technology Letters, Vol. 29, No. 1, pp. 62-66, April 2001.

[7] Q.-X. Chu and M. Hou, “An H-shaped harmonic suppression active integrated antenna”, International Journal of RF and Microwave Computer-aided Engineering, Vol. 16, No. 3, pp. 245-249, May 2006.

[8] H. Kim and Y.J. Yoon, “Microstrip-fed slot antennas with suppressed harmonics”, IEEE Transactions on Antennas and Propagation, vol. 53, no. 9, pp. 2809-2817, September 2005.

[9] D.A. Coley, “An introduction to Genetic Algorithms for Scientists and Engineers”, World Scientific, Singapore, 1999.

[10] H.H. Ammar and Y. Tao, “Fingerprint registration using Genetic Algorithms”, IEEE Symposium on Application Specific Systems and Software Engineering Technology, pp. 148-154, March 2000.

[11] Y. Rahmat–Samii and E. Michielssen, “Electromagnetic optimisation by Genetic Algorithms”, John Wiley & Sons, Canada, 1999.

[12] E.E. Altshuler and D.S. Linden, “Wire-antenna designs using genetic algorithms”, IEEE Antennas Propag, Mag. Vol. 39, pp. 33-43, 1997.

[13] E.A. Jones and W.T. Joines, “Design of Yagi-Uda Antennas Using Genetic Algorithms”, IEEE Transactions on Antennas and Propagation, Vol. 45, No. 9, 1386-1392, 1997.

[14] W.-C. Liu, “Design of a CPW-fed notched planar monopole antenna for multiband operations using a genetic algorithm”, IEE Proc. - Microwaves Antennas and Propagation, Vol. 152, No 4, 273-277, 2005.

[15] S.W.J. Chung, R.A. Abd-Alhameed, P.S. Excell. C.H. See, D. Zhou and J.G. Gardiner, “Resistively Loaded Wire Bow-tie Antenna for Microwave Imaging By Means of Genetic Algorithms”, International Multi-Conference on Engineering and Technological Innovation Proceedings, Orlando, Florida, USA, 2008, Pp 303-306.

[16] M.M. Abusitta, R.A. Abd-Alhameed, D. Zhou, C.H. See, SMR Jones and P.S. Excell, “New Approach for Designing Beam Steering Uniform Antenna Arrays using Genetic Algorithms”, Loughborough Antennas and Propagation Conf., 2009, Loughborough, UK, pp. 617-620.

[17] P.D. Karamalis, N.D. Skentos, and A.G. Kanatas, “Selecting array configurations for MIMO systems: an evolutionary computation approach”, IEEE Trans. on Wireless Communications, Vol. 3, No. 6, pp. 1994-1998, 2004.

[18] P.D. Karamalis, N.D. Skentos, and A.G. Kanatas, “Adaptive Antenna Subarray Formation for MIMO Systems”, IEEE Trans on Wireless Communications, Vol. 5, No. 11, pp. 2977-2982, 2006.

[19] M.A. Mangoud, R.A. Abd-Alhameed and P.S. Excell, “Optimisation of Channel Capacity for Indoor MIMO Systems Using Genetic Algorithm”, Proceedings of the Third International Conference on Internet Technologies and Applications (ITA 09), 2009, Glyndwr University, Wrexham, Wales, UK, pp. 431-439.

[20] P.D. Karamalis, A.G. Kanatas and P. Constantinou, “A Genetic Algorithm Applied for Optimisation of Antenna Arrays Used in Mobile Radio Channel Characterization Devices”, IEEE Trans on Intrumentation and Measurements, Vol. 58, No. 8, pp. 2475-2487, 2009.

[21] D.L. Carroll, FORTRAN Genetic Algorithm Driver, Version 1.7a, Download from: http://www.cuaerospace.com/carroll/ga.html, 4/2/2001.

[22] R.A. Abd-Alhameed, P.S. Excell and J. Vaul, “Currents Induced on wired I.T. Networks by Randomly distributed phones – A Computational study”, IEEE Trans on Electromagnetic Compatibility, Vol. 48, No. 2, pp. 282-286, May 2006.

[23] C.H. See, R.A. Abd-Alhameed, D. Zhou, P.S. Excell and Y.F. Hu, “A new design of circularly-polarised conical-beam microstrip patch antennas using a genetic algorithm”, Proceedings of the European Conference on Antennas and Propagation: EuCAP 2006, Session 4PA1, Paper no.100, Nice, France, 2006.

[24] D. Zhou, R.A. Abd-Alhameed and P.S. Excell, “Bandwidth enhancement of balanced folded loop antenna design for mobile handsets using genetic algorithms”, PIERS Online, Vol. 4, No. 1, pp.136-139, 2008.

[25] D. Zhou, R.A. Abd-Alhameed, C.H. See, P.S. Excell, F.Y. Hu, K. Khalil and N.J. McEwan, “Quadrifilar helical antenna design for satellite-mobile handsets using genetic algorithms”, Microwave and Optical Technology Letters, Vol. 51, No. 11, pp. 2668-2671, November 2009.

[26] D. Zhou, R.A. Abd-Alhameed, C.H. See, M.S. Bin-Melha, E.T.I. Elferganai and P.S. Excell, “New antenna designs for wideband harmonic suppression using adaptive meshing and genetic algorithms”, In proceeding of Mosharaka International Conference on Communications, Propagation and Electronics (ISBN: 978-9957-486-06-8), Amman, Jordan, 5-7 March 2010, Technical Session 1, pp. 5-9.

[27] W. L. Stutzman and G. A. Thiele, *Antenna theory and design*, 2nd ed. New York: John Wiley & Sons, 1998.

[28] K. Sawaya, "Antenna design by using method of moments," *IEICE Transaction Communication*, vol. E88-B, pp. 1766-1773, 2005

[29] R. E. Collin, *Field theory of guided waves*, 2nd ed. New York: The Institute of Electrical and Electronics Engineers Inc., 1995

CHAPTER SIX

6 Harmonic Suppression Antennas Using Genetic Algorithm

6.1 Introduction

This chapter examines the design of microstrip patch antenna for harmonic suppression with the aid of a generic algorithm. Active antennas generally have considerable non-linearity and are compact in their specification. For this reason, the transistor drain would be generating harmonic current in to the radiator and would invariably be radiating undesirable power. In active antenna design, these undesirable harmonic elements could be removed with the aid of the radiating element. To achieve this, the circuit can be designed in a compact form without additional circuitry for harmonic tuning.

To increase the effectiveness of the harmonic suppression the rectangular patch antenna shape was modified with a series of shorting pins added to the patch centre line, included to shape the radiated second harmonic from the active amplifying-type antenna. Since the intended antenna does not provide the termination harmonic, a circular sector patch antenna with 120 degrees cut out was analysed and it provided

additional harmonic termination for the third harmonic. To overcome, the unwanted harmonic radiation, an oscillator type integrated antenna was included.

The micro strip patch antenna acts as a radiator and also provides circuit functionality by matching circuit and band pass filter. However, if the harmonic radiation is not suppressed it could cause unwanted electromagnetic interference (EMI) in the system. To address this limitation, shorting pins, slots photonic band gap structures or matching stubs can be used on the antenna feeding line.

A microstrip line fed slot antenna was developed for harmonic suppression without using reference antenna and this resulted in complex geometry for 5 GHz operation. However, if the frequency is altered in a way, then the complete antenna structure needed to be modified.

Good matching impedance at the fundamental design frequency (fo) with an ideal maximum first two harmonic (2fo and 3fo) is considered to be a harmonic suppression antenna (HSA). However, the response of the HSA, bearing in mind the antenna return loss (S11), is that of a band pass filter having an ideal rejection outside the concerned frequency bands. In certain HSA specifications the antennas may have resonances at frequencies beyond the intended frequency (fo, 2fo and 3fo) but are still considered as antennas for harmonic suppression.

An additional constraint in the HSA regards the input impedance. This has to be reactive at the harmonic frequencies, since the HSA was initially intended for harmonic termination to get class F operation for the amplifying category antenna.

The primary criteria of antenna for harmonic suppression is return loss and input impedance. In this study, a sample of designs are examined and presented and are all designed to operate at 2.4 GHz.

6.2 Microstrip Patch Antenna with Fully Shorted Wall

The design of harmonic suppression antenna with a shorted wall can be seen in Figure 6.1. This gives an overview of the proposed antenna sub-divided into four trilaterals and two quadrilaterals. It has six parameters to be assigned in Figure 6.1 and Figure 6.2 illustrates the 3D of the adaptive wire grid segmentation results.

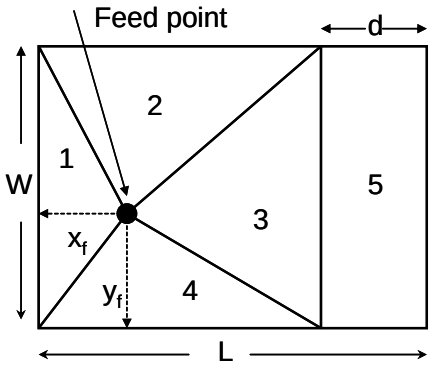

Figure 6:1: **Top elevation view of antenna geometry used for adaptive meshing using GA.**

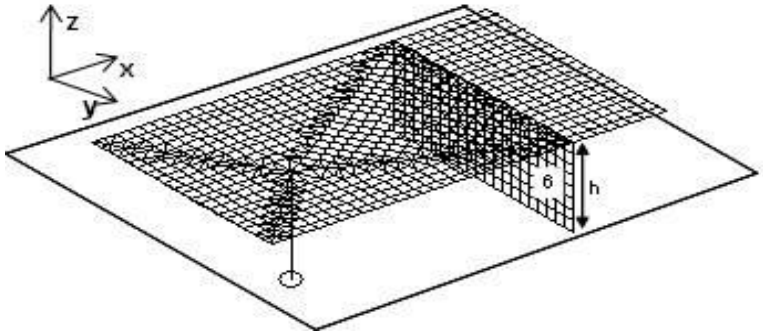

Figure 6:2: **Top elevation view of resulted wire mesh used for Figure 6.1.**

Table 6.1 shows the GA input parameters with likely values for the GA chromosomes for the optimisation, that were applied. In this chapter, first, second and also fundamental frequencies were considered for the GA cost function. The randomly generated antenna configurations were calculated for maximum fitness using the cost function below:

$$F = \left[1 + w_1 \left| \frac{Z(f_o) - 50}{50} \right| + \sum_{i=2}^{n} w_i \left\{ \left| \Gamma(if_\circ) - 1 \right| + \frac{R(if_o)}{50} \right\} \right]^{-1} \qquad (1)$$

Where F represents the fitness of the cost function, n = 3, w_1, w_2 and w_3 are the weight coefficients of the cost function and they are optimally found to be 0.6, 0.4 and 0.4; the geometry configuration of the optimal antenna was within the maximum generation and is given in Figure 6.1.

The computation time taken for each of the randomly generated antenna samples ranged from 60-70 seconds using various length, width and height of the patch antenna selected of the given antenna configuration.

Table 6.1: Summary of GA input parameters, antenna variables and optimum solutions.

GA parameters	Harmonic suppression antenna parameters	Fully shorted
	Parameters (m)	Optimal (m)
	Antenna length (L) (0.03-0.06)	0.03950
No. of population size = 4,	Antenna width (W) (0.02-0.06)	0.03305
No. of parameters: 6 (Figure 1 (a1)), 7 (Figure 1 (a2)), 8 (Figure 1 (a3)),	Shorting or folded wall position (d) (0.002-0.03)	0.00972
Probability of mutation =0.02,	Antenna height (h) (0.003-0.01)	0.0079
Maximum generation =500,	Feeding point at x-axis (X_f) (0.004-0.02)	0.00723
No. of possibilities=32768,	Feeding point at y-axis (Y_f) (0.004-0.02)	0.01752
	Variable shorting wall width (Ws) (0.001-0.03)	-
	Extend folded wall length (L_f) (0.005-0.015)	-
	Extend folded wall height (h_f) (0.001-0.0035)	-

A prototype GA optimised harmonic suppression antenna with a shorted wall is presented in Figure 6.1. A copper sheet with thickness of 0.5mm is used for the antenna patch, shorting wall and the ground plane with measurement 140mm x 140mm. The return loss was validated and the rejection of 2nd and 3rd harmonics was satisfactory. The prototype antenna resonates at 2.47GHz and has a bandwidth of 500MHz, with reflection coefficient of 1.71dB and 2.47dB for the first and second harmonics. The observed resonance frequency agreed with the predicted value.

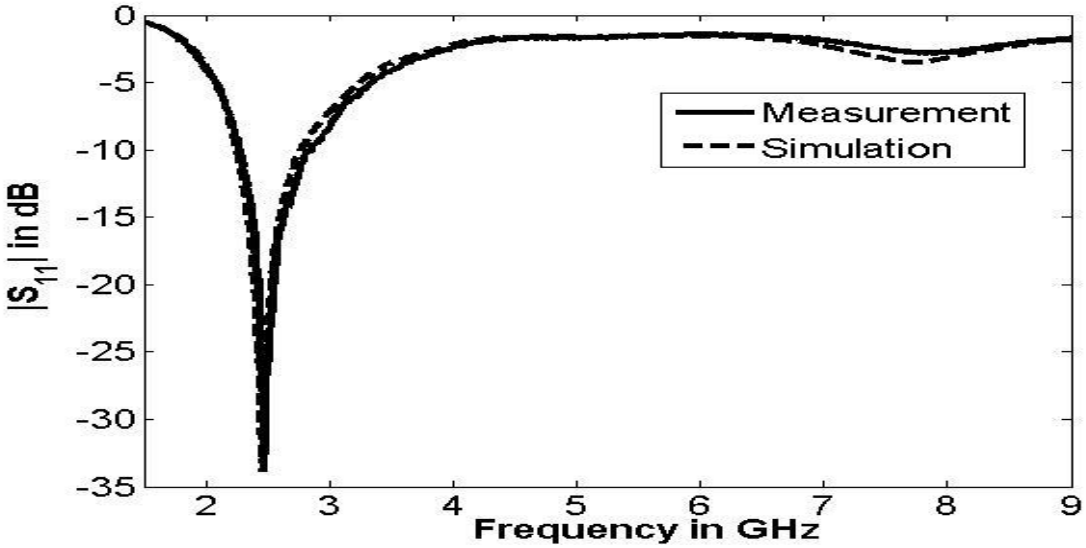

Figure 6:3: The measured and simulated return loss of the patch antenna with fully shorted wall.

Furthermore, the input impedance of the proposed antenna was equally measured over a wide frequency band and is given in Figure 6.4. An additional input impedance plot is also presented, in Figure 6.5, showing a constant input impedance of under 10 Ω at harmonic frequency bands.

The measured input impedance of the harmonic rejection antenna with shorted wall for fundamental frequency and with its first harmonic rejection antenna is illustrated in Table 6.2. It gave matching of 50 Ω at fundamental frequency and resistive impedance at harmonics was found thus agreeing with the objective of the design.

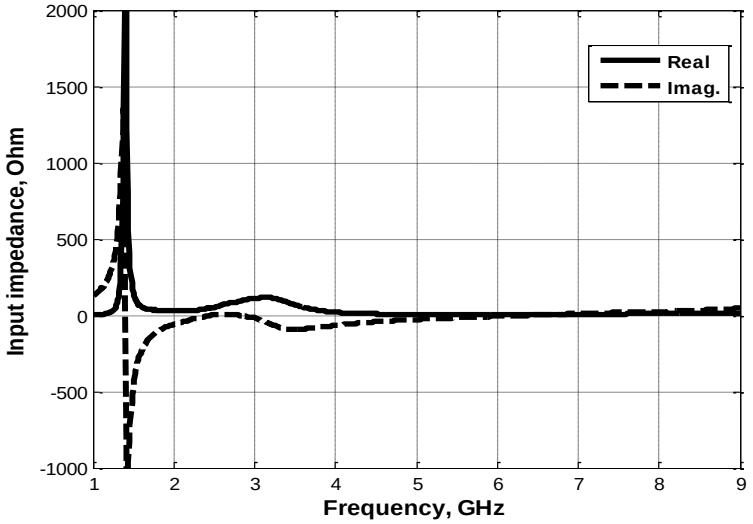

Figure 6:4: **The overall measured input impedance of patch antenna with fully shorted wall.**

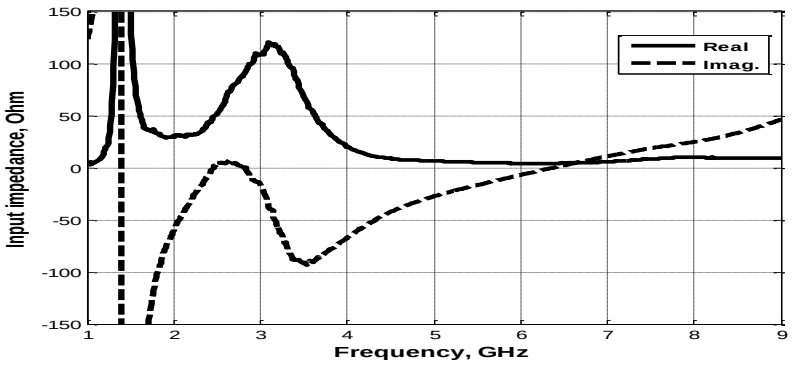

Figure 6:5: Measured input impedance of the harmonic suppression antenna for fully shorted wall.

Table 6.2 : **Performance of antenna input impedance of the harmonic rejection antenna with shortened wall at the fundamental and first and second harmonics.**

Full-width shorted wall		
Frequency (GHz)	Antenna input impedance (Ω)	
F	Real	Imaginary
f_o : 2.47	49.87	-0.587
$2f_o$: 4.94	6.283	-28.917
$3f_o$: 7.1	839	7.64

The measurements for the far field radiation patterns of the prototype were done in a far field anechoic chamber. The fixed antenna (broadband horn) had a spacing of 4m between the antenna and the horn. Two pattern cuts were taken for four selected operating frequencies that cover the complete bandwidth. The radiation patterns in *zx* plane and *zy* plane for the GA-optimised HSA with shortened wall at fundamental, second and third harmonic frequencies were measured. These results are given in Figure 6.6 showing 2nd and 3rd harmonic radiations of the HSA with shortened wall to be less than 13dB and 18dB for the *zx* plane and 10dB and 9dB for the *zy* plane subject to the normalised accepted power of the fundamental frequency. The measured maximum gain of the GA optimised antenna is give as 4.14dB.

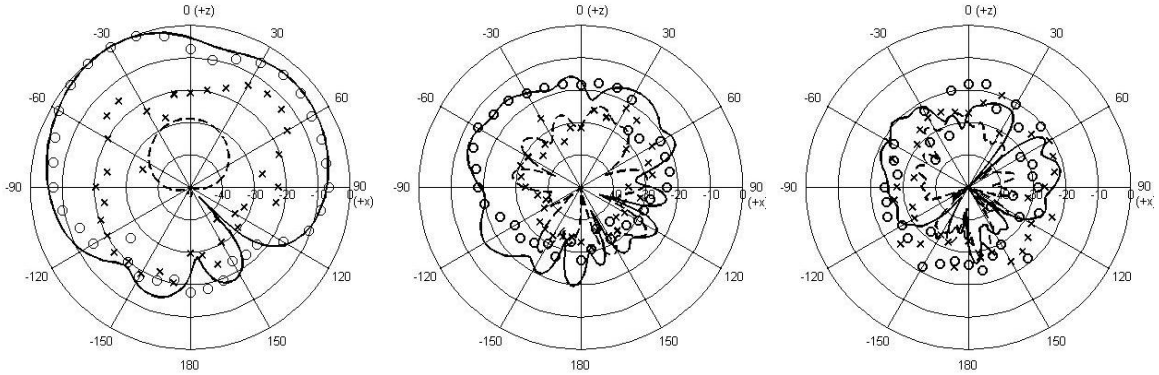

f_0=2.47 GHz f_1=4.94 GHz f_2=7.41GHz

(a)

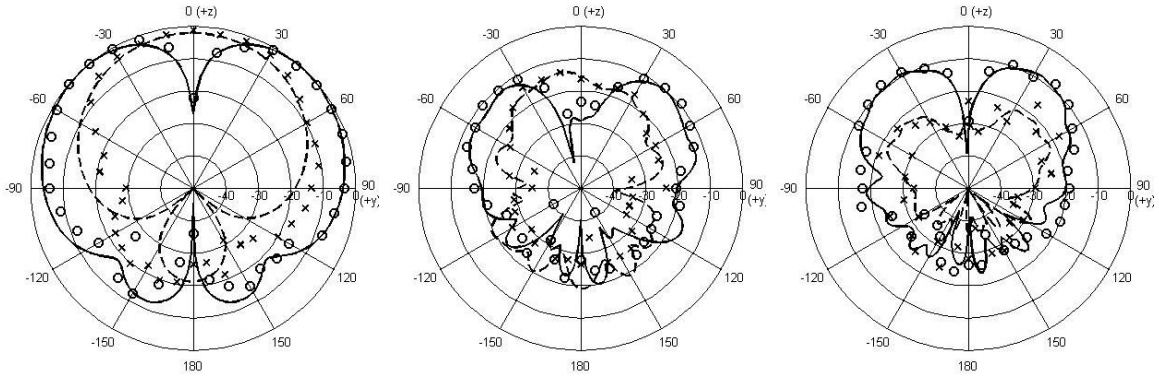

f_0=2.47 GHz f_1=4.94 GHz f_2=7.41GHz

(b)

Figure 6:6: Measured and simulated radiation patterns of the proposed GA-optimised HSA with full-width shorted wall for 2.47 GHz, 4.94 GHz and 7.41 GHz over: (top) z-x plane; (bottom) z-y plane; ('——'measured E_θ, ('o o o'simulated E_θ, '- - - -' measured E_ϕ, 'x x x' simulated E_ϕ).

6.3 Microstrip Patch Antenna with Partially Shorted Wall

After the design of harmonic suppression antenna with a partially shorted wall a new design can be made to control the harmonics with the variation of the width of the shorting wall. This design operates at 2.4GHz. The antenna geometry for this is shown in Figure 6.7.

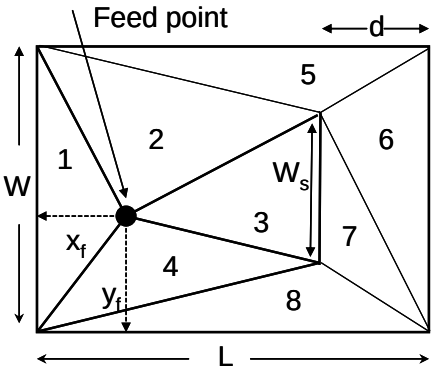

Figure 6:7: Top elevation view of antenna geometry used for adaptive meshing using GA.

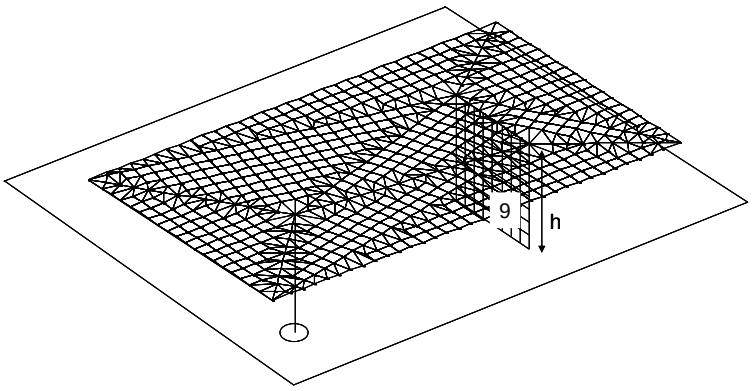

Figure 6:8: Top elevation view of resulted wire mesh used for Figure 6.7.

Table 6.3 presents the GA input parameters in which the possible range of values is shown for shorted wall. Similar optimisation process was applied as to the previous example except the optimal weight coefficients of the cost function were found to be 0.6, 0.4 and 0.4 after a few trials.

Table 6.3: Summary of GA input parameters; antenna variables and optimum solutions.

GA parameters	Harmonic suppression antenna parameters	Truncated shorted
	Parameters (m)	Optimal (m)
	Antenna length L) (0.03-0.06)	0.033 0
No. of population size =4,	Antenna width (W) (0.02-0.06)	0.03820
No. of parameters: 6 (Figure 1 (a1)), 7 (Figure 1 (a2)), 8 (Figure 1 (a3)),	Shorting or folded wall position (d) (0.002-0.03)	0.00986
Probability of mutation =0.02,	Antenna height (h) (0.003-0.01)	0.00336
Maximum generation =200,	Feeding point at x-axis	0.01685

	(X_f) (0.004-0.02)	
No. of possibilities=32768,	Feeding point at y-axis (Y_f) (0.004-0.02)	0.01923
	Variable shorting wall width (Ws) (0.001-0.03)	0.02474
	Extend folded wall length (L_f) (0.005-0.015)	-
	Extend folded wall height (h_f) (0.001-0.0035)	-

For validation, prototypes of the GA-optimised harmonic-suppression antennas (HSAs) of the three models shown in Fig. 6.7 were designed and tested. Copper sheet with thickness of 0.5 mm was used for the patch antenna, shorted/folded wall and the ground plane. The ground plane size was set to 140 mm x 140 mm, the relatively large size was chosen in order to attenuate the effect of the edges of the finite ground plane. The return losses were validated and measured results compared with calculations are shown in Figure 6.9. As can be seen, the results for rejection levels of 2^{nd} and 3^{rd} harmonics were quite encouraging and no other resonances or ripples were found over the harmonic frequency bands.

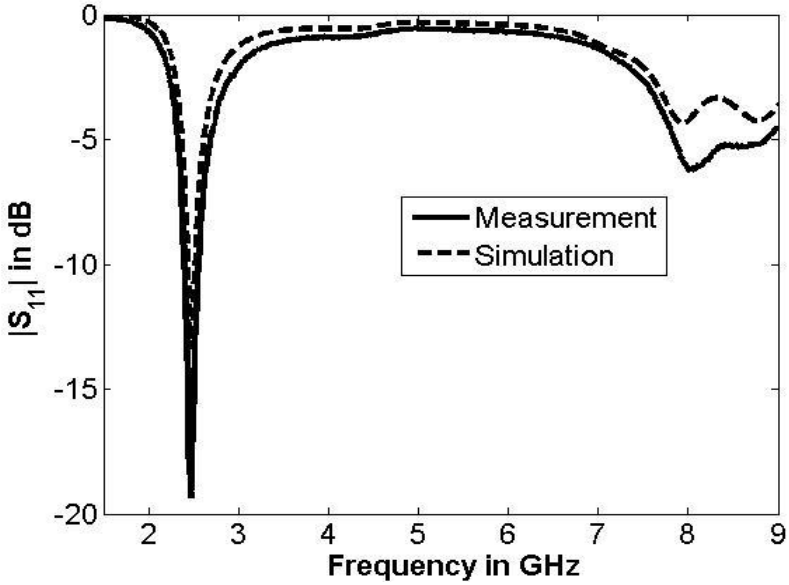

Figure 6:9: The measured and simulated return loss of the patch antenna with a partially shorted wall.

It was found that the full-width shorted-wall prototype antenna was resonant at 2.47 GHz and presents quite a wide bandwidth of around 500 MHz. The reflection coefficient level at the first and second harmonic frequencies was found to be 1.71 dB and 2.45 dB, respectively.

These results are quite acceptable, as compared with HSAs published in the open literature [27]. It is notable that the measured resonant frequency of the prototype antenna shows good agreement with the prediction. The second prototype antenna was resonant at 2.48 GHz and presented a narrower bandwidth (around 150 MHz), compared to the first design. This is mainly because the height of this antenna is much

lower (about 3.36 mm) than the first design (7.9 mm), correlating with previous experience that has shown that the antenna height has a most important influence on bandwidth enhancement of microstrip patch antennas. The third prototype exhibited approximately 380 MHz bandwidth, centred at a 2.45 GHz resonance frequency. The rejection levels of the 2nd and 3rd harmonics were about 1.5 dB and 1.9 dB respectively.

The input impedances of the prototype antennas were also measured over a wide frequency band as shown in Figure 6.10. The measured input impedance of these antennas at the fundamental operating frequency and its first two harmonics shows that almost perfect matching to 50 Ω was attained at the fundamental frequency, while fairly small resistive impedances at harmonic frequencies were observed, as illustrated in Table 6.4.

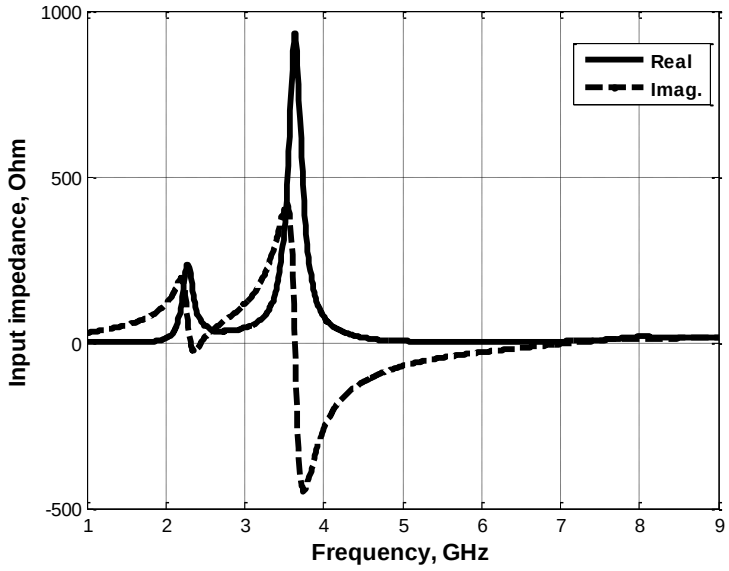

Figure 6:10: The overall measured input impedance of the patch antenna with a partially shorted wall.

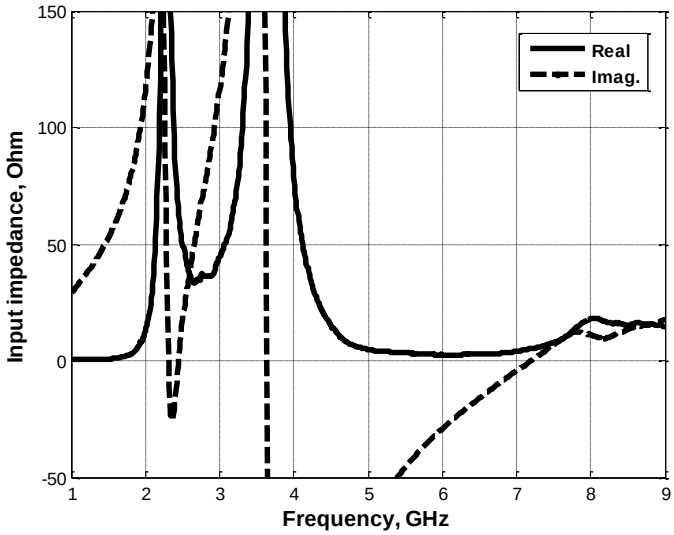

Figure 6:11: Measured input impedance of the harmonic suppression antenna with a partially shorted wall.

Table 6.4 : Performance of antenna input impedance of the harmonic rejection antenna with shortened wall at the fundamental and first and second harmonics.

Truncated shorted wall		
Frequency (GHz)	Antenna input impedance (Ω)	
	Real	Imaginary
f_o : 2 48	52.75	7.828
$2f_o$: 4.96	.254	-73.672
$3f_o$: 7.44	5.332	15.54

The radiation patterns in *zx* plane and *zy* plane for the GA-optimised HSA with partially shorted wall at fundamental, second and third harmonic frequencies were measured. These results are given in Figure 6.12 showing 2nd and 3rd harmonic radiations of the HSA with shortened wall to be less than 13dB and 18dB for the *zx* plane and 10dB and 9dB for the *zy* plane subject to the normalised accepted power of the fundamental frequency. The measured maximum gain of the GA optimised antenna is 4.14dB.

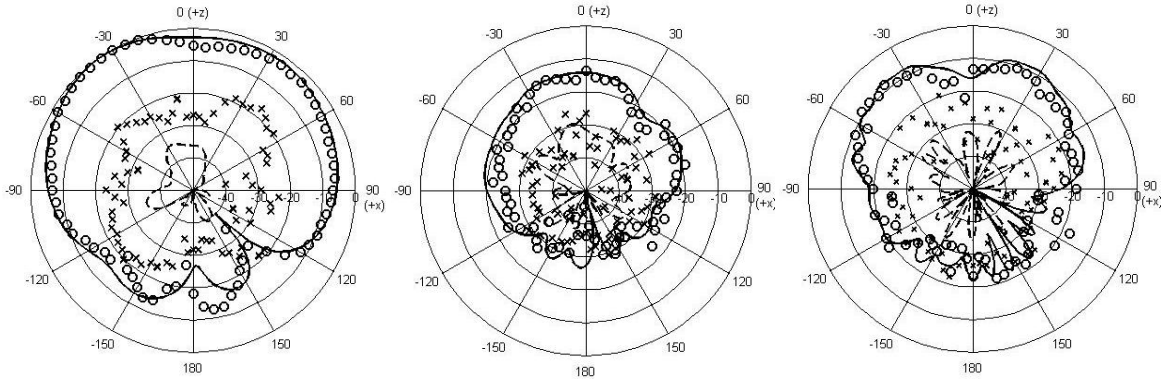

f_0=2.48 GHz f_1=4.96 GHz f_2=7.44GHz

(a)

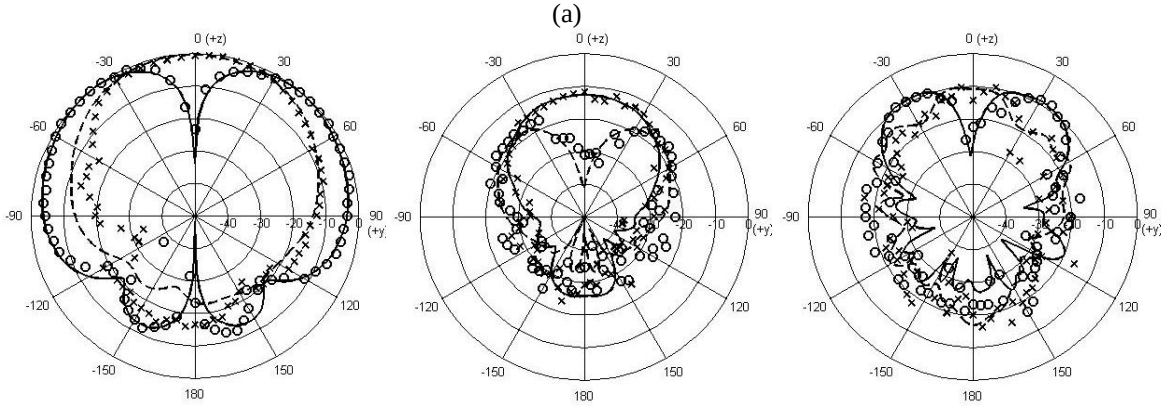

f_0=2.48 GHz f_1=4.96 GHz f_2=7.44GHz

(b)

Figure 6:12: Measured and simulated radiation patterns of the proposed GA-optimised HSA with a truncated shorted wall for 2.48 GHz, 4.96 GHz and 7.44 GHz over: (top) z-x plane; (bottom) z-y plane; ('——'measured E_θ, ('o o o'simulated E_θ, '- - - -' measured E_ϕ, 'x x x' simulated E_ϕ).

6.4 Microstrip Patch Antenna with Folded Patch

Here a new design for patch antenna for harmonic suppression using GA is extended. A novel coaxial-fed, air-dielectric with folded patch at 2.4 GHz is designed. The antenna geometry for this is shown in Figure 6.13.

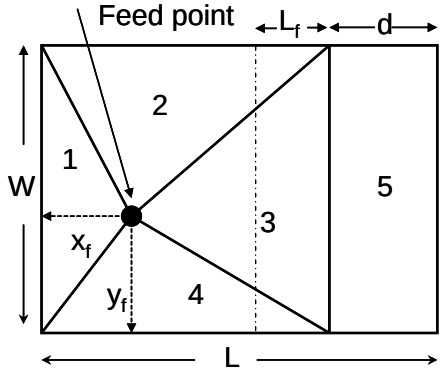

Figure 6:13: Top elevation view of antenna geometry used for adaptive meshing using GA.

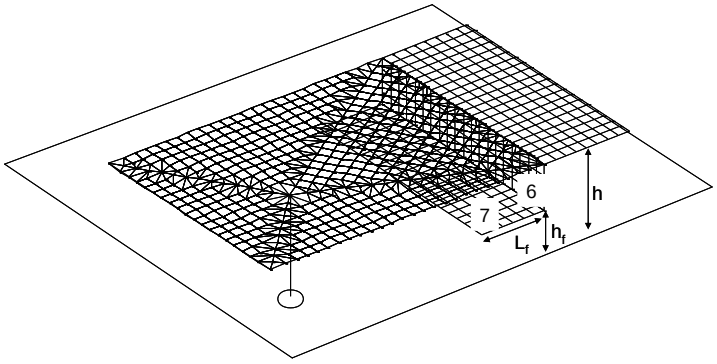

Figure 6:14: Top elevation view of resulted wire mesh used for Figure 6.13.

Table 6.5 presents the GA input parameters in which the possible range of values is shown for folded patch. It has a folded patch extended underneath the main patch as

shown. The weight coefficients of the cost function used in this example is similar to the previous example.

Table 6.5: Summary of GA input parameters; antenna variables and optimum solutions

G parameter	Harmonic suppression antenna parameters	Folded wall
	Parameters (m)	Optimal (m)
	Antenna length (L) (0.03- . 6	0. 4540
No. of population size = 4,	Antenna width (W) (0.02-0.06)	0.03006
No. of parameters: 6 (Figure 1 (a1)), 7 (Figure 1 (a2)), 8 (Figure 1 (a3)),	Shorting or folded wall position (d) (0.002-0.03)	0.00748
Probability of mutation =0.02,	Antenna height (h) (0.003-0.01)	0.00989
Maximum generation =500,	Feeding point at x-axis (X_f) (0.004-0.02)	0.00571
No. of possibilities=32768,	Feeding point at y-axis (Y_f) (0.004-0.02)	0.01392
	Variable shorting wall width (Ws) (0.001-0.03)	-
	Extend folded wall length (L_f) (0.005-0.015)	0.01327
	Extend folded wall height (h_f) (0.001-0.0035)	0.00159

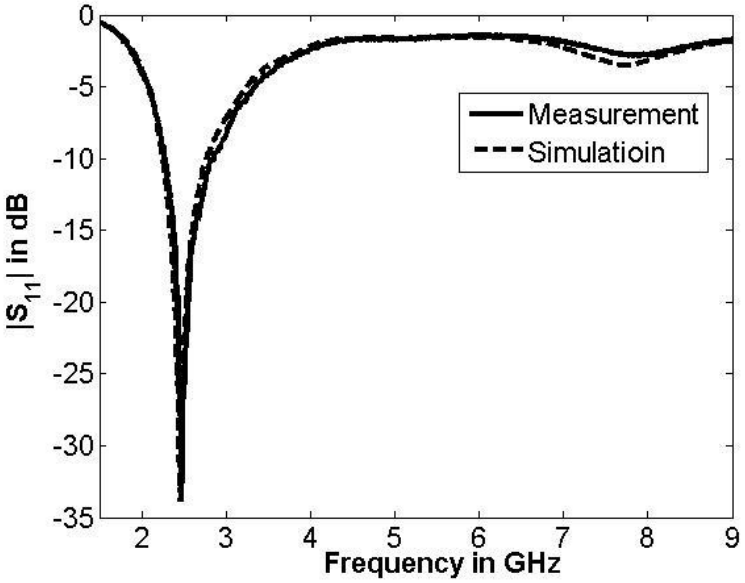

Figure 6:15: The measured and simulated return loss of the patch antenna with a folded patch.

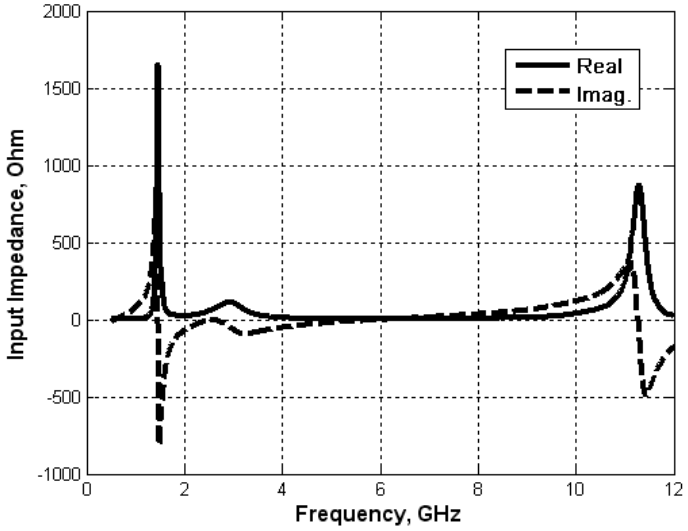

Figure 6:16: The overall measured input impedance of the antenna with folded patch.

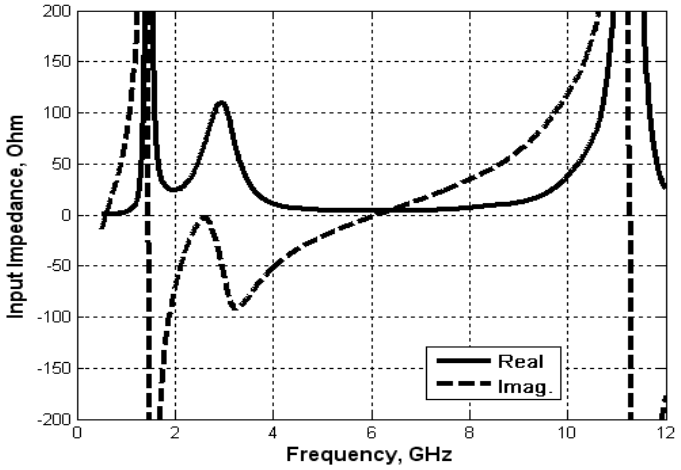

Figure 6:17: Measured input impedance of the harmonic suppression antenna a folded patch.

Table 6.6 : Performance of antenna input impedance of the harmonic rejection antenna with shortened wall at the fundamental and first and second harmonics.

Folded wall Patch Antenna		
Frequency (GHz)	Antenna input impedance (Ω)	
F	Real	Imaginary
f_o : 2.45	49.33	-11.88
$2f_o$: 4.90	5.021	-24.81
$3f_o$: 7.35	4.606	27

The radiation patterns in *zx* plane and *zy* plane for the GA-optimized HSA with folded wall at fundamental, second and third harmonic frequencies were measured. These results are given in Figure 6.18 showing 2nd and 3rd harmonic radiations of the HSA

with folded wall to be less than 13dB and 18dB for the *zx* plane and 10dB and 9dB for the *zy* plane subject to the normalised accepted power of the fundamental frequency. The measured maximum gain of the GA optimised antenna is 4.14dB.

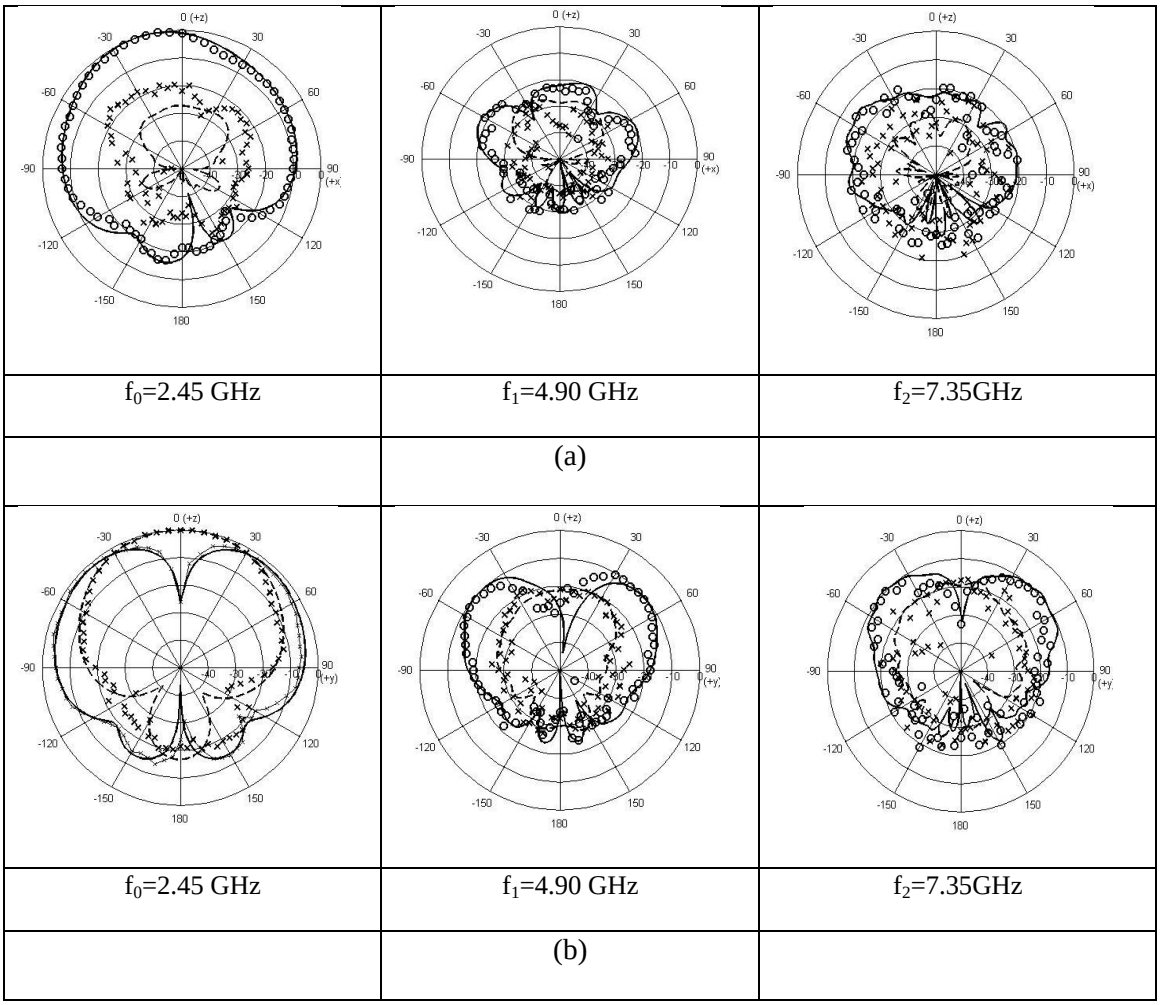

f_0=2.45 GHz	f_1=4.90 GHz	f_2=7.35GHz
	(a)	
f_0=2.45 GHz	f_1=4.90 GHz	f_2=7.35GHz
	(b)	

Figure 6:18: Measured and simulated radiation patterns of the proposed GA-optimised HSA with a folded wall for 2.45 GHz, 4.90 GHz and 7.35 GHz over: (top) z-x plane; (bottom) z-y plane; ('——'measured E_θ, ('o o o'simulated E_θ, '- - -' measured E_ϕ, 'x x x' simulated E_ϕ).

6.5 Conclusions

A novel technique for the design and optimisation of harmonic-suppression patch antenna, applying adaptive surface patch models and genetic algorithms, has been presented. Hardware realisations of three coaxially-fed air-dielectric microstrip patch antennas were used to assess and confirm the design theory. The return losses were validated for microstrip patch antennas with full and partial shorted walls, and for microstrip patch antenna with folded patch. The results showed good suppression at both the second and third harmonics. The measured input impedance of these antennas at the fundamental frequency showed almost perfect matching to 50 Ω, while fairly small resistive impedances were observed at the first two harmonic frequencies.

The comparison of return loss and far field radiation pattern measurements exhibited good agreement with the predictions. The examples presented confirmed the capability of the proposed method for antenna design using GA and adaptive surface meshing, showing reasonable stability and accuracy in the results.

6.6 References

[1] E. Elkhazmi, N.J. McEwan and J. Moustafa, “Control of harmonic radiation from an active microstrip patch anrtenna”, Journees Internationale de Nice sur les Antennes, pp. 313-316, November 1996.

[2] V. Radisic, Y. Qian, and T. Itoh, “Class F power amplifier integrated with circular sector microstrip antenna,” IEEE MTT-S Symposium Digest, pp. 687-690, 1997.

[3] H. Kim, K.S. Hwang, K. Chang and Y.J. Yoon, “Novel slot antennas for harmonic suppression”, IEEE Antennas and Wireless Components Letters, Vol. 14, No. 6, pp. 286-288, 2004.

[4] Y.J. Sung and Y.-S. Kim, “An improved design of microstrip patch antennas using photonic bandgap structure”, IEEE Transactions on Antennas and Propagation, Vol 53, No. 5, pp. 1799-1804, 2005.

[5] V. Radisic, S.T. Chew, Y. Qian, and Tatsuo Itoh, “High efficiency power amplifier integrated with antenna”, IEEE Microwaves and Guided Wave Letters, Vol. 7, No. 2, pp. 39-41, February 1997.

[6] A.F. Sheta, “A novel H-shaped patch antenna”, Microwave and Optical Technology Letters, Vol. 29, No. 1, pp. 62-66, April 2001.

[7] Q.-X. Chu and M. Hou, “An H-shaped harmonic suppression active integrated antenna”, International Journal of RF and Microwave Computer-aided Engineering, Vol. 16, No. 3, pp. 245-249, May 2006.

[8] H. Kim and Y.J. Yoon, “Microstrip-fed slot antennas with suppressed harmonics”, IEEE Transactions on Antennas and Propagation, vol. 53, no. 9, pp. 2809-2817, September 2005.

[9] D.A. Coley, “An introduction to Genetic Algorithms for Scientists and Engineers”, World Scientific, Singapore, 1999.

[10] H.H. Ammar and Y. Tao, “Fingerprint registration using Genetic Algorithms”, IEEE Symposium on Application Specific Systems and Software Engineering Technology, pp. 148-154, March 2000.

[11] Y. Rahmat–Samii and E. Michielssen, “Electromagnetic optimisation by Genetic Algorithms”, John Wiley & Sons, Canada, 1999.

[12] E.E. Altshuler and D.S. Linden, “Wire-antenna designs using genetic algorithms”, IEEE Antennas Propag, Mag. Vol. 39, pp. 33-43, 1997.

[13] E.A. Jones and W.T. Joines, “Design of Yagi-Uda Antennas Using Genetic Algorithms”, IEEE Transactions on Antennas and Propagation, Vol. 45, No. 9, 1386-1392, 1997.

[14] W.-C. Liu, “Design of a CPW-fed notched planar monopole antenna for multiband operations using a genetic algorithm”, IEE Proc. - Microwaves Antennas and Propagation, Vol. 152, No 4, 273-277, 2005.

[15] S.W.J. Chung, R.A. Abd-Alhameed, P.S. Excell. C.H. See, D. Zhou and J.G. Gardiner, “Resistively Loaded Wire Bow-tie Antenna for Microwave Imaging By Means of Genetic Algorithms”, International Multi-Conference on Engineering and Technological Innovation Proceedings, Orlando, Florida, USA, 2008, Pp 303-306.

[16] M.M. Abusitta, R.A. Abd-Alhameed, D. Zhou, C.H. See, SMR Jones and P.S. Excell, “New Approach for Designing Beam Steering Uniform Antenna Arrays using Genetic Algorithms”, Loughborough Antennas and Propagation Conf., 2009, Loughborough, UK, pp. 617-620.

[17] P.D. Karamalis, N.D. Skentos, and A.G. Kanatas, “Selecting array configurations for MIMO systems: an evolutionary computation approach”, IEEE Trans. on Wireless Communications, Vol. 3, No. 6, pp. 1994-1998, 2004.

[18] P.D. Karamalis, N.D. Skentos, and A.G. Kanatas, “Adaptive Antenna Subarray Formation for MIMO Systems”, IEEE Trans on Wireless Communications, Vol. 5, No. 11, pp. 2977-2982, 2006.

[19] M.A. Mangoud, R.A. Abd-Alhameed and P.S. Excell, “Optimisation of Channel Capacity for Indoor MIMO Systems Using Genetic Algorithm”, Proceedings of the Third International Conference on Internet Technologies and Applications (ITA 09), 2009, Glyndwr University, Wrexham, Wales, UK, pp. 431-439.

[20] P.D. Karamalis, A.G. Kanatas and P. Constantinou, “A Genetic Algorithm Applied for Optimisation of Antenna Arrays Used in Mobile Radio Channel Characterization Devices”, IEEE Trans on Intrumentation and Measurements, Vol. 58, No. 8, pp. 2475-2487, 2009.

[21] D.L. Carroll, FORTRAN Genetic Algorithm Driver, Version 1.7a, Download from: http://www.cuaerospace.com/carroll/ga.html, 4/2/2001.

[22] R.A. Abd-Alhameed, P.S. Excell and J. Vaul, "Currents Induced on wired I.T. Networks by Randomly distributed phones – A Computational study", IEEE Trans on Electromagnetic Compatibility, Vol. 48, No. 2, pp. 282-286, May 2006.

[23] C.H. See, R.A. Abd-Alhameed, D. Zhou, P.S. Excell and Y.F. Hu, "A new design of circularly-polarised conical-beam microstrip patch antennas using a genetic algorithm", Proceedings of the European Conference on Antennas and Propagation: EuCAP 2006, Session 4PA1, Paper no.100, Nice, France, 2006.

[24] D. Zhou, R.A. Abd-Alhameed and P.S. Excell, "Bandwidth enhancement of balanced folded loop antenna design for mobile handsets using genetic algorithms", PIERS Online, Vol. 4, No. 1, pp.136-139, 2008.

[25] D. Zhou, R.A. Abd-Alhameed, C.H. See, P.S. Excell, F.Y. Hu, K. Khalil and N.J. McEwan, "Quadrifilar helical antenna design for satellite-mobile handsets using genetic algorithms", Microwave and Optical Technology Letters, Vol. 51, No. 11, pp. 2668-2671, November 2009.

[26] D. Zhou, R.A. Abd-Alhameed, C.H. See, M.S. Bin-Melha, E.T.I. Elferganai and P.S. Excell, "New antenna designs for wideband harmonic suppression using adaptive meshing and genetic algorithms", In proceeding of Mosharaka International Conference on Communications, Propagation and Electronics (ISBN: 978-9957-486-06-8), Amman, Jordan, 5-7 March 2010, Technical Session 1, pp. 5-9.

[27] S. Kwon, B.M. Lee, Y.J. Yoon, W.Y. Song and J.-G. Yook, "A harmonic suppression antenna for an active integrated antenna", IEEE Antennas and Wireless Propagation Letters, Vol. 13, No. 2, pp. 54-56, February 2003.

CHAPTER SEVEN

7 Harmonic Rejection Triangular Patch Antenna

7.1 Introduction

Good antenna designs feature low manufacturing cost, high reliability and compact size for acceptable performance. For electrically small antennas, performance criteria place most emphasis on impedance matching, bandwidth and radiation efficiency and there is limited scope for controlling the pattern. Microstrip patch antennas satisfy the first two criteria fairly well. One of their biggest advantages is that they are low in cost as well as being light in weight. Various shapes of patch antenna design have been tried but the most common shapes are rectangular, circular and triangular [1]. Within this class of antennas, the Triangular Patch Antenna (TPA) has received relatively little attention, yet it has been claimed to have very small size for a given resonant frequency [1]. Like other patch antennas, it can be further miniaturised by increasing the permittivity of the dielectric material used for the antenna. On the other hand a major disadvantage associated with such types of antennas is that they are prone to excess harmonic radiations especially at high frequencies. This means that they provide little rejection of harmonic frequencies if these are present at the input of the antenna. Fortunately several

methods have been proposed to overcome such downsides in these types of antennas. One of the modern techniques is known as an electromagnetic band gap structure (EBG) which is especially used in microstrip patch antenna design. EBG structures are quite useful for high gains of about 20dBi. EBG structures have been found very useful to reject higher harmonics and this makes them attractive in the design of filters and other microwave circuits [2][3][4][5].

Besides the EBG, another useful approach to rejecting higher harmonics and reducing harmonic radiation from microstrip patch antennas EBG is known as a Defected Ground Structure (DGS). DGS is a convenient method to recognise the effect caused by the slow wave nature. DGS on one hand is used to miniaturise the size of the antenna, and on the other hand it may be used with different defect patterns to reduce the harmonic radiations.

Some of the common patterns include a “dog bone” structure, spiral DGS and rectangular DGS. Another common problem associated with the EBG is the backspace radiations due to cut-out slots just below the patch radiator. The DGS is quite useful under such circumstances because it helps in curing the problems by minimising the effects of back side radiation, providing that the proper shape of DGS is used, e.g. a cross shape is useful for polarisation and good radiation pattern [4][5].

The shape of a DGS structure is significant in an antenna design in order to suppress radiation of a particular harmonic. Circular and dumbbell shapes are particularly

important to suppress a particular harmonic. Each harmonic of a particular order has to be treated separately because of its different wavelength [6][7].

An attractive feature of the triangular patch antenna is that it is possible to obtain a given natural frequency by using less area as compared with many other shapes e.g. rectangular, equilateral etc. The shorting pin technique is also useful in patch design, whether for size reduction or control of harmonic radiation. This method helps in reducing the size of an antenna to around 75% of its original size which is useful in various applications where size remains a key issue [10]. Another technique of size reduction is to split an antenna patch into equal parts each having half of the full size. One of the equal parts can be discarded while the same resonant frequency can be retained. The split can be made along a plane of symmetry of the structure or along a voltage or current null line of the resonant mode. This procedure has a penalty as it is important to realise that there is always a trade-off between the size of the antenna and both its bandwidth and efficiency. Other factors which can effect the antenna size are the substrate permittivity and permeability [11].

Minimum return loss, maximum bandwidth, compact size and high efficiency are all factors which are important considerations for an antenna design engineer. Other major requirements in modern communications include multi frequency and broadband communication modes. These can be achieved by using slot patches for radiating elements. In applications such as Wi-Fi significant impedance bandwidth can be achieved by using this technique, which has the attractive feature that it keeps the size

of the antenna as compact as it can be and the overall layout remains simple which is important for communication systems [12]. More enhancement in the input impedance bandwidth can be made by using a truncated tip in a single probe feed triangular patch antenna. In [12] the impedance bandwidth can be enhanced to 9% of the working Wi-Fi, here the impedance can be enhanced to over 11% of the working Wi-Fi. This shows that antenna design research has advanced considerably in recent times and much has been done to improve the antenna design technology for modern communications [13][14]. One useful design is the corner- truncated short circuited antenna with triangular shape. This type of antenna provides very good impedance matching and the size of the antenna remains small as well. Another good point about such an antenna is that it can cover dual frequency bands and it remains low in profile and light in weight [14][15]. Replacing dielectrics with air where possible also plays an important role, and can have effects on the gain, directivity and the bandwidth of antenna. When there is an air gap, an antenna may resonate at two different frequencies and this may also provide improved bandwidth [16][17]. The right- angled isosceles design is another good option for a patch radiator. In right- angled types of design, computations are made in order to calculate harmonics of the antenna. Inputs of the antenna consist of two possible configurations with computations involved to get best possible results [18][19].

In this chapter a triangular patch antenna has been proposed with a coplanar feed strip and an integrated stubline. The design aims to obtain a good impedance match to 50 Ω at the fundamental frequency while suppressing radiation of the harmonics, which is achieved by having a reflection coefficient near unity in a 50 Ω system at the harmonic

frequencies. The work is similar to [8], but the performance of the design has been optimised.

7.2 Antenna Design Concept

The triangular patch antenna designed for this investigation is shown in the Figure 7.1. Key design details are that the material used is FR4, thickness is 1.6mm, and relative permittivity (ε_R) is 4.4. The dimensions of the printed antenna patch are 90 × 25 mm and it lies above a complete copper ground plane of 135 × 65 mm on the reverse side. To match impedance to 50Ω, a through-board feed pin can be placed at any point within the triangular patch. If the strip feed technique is used, it can be placed at any point on the periphery of the patch, and it has more flexibility for incorporating additional printed structures. To design the antenna, Ansoft's High Frequency Simulation Software (HFSS) has been used [9]. The design uses an additional stub line whose length, optimised together with the position of the attachment point on the main patch, allows good impedance match to be obtained at the resonant frequency while providing good rejection at harmonics. This proposed antenna had a resonant frequency of 3.43 GHz and impedance bandwidth of 380 MHz or 11% with stable gain and cross polarization characteristics. This makes the antenna useful in applications such as modern communication systems where multi-frequency operating modes are required.

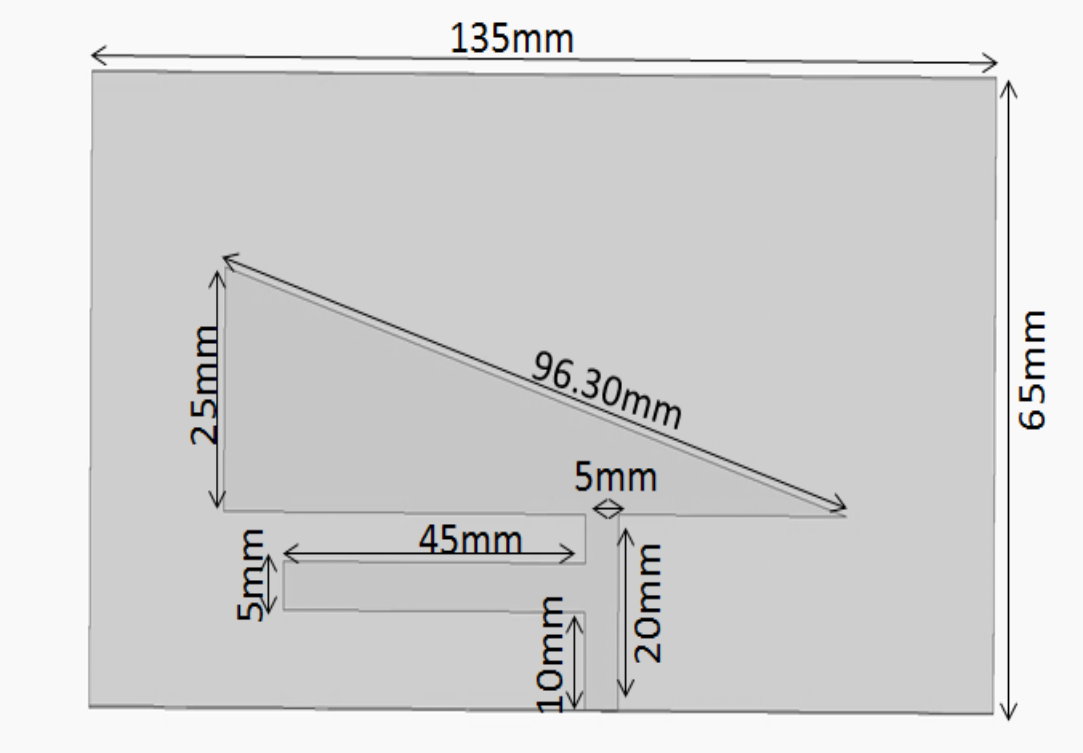

Figure 7:1: Basic geometry of the proposed antenna.

7.3 Result and Discussions

Figure 7.2 shows the reflection co-efficient for the above designed antenna. It can be seen from the results that antenna is designed for a fundamental frequency of 1.02GHz. The corresponding second and third harmonics are at frequencies of 2.04 and 3.06 GHz respectively. Impedance matching has been obtained very easily at 1.02GHz

fundamental frequency by adjusting the location of the feeding strip. At the fundamental frequency the harmonic suppression does not produce any noticeable harmful effects in impedance matching. The results obtained as results of simulations have been carried out all by using HFSS.

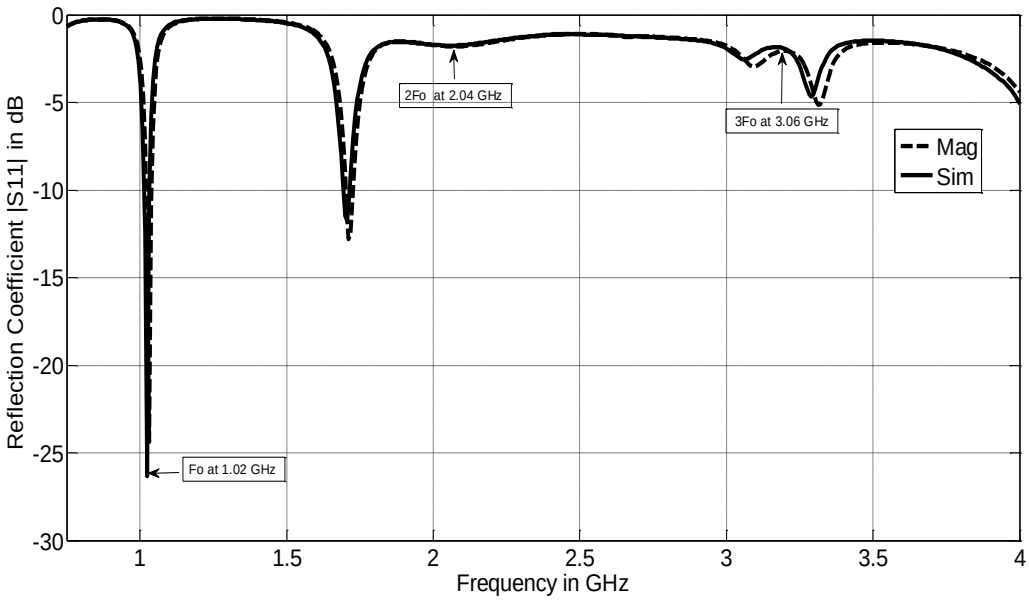

Figure 7:2: Reflection Coefficient |S11| VS Frequency.

It can be noticed that the return loss at 1.02GHz is less around -26dB, which is well within the requirements of the design; in addition the results satisfy the fundamental requirements of such design in terms the significant harmonics levels for practical realization.

Table 7.1: Return Loss in dB vs Frequency in GHz for Fundamental and two Harmonics Frequency.

Name	Frequency (f) in GHz along X-Axis	Return loss in dB along Y-Axis
Frequency Fundamental(f1)	**1.02**	**- 26.31**
Frequency 2nd(2f1)	**2.04**	**- 1.75**
Frequency 3ed(3f1)	**3.06**	**- 2.53**

Table 7.1 is the measured return loss values in dBs at the fundamental and the first two harmonics. It can be seen from the table that at frequency of 1.02GHz which is the fundamental frequency the return loss is measured as -26.31 dB. The return loss is less than -20 dB over the stated bandwidth at the fundamental frequency which satisfies the requirement specifications of the design. For all harmonics the return loss should be as small as possible, and from the table above it can be seen that for the first two harmonics of the design the return loss remains less than 3dBs. The design characteristics of the above design triangular patch antenna meet the requirement specifications for the antenna as outlined in the requirement specifications for the first and second harmonics of the antenna. The antenna had a size reduction of 38% as compared to triangular patch antenna without the tri-slot at the same target frequency.

The circuit impedance has also been measured in order to check and normalise according to the requirements. The simulation results of the impedance are shown in the figures below consisting of both real and imaginary parts of the impedance.

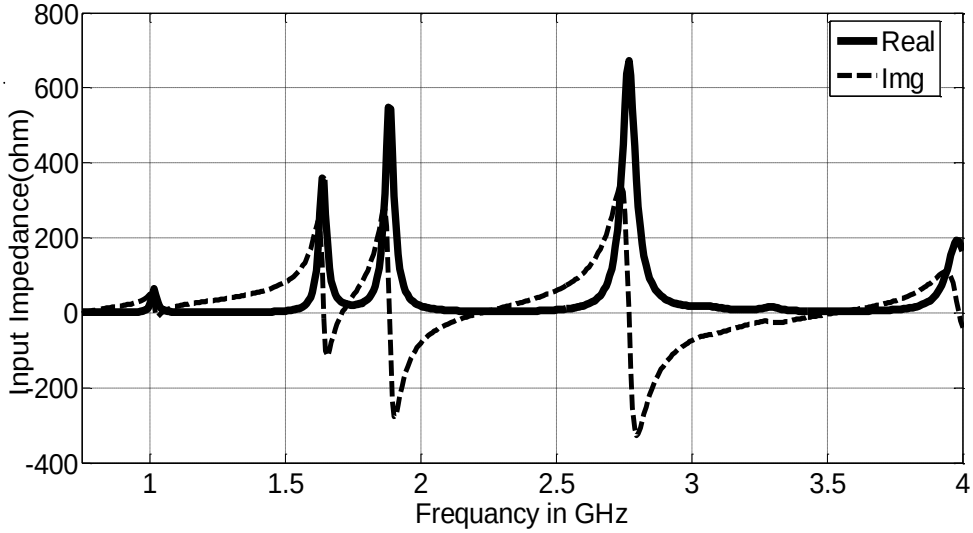

Figure 7:3: Circuit Impedance consisting of real and imaginary parts.

Table 7.2:Impedance measured in (Ω) VS Frequqncy measured in GHz for Fundamental, first and second Harmonics.

Name	**Frequency (f) in GHz along X-Axis**	**Impedance Measured in (Ω) along Y-Axis**
Frequency Fundamental(f1)	**1.02**	**50.24**
Frequency 2nd($2f_1$)	**2.04**	**10.23**
Frequency 3rd($3f_1$)	**3.06**	**17.55**

The table above shows the comparison of impedance measured in ohm's versus the frequency measured in GHz; in which at the fundamental frequency of 1.02GHz, the impedance value measured is given as 50.24Ω. This impedance value is quite satisfactory at the fundamental harmonic. The impedance value at 2^{nd} harmonic are given as 10.23 Ω, which are not very much closer to the one obtained at fundamental harmonic. The values of impedance at 3^{rd} are given as 17.55 Ω. The impedances matching for the harmonics of the antenna design show almost perfect matching however fairly small resistive impedance at harmonic frequencies has also been observed. From the simulation results achieved it can be seen that both imaginary and real part of the impedance at the fundamental frequency meet the requirement specifications laid down, both values are well below 1.

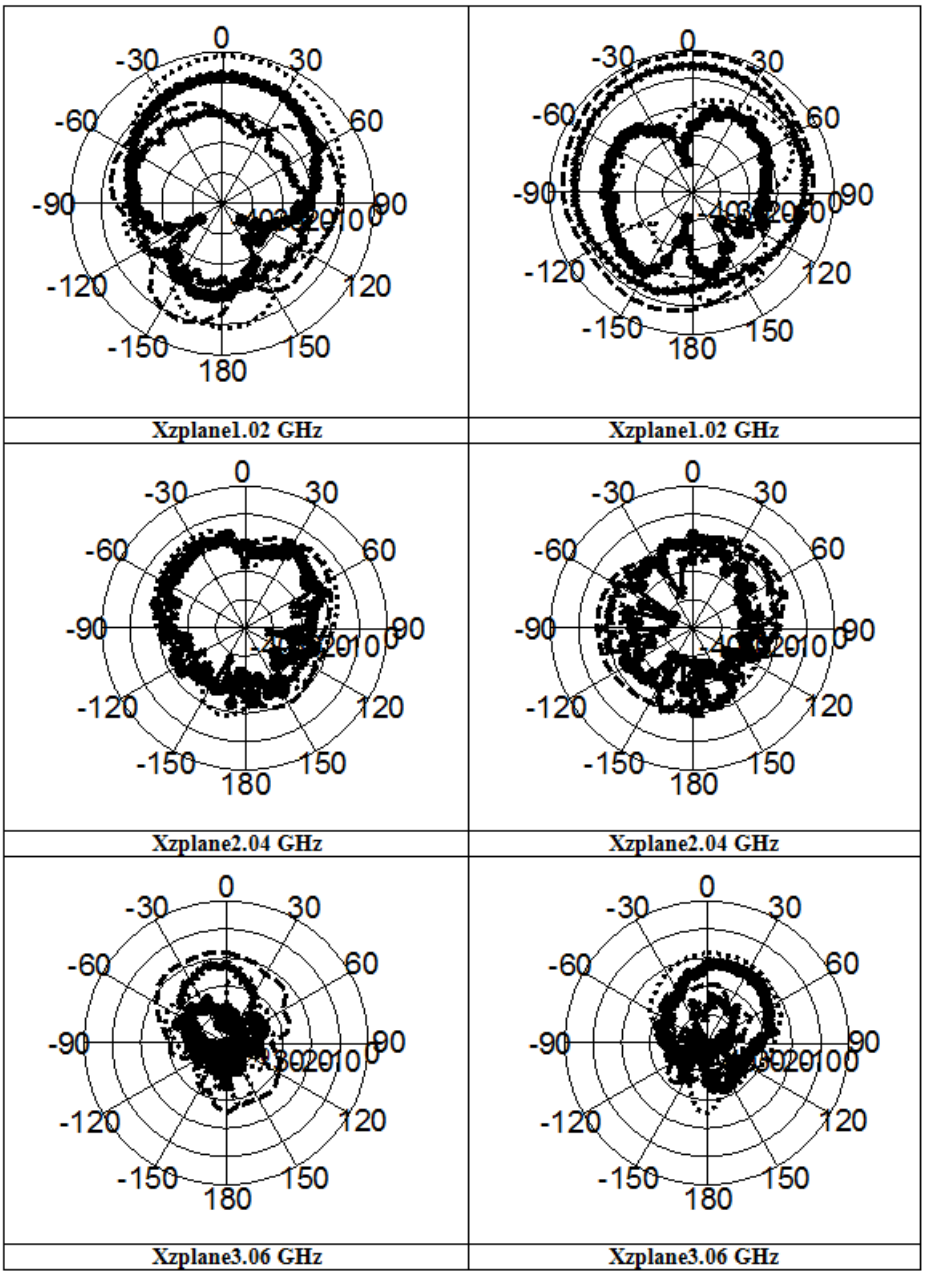

Figure 7:4: Measured and simulated radiation patterns for 1.02 GHz, 2.04 GHz and 3.06 GHz over: (top) z-x plane; (bottom) z-y plane; ('x x x' measured E_θ, ('- - -'simulated E_θ, 'o o o' measured E_ϕ, '——' simulated E_ϕ).

Figure 7.4 shows the radiation pattern for all harmonics of the antenna designed above. The radiation patterns have been measured inside the anechoic chamber at Bradford University. Radiation pattern is categorised with main beam with 3dB beam width with side lobes at different harmonics. Radiation patterns are shown in YZ plane as well as in XZ plane for all harmonics. XZ is the horizontal plane whereas YZ is the vertical plane to show the radiation pattern. Radiation pattern of antenna at fundamental frequency (1.02GHz) shows that antenna has an omnidirectional pattern in the YZ plane. Comparing results of antenna at fundamental frequency and at all harmonics, it shows that radiation pattern fulfils the requirements of the design at almost all frequencies. Harmonic rejection antenna has the differences in the radiation pattern at 1.02 GHz and all harmonics of about 2dBi in YZ plane and about 4dBi in XZ plane. These are quite satisfying values of the radiation pattern comparing with many different design with various different shapes of the antenna. At the given dimensions of the antenna this design radiation pattern shows almost the ideal values which are quite satisfying for this design. The dimensions of the antenna are quite small compared with the wavelength at the fundamental and first two harmonic frequencies. From the comparison of radiation patterns of all harmonics with each other it can be said that the radiation pattern of the antenna at 1.02 GHz is better than at all harmonics. Results achieved in both planes YZ as well as XZ plane are almost perfect for such a type of triangular patch antenna.

7.4 Conclusion

In this design, an edge-fed technique has been proposed and investigated for designing a triangular patch for operation at 1.02 GHz with suppression characteristics over harmonic frequency bands. The reflection coefficient was about -1.75 dB at the second harmonic and -2.53 dB at the third harmonic. According to the results obtained, this antenna with its simple harmonic suppression structures is quite effective. Therefore, the proposed antenna can be suitable for active integrated antennas where generation of harmonics in the active device can be substantial. Antenna design parameters were almost perfect with satisfactory impedances at the fundamental frequency and dominant harmonics, and measured results were in good agreement with simulation. An acceptable omnidirectional pattern was obtained at the fundamental frequency. It is suggested that by employing the array technique the gain, directivity and selectivity can be enhanced and design can be made even better as well. It can be concluded that the antenna design was successful and fulfilled all the design requirements and specifications in terms of return loss, impedance matching and radiation pattern.

7.5 References

[1] Saunders, S. R. and A. Aragon-Zavala, Antenna and Propagation for Wireless Communication Systems, John Wiley & Sons, England, 2007.

[2] Y. Horri and M. Tsutsumi, Harmonic control by photonic bandgap on microstrip patch antenna, IEEE Microwave Guided Wave Lett 9 (1999), 13–15.

[3] Y.J. Sung, M. Kim, and Y.S. Kim, Harmonics reduction with defected ground structure for a microstrip patch antenna, IEEE Antennas Wireless Propag Lett 2 (2003), 111–113.

[4] H. Liu, Z. Li, X. Sun, and J. Mao, Harmonic suppression with photonic bandgap and defected ground structure for a microstrip patch antenna, IEEE Microwave Wireless Compon Lett 15 (2005), 55, 56.

[5] Y.J. Sung and Y.-S. Kim, An improved design of microstrip patch antennas using photonic bandgap structure, IEEE Trans Antennas Propag 53 (2005), 1799–1804.

[6] M. K. Mandal, P. Mondal, S. Sanyal, and A. Chakrabarty, "An Improved Design of Harmonic Suppression for Microstrip Patch Antennas," Microwave and Optical Technology Letters, Vol. 49, No. 1, January 2007, pp. 103-105.

[7] Luis Inclán-Sánchez, José-Luis Vázquez-Roy, and Eva Rajo-Iglesias, "Proximity Coupled Microstrip Patch Antenna With Reduced Harmonic Radiation," IEEE Transactions on Antennas and Propagation, Vol. 57, No. 1, January 2009, pp. 27-32.

[8] M. M. Olaimat and N. I. Dib, "A Study of 15°-75°-90° Angles Triangular Patch Antenna, *Progress In Electromagnetics Research Letters.,* vol. 21, pp. 1-9, 2011.

[9] Ansoft High Frequency Structure Simulator v10 Uses Guide, CA, USA.

[10] M. M. Olaimat and N. I. Dib, "A Study of 15°-75°-90° Angles Triangular Patch Antenna,"*Progress In Electromagnetics Research Letters.*, vol. 21, pp. 1-9, 2011.

[11] M.S. El-Sallamy, M.Y. Omar, D. Abdelaziz, "Tri-Slot Loaded Equilateral Triangular Microstrip Antenna for Compact And Dual-Frequency Operation," National Radio Science Conference, pp. 1-6, 2009.

[12] Y. Bhomia, A. Kajla, and D. Yadav, "Slotted right angle triangular microstrip patch antenna," *International Journal of Electronic Engineering Research*, vol. 2, no. 3, pp. 393-398, 2010.

[13] A. Chaturvedi, Y. Bhomia, D. Yadav, "Truncated tip triangular microstrip patch antenna," International Symposium on Antennas Propagation and EM Theory (ISAPE), pp. 212-214, 2010.

[14] N. Singh, D.P. Yadav, S. Singh, R.K. Sarin, “Compact corner truncated triangular patch antenna for WiMax application,” Mediterranean Microwave Symposium (MMS), pp. 163-165, 2010.

[15] A. Kimothi, V. Tiwari, V.K. Saxena, J.S. Saini, D. Bhatnagar, “Radiations from a right triangular patch antenna with and without air gap,” International Conference on Recent Advances in Microwave Theory and Applications, pp.154-156, 2008.

[16] E. G. Lim, E. Korolkiewicz, S. Scott, A. Sambell, and B. Aljibouri , "An Efficient Formula for the Input Impedance of a Microstrip Right-Angled Isosceles Triangular Patch Antenna" *IEEE Antennas And Wireless Propagation Letters*, vol. 1, pp. 18-21, 2002.

[17] Indra Surjati, “Dual frequency operation triangular microstrip antenna using a pair of slit,” *11th Asia Pacific Conference on Communications*, Perth, Western Australia, 2005.

[18] Yuan Li, R. Chair, K. M. Luk, and K. F. Lee, “Broadband Triangular Patch Antenna With a Folded Shorting Wall,” IEEE Antennas and Wireless Propagation Letters, vol. 3, pp. 189-192, 2004.

[19] Guha, D. and J. Y. Siddiqui, “Resonant frequency of equilateral triangular microstrip patch antenna with and without air gaps,”*IEEE Trans. Antennas Propagat.*, Vol. 52, No. 8, 2174-2177, Aug. 2004.

CHAPTER EIGHT

8 Conclusions and Future Work

8.1 Conclusions

This work has been based on the design of band - rejected antennas using adaptive meshing and genetic algorithms (GA). The new type of antennas designed and proposed in this work can be used in any wireless communications devices such as mobile handsets and communication terminals in order to increase the systems performance with reduced noise levels and interefernce between electromagnetic components by reducing the harmonic radiations at the secong and third frequencies and will also serve as a bandpass filter.The main target frequency was 1.8 GHz, combined with rejection of its second harmonic (3.6 GHz) and the third harmonic (5.4 GHz). To meet the given design frequencies modelling have been done by adaptive meshing whereas the optimal parameters for the design have been determined by using the genetic algorithms (GA). GA has proved an excellent optimisation tool in antenna design technology in recent years. With the requirements of compact size and harmonic rejection, GA is the one of the fundamental tools which can be exploited. The good thing about GA is that it can evolve a generic optimum point by applying the pressure on the given group with multiple outcomes and by managing the results. The square patch antenna fed by 50 Ω

inset microstrip-line for 1.8 GHz operation showed good suppression at the first two harmonic frequencies. The sensing patch measurement technique for the microstrip patch antenna has been shown to achieve good accuracy for the second and third harmonic measurements. Several examples were demonstrated, all including design of coaxially-fed, air-dielectric patch antennas implanted with shorting and folded walls. The measurement results for the radiation pattern showed good agreement with the predictions. The presented results showed a good impedance matching at the fundamental frequency with good suppression achieved at the first two harmonic frequencies. A computational technique using adaptive surface meshing driven by GA was adopted for optimizing the antenna design parameters and theresults produced allowed us to conclude that the GA method can provide outstanding optimization parametrs in order to provide high-speed, accurate and reliable solutions for the proposed antenna design structures.

Chapter 1 introduced the aims and objectives of this research, and reviewed the adaptive meshing and GA methods and their usefulness in antenna design.

Chapter 2 is about background study. It reviews the similar work already been done in the field of antenna design. Significant amount of work has been review and studied and has been included in the review. Main study has been done in key areas including harmonic suppression, harmonic control, adaptive meshing, genetic algorithms and triangular patch antenna for mobile and wireless communications.

Chapter 3 described the major design study and presented a square microstrip antenna design for a fundamental frequency of 1.8 GHz with harmonic control. Simulated results of square microstrip antenna fed by 50Ω inset microstrip line at given specifications have presented. As the design is based on the fundamental frequency, the aim of this design is to check the reception of harmonic as well as observe any sort of specious radiations.

Chapter 4 treated the harmonic radiation measurement for active patch antenna using sensor patches. This method is applicable to active integrated antenna designs and solves the problem of measuring the total harmonic radiation from the active antenna where it is difficult both to measure the power incident on the radiating structure at harmonic frequencies and to integrate the total radiated flux density over all angles. This design work is extension of the design in chapter 3 as it explores a method of evaluating the radiation of wanted power at the fundamental frequency as well as unwanted power at second and third harmonics. A parametric study of the sensor patch design was conducted using S-parameters between the input feed line of the antenna and the sensor's output, measured by using HP8510C network analyser from 2GHz to 8GHz.

In chapter 5 further detailed discussion of the genetic algorithm (GA) and adaptive meshing has been provided. The chapter explored how GA can be used in conjunction with an electromagnetic simulator, making GA an efficient tool for search, optimisation and machine learning. In addition to its use for design of air and dielectric filled patch antennas, the chapter also demonstrated GA's use for wideband antenna designs based

on the fundamental requirements of near field imaging tools such as are needed for microwave detection of breast cancer, and for the design enhancement of MIMO applications.

In chapter 6 a micro strip patch antenna, designed for harmonic suppression with the aid of a genetic algorithm, has been explored. Return loss and input impedance of a conventional patch antenna as well as the input impedance of a harmonic suppression antenna with fully shorted walls were measured, simulated and compared. Also, the same parameters were measured and simulated for partially shorted wall antennas, and microstrip patch antennas with a folded patch were also explored.

Chapter 7 explored a harmonic rejection antenna based on the triangular patch. A novel design including an integrated stub line was described. This has good match at the fundamental frequency with a reduced resonant size, as well as low transmission of second and third harmonics. This chapter introduces new ideas for design of compact, low cost, efficient antennas with good harmonic rejection. The measured and simulated results were very good and design seemed quite successful useful. Overall it can be concluded that this research has contributed significantly to bring new ideas in antenna design technology for wireless communication systems.

8.2 Future Work

The research has brought significant areas for further study. Major considerations for future work can be summarised as below:

- Design of active patch antenna can be extended for wider frequency operation. In an active transmitting antenna, the trade-off between rejection of harmonic radiation and optimisation of harmonic frequency inpedances for amplifier efficiency can be explored in more detail. It has been found that nonlinearity due to using active devices in an integrated antenna is an attractive subject of research.
- The other new subject that can be tackled is the performance of these devices near high scattering electromagnetic fields environment.
- The GA optimisation can be applied to the design of planar monopole antennas, which exhibit both ultra-wide-band (UWB) operation and a narrow-band frequency notch. It would also be worth looking at implementing notch filters for other microstrip antenna designs.
- The work can be extended for MIMO applications where the design could consider using new innovations beyond EBG, such as Met materials, for design of MIMO antennas for wireless communications. Such new techniques can be investigated in order to minimise the size of the antenna as well as reducing the natural frequency by artificially creating the antenna filling and support materials. The idea of negative refractive index can be an innovative and useful tool in antenna design technology for future systems.
- In order to enhance system performance adaptive techniques can be implemented between different MIMO schemes which can be based on the statistics of the channel to enhance the overall performance of the system. For

systems employing multiple users, adaptive MIMO algorithms can be implemented for multiple transmissions.

9 AUTHORS PUBLICATION RECORD

LIST OF PUBLICATIONS

9.1 CONFERENCES AND WORKSHOPS

1) **Mohammad S. Bin-Melha**, Raed A. Abd-Alhameed, Dawei Zhou, Z. B. Zainal-Abidin, Chan H. See, Issa T. E. Elfergani, and Peter S. Excell "Harmonic-suppression Using Adaptive Surface Meshing and Genetic Algorithms" PIERS Online, Marrakesh, Morocco, March 20-23, 2011, pp. 1627-1631.

2) **Mohammad S. Bin-Melha**, N.A Jan, M. Usman, C.H. See and R.A. Abd-Alhameed, Investigation of Harmonic Rejection for Triangular Patch microstrip antenna, ITA 2013, Wrexham, Wales, Sept 2013, EERT Workshop.

3) **Mohammad S. Bin-Melha**, Chan H. See, Raed A. Abd-Alhameed M. S. Alkambashi, D. Zhou, SMR Jones and PS Excell, Two miniaturized printed dual-band spiral antenna designs for satellite communication systems, PSATS 2012 - 4th International Conference on Personal Satellite Services, March 22-23 - Bradford, UK, , Technical Session 2, Paper 5, pp. 1-6.

4) **Mohammad S. Bin-Melha**, R. A. Abd-Alhameed, C. H. See, M. Usman, I. T. E. Elfergani, and J. M. Noras, Harmonic Rejection Triangle Patch Antenna, PIERS Proceedings, Kuala Lumpur, MALAYSIA, March 27-30, 2012, pp. 1463-1466.

5) Ogbonnaya O. Anoh, Raed A. Abd-Alhameed, Steve M. R. Jones, Yousef A. S. Dama, and **Mohammad S. Bin-Melha** "On the Wavelet Families for OFDM System - Comparisons over AWGN and Rayleigh Channels "PSATS 2012, 22-23 March 2012 in Bradford, Technical Session 2, Paper 3, pp. 1-8.

6) D. Zhou, R.A. Abd-Alhameed, **M.S. Bin-Melha**, I.T.E. Elfergani, C.H. See and P.S.Excell" New Antenna Design For Wide Harmonic Suppression Using Adaptive Meshing And Genetic Algorithms" In proceeding of Mosharaka International Conference on Communication , propagations and Electronics, Amman, Jordan, 3-5 March 2010, Technical Session 1, pp. 5-9.

7) A. G. Alhaddad, R. A. Abd-Alhameed, D. Zhou, I. T. E. Elfergani, C. H. See, P. S. Excell, and **M. S. Bin-Melha**, "Low Profile Balanced Handset Antenna with Dual-Arm Structure for WLAN Application," *Proceedings of Mosharaka* International Conference on Communications, Propagation, and Electronics (ISBN: 978 - 9957- 486 - 10 - 5), Amman, Jordan, pp. 1-4, 5-7 March 2010.

8) S.Adnan, R. A. Abd-Alhameed, H. I. Hraga, **M S Bin-Melha** and M Alghazimi, “Modified Printed Monopole Antenna for Ultra-wideband Application" 4th European conference on antenna and propagation. Barcelona, Spain, 12-16 April 2010, Paper No 16, pp. 1-4

9) I.T.E. Elfergani, Hussaini A.S, Abd-Alhameed R.A, See C.H, Hraga H.I, **Bin-Melha, M.S,** Excell P.S, Rodriguez J, " A dual-band frequency tunable planar inverted F antenna", In proceedings of The European Conference on Antennas and Propagation: EuCAP 2011, pp. 235-239 Rome, Italy, 11-15 April 2011.

10) I.T.E. Elfergani, Raed Abd-Alhameed, **M.S. Bin-Melha,** Chan See, Da-Wei Zhou, Mark Child, and Peter Excell “Frequency Tunable PIFA Design for Handset Applications" The 6th International Mobile Multimedia Communications Conference, 6-8 September 2010 - Lisbon, Portugal, Paper No. 5, pp. 1-8.

9.2 JOURNAL ARTICLES

1) D. Zhou, R.A. Abd-Alhameed, **M.S. Bin-Melha**, C.H. See, Z.B. Zainal-Abdin, P.S. Excell, "New Antenna Designs for Wideband Harmonic-Suppression Using Adaptive Surface Meshing and Genetic Algorithms" IET MAP Journal, vol. 5, No. 9, June 2011, pp. 1054 - 1061.

2) I.T. Elfergani, Raed Abd-Alhameed, **Mohammad S. Bin-Melha**, Chan See, Da-Wei Zhou, Mark Child, Peter Excell, A Frequency Tunable PIFA Design for Handset Applications, Lecture Notes of the Institute for Computer Sciences (LNICST), Social Informatics and Telecommunications Engineering, vol. 77, pp. 688-693, 2012

3) Z.Z. Abidin, Y.Ma, R.A. Abd-Alhameed, K.N. Ramli, D Zhou, **M.S. Bin-Melha**, J. M. Noras and R. Halliwell “Design of 2×2 U-shape MIMO slot antennas with EBG material for mobile handset applications" PIERS Online, 2011, pp. 1275-1278.

4) D. Zhou, R. A. Abd-Alhameed, C. H. See, N. T. Ali and **M. S. Bin-Melha** "Harmonics Measurement on Active Patch Antenna Using Sensor Patches" Progress In Electromagnetics Research C, Vol. 17, 121-130, 2010.

SELECTED AUTHOR’S PUBLICATIONS

Harmonic-suppression Using Adaptive Surface Meshing and Genetic Algorithms

M. S. Bin-Melha[1], R. A. Abd-Alhameed[1], D. Zhou[1], Z. B. Zainal-Abdin[1], C. H. See[1], I. T. E. Elfergani[1], and P. S. Excell[2]

[1]Mobile and Satellite Communications Research Centre, University of Bradford, Bradford, UK
[2]Centre for Applied Internet Research, Glyndwr University, Wrexham, UK

Abstract— A novel design strategy for microstrip harmonic-suppression antennas is presented. The computational method is based on an integral equation solver using adaptive surface meshing driven by a genetic algorithm. Two examples are illustrated, all involving design of coaxially-fed air-dielectric patch antennas implanted with shorting and folded walls. The characteristics of the antennas in terms of the impedance responses and far field radiation patterns are discussed theoretically and experimentally. The performances of all of the GA-optimised antennas were shown to be excellent and the presented examples show the capability of the proposed method in antenna design using GA.

1. REVIEW AND SUMMARY OF THE METHOD

Harmonic suppression antennas (HSAs) are used to suppress power radiation at harmonic frequencies from active integrated antennas. An antenna that presents a good impedance match at the fundamental design frequency (f_o) and maximised reflection at harmonic frequencies is said to be a harmonic suppression antenna. In addition, the input impedance of any HSA design has to have minimised resistance at the harmonic frequencies and hence will be largely reactive [1, 2]. Several techniques have been proposed to control such harmonics, such as shorting pins, slots or photonic bandgap structures [3, 4]. In [5], the modified rectangular patch antenna with a series of shorting pins added to the patch centre line was applied to shape the radiated second harmonic from the active amplifying-type antenna, in order to increase the transmitter efficiency. Unfortunately, the proposed design does not provide the termination for the third harmonic. A circular sector patch antenna with 120° cut out was investigated and proved to provide additional harmonic termination for the third harmonic, also claiming a further enhancement in the transmitter efficiency [2]. Further, an H-shaped patch antenna was designed and applied in oscillator-type active integrated antennas for the purpose of eliminating the unwanted harmonic radiation [6, 7]. The present work presents a clear motivation to develop a coherent design strategy for microstrip HSA in active integrated applications. The technical work, adopts a computational technique using adaptive surface meshing driven by a genetic algorithm.

The benefit of applying GA methods is that they provide fast, accurate and reliable solutions for antenna structures. A genetic algorithm driver [8–10], written in Fortran, was adopted in this work in conjunction with the authors' Fortran source code [11], which was used to evaluate the randomly-generated antenna samples. Several antenna designs, derived using GA in previous work by the authors [12–14], have shown that the GA method to be an efficient optimiser tool that can be used to search and find rapid solutions for complex antenna design geometries.

An adaptive meshing program was also written in Fortran by the present authors and added as a subroutine to the GA driver, with the primary objective of simulating air-dielectric planar microstrip patch antenna designs: this used a surface patch model in cooperation with a GA. In addition to microstrip patch designs, the program can support the design of any 3D antenna geometry structure, including moderate amounts of dielectric materials. The present work is an extended version of preliminary work reported in [15]. The design of coaxially-fed air-dielectric microstrip harmonic-rejecting patch antennas for 2.4 GHz was investigated, enforcing suppression of the first two harmonic frequencies, using a genetic algorithm. The designs included patch antennas with shorted and folded walls.

2. SIMULATION AND RESULTS

Simple coaxially-fed air-dielectric patch antennas with shorted and folded walls, mounted on an infinite ground plane and operating at 2.4 GHz, were selected for this study as a simple exemplar to demonstrate acceptable harmonic rejection [5].

The proposed outline antenna designs are shown in Fig. 1. The full width shorted patch is subdivided into four trilaterals and two quadrilaterals, including the conducting shorted wall, as illustrated in Figs. 3(a) and 3(b). This design required six parameters to be defined. The second design example is similar to the first, but uses a modified folded wall, as shown in Figs. 3(c) and 3(d), in which the total surface area was subdivided into four trilaterals and three quadrilaterals. The fold in the wall means that it is no longer electrically connected to the ground plane, although the folded portion will provide strong capacitive coupling. In this model eight GA parameters were considered.

Table 1 presents the GA input parameters in which the possible range of values is shown for two examples considered. For this optimisation process, real-valued GA chromosomes were used. It should also be noted that the fundamental, first and second harmonic frequencies were considered within the GA cost function.

For validation, prototypes of the GA-optimised harmonic-suppression antennas (HSAs) of the two models were designed and tested. Copper sheet with thickness of 0.5 mm was used for the patch antenna, shorted/folded wall and the ground plane. The ground plane size was set to 140 mm × 140 mm, this relatively large size being chosen in order to attenuate the effect of the edges of the finite ground plane. The return losses were validated and measured results compared with calculations are shown in Fig. 2. As can be seen, the results for rejection levels of 2nd and 3rd harmonics were quite encouraging and no other resonances or ripples were found over the harmonic frequency bands.

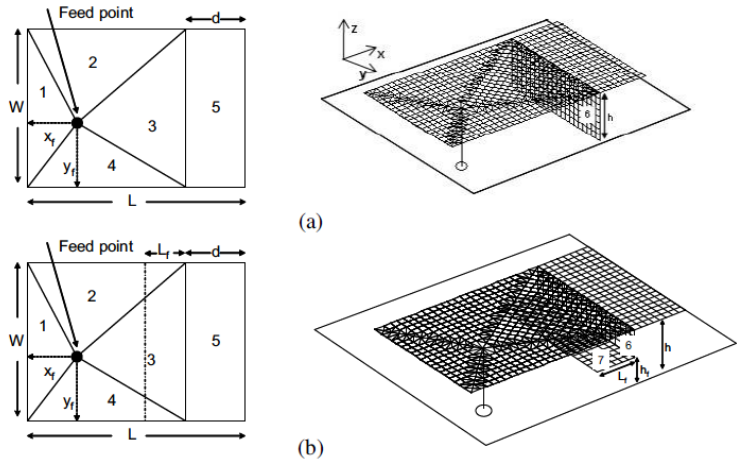

Figure 1: (a), (b) The proposed antenna models for full-width shorted wall; and (c), (d) folded wall. (a), (c): Top view; (b), (d): 3D view of surface patch meshing.

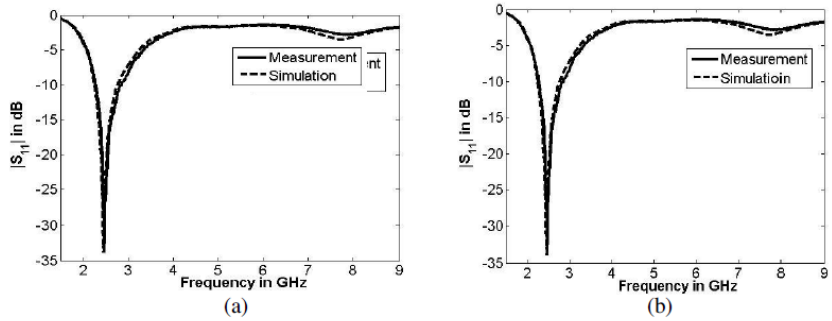

Figure 2: Performance of the measured and calculated return losses of the GA-optimised HSAs; (a) full-width shorted wall; and (b) folded wall.

Table 1: Summary of GA input parameters, antenna variables and best solutions for the proposed designs, including shorted and folded walls.

GA parameters	**Harmonic suppression antenna parameters**	**Fully shorted**	**Folded wall**
	Parameters (m)	Optimal (m)	Optimal (m)
	Antenna length (L) (0.03–0.06)	0.03950	0.04540
No. of population size = 4	Antenna width (W) (0.02–0.06)	0.03305	0.03006
No. of parameters: 6 (Figure 1(a1)), 7 (Figure 1(a2)), 8 (Figure 1 (a3))	Shorting or folded wall position (d) (0.002–0.03)	0.00972	0.00748
Probability of mutation = 0.02	Antenna height (h) (0.003–0.01)	0.0079	0.00989
Maximum generation = 500	Feeding point at x-axis (X_f) (0.004–0.02)	0.00723	0.00571
No. of possibilities = 32768	Feeding point at y-axis (Y_f) (0.004–0.02)	0.01752	0.01392
	Variable shorting wall width (W_s) (0.001–0.03)	-	-
	Extend folded wall length (L_f) (0.005–0.015)	-	0.01327
	Extend folded wall height (h_f) (0.001–0.0035)	-	0.00159

Table 2: Simulated and measured gain values at the fundamental frequency for the two antennas shown in Fig. 1.

Type of antenna		**Full shorted wall**		**Folded wall**	
Antenna gain (dBi)		Measured	Simulated	Measured	Simulated
Frequency (GHz)		$f_o = 2.47$		$f_o = 2.45$	
x-z plane	H.P.[1]	−8.35	−24.74	−13.45	−23.71
	V.P.[1]	4.14	4.06	5.01	5.03
y-z plane	H.P.	1.71	2.29	3.11	3.98
	V.P.	0.54	0.16	2.04	2.50

The input impedances of the prototype antennas were also measured over a wide frequency band as shown in Fig. 3. The measured input impedance of these antennas at the fundamental operating frequency and its first two harmonics shows that almost perfect matching to 50 Ω was attained at the fundamental frequency, while fairly small resistive impedances at harmonic frequencies were observed.

The simulated and measured radiation patterns in the z-x plane for the prototype antenna shown in Fig. 1 is presented in Fig. 4 the fundamental, second and third harmonic frequencies. The results are in good agreement and confirm viable levels of suppression of 2nd and 3rd harmonic levels. The fields for the second antenna design is quite similar thus are not shown here. These levels may be summarised as follows: for the fully-shorted wall design the maximum 2nd and 3rd harmonic radiation amplitudes were lower than 13 dB and 18 dB (respectively) below the fundamental for the z-x plane and 10 dB and 9 dB below for the z-y plane.

The simulated and measured gain values at the fundamental frequency for the two antennas shown in Fig. 1 are presented in Table 2. The simulated and measured co-polar gain values show reasonable agreement, although the differences in the cross-polar gain values are more significant. The cross-polar results are inherently weaker and hence more susceptible to minor deviations in the practical test implementation.

It was found that the full-width shorted-wall prototype antenna was resonant at 2.47 GHz and presents quite a wide bandwidth of around 500 MHz. The reflection coefficient level at the first and

second harmonic frequencies was found to be 1.71 dB and 2.45 dB, respectively. These results are quite acceptable, as compared with HSAs published in the open literature [15]. It is notable that the measured resonant frequency of the prototype antenna shows good agreement with the prediction. The third prototype exhibited approximately 380 MHz bandwidth, centred at a 2.45 GHz resonance frequency. The rejection levels of the 2nd and 3rd harmonics were about 1.5 dB and 1.9 dB respectively.

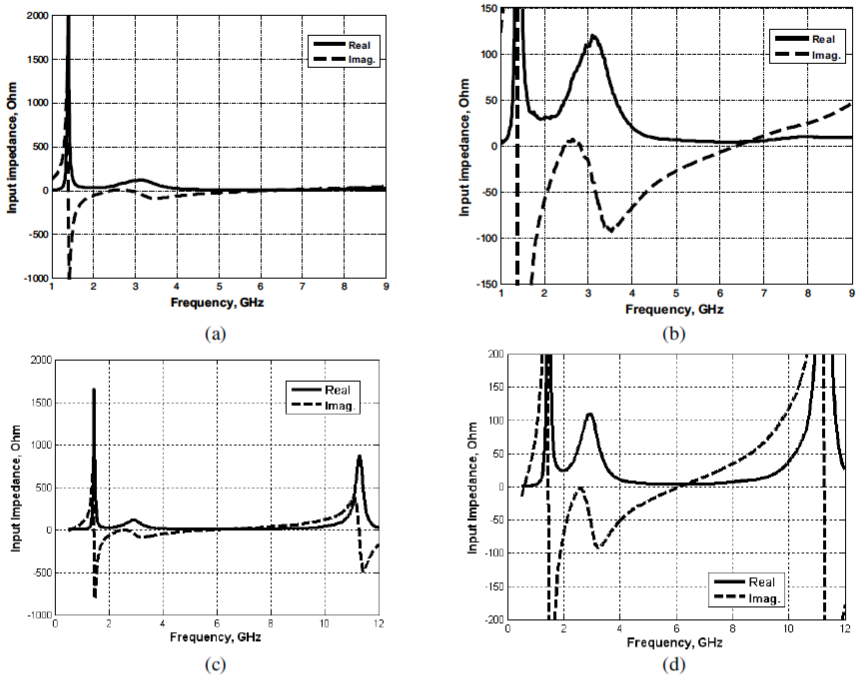

Figure 3: The overall measured input impedance of the patch antennas; (a), (b) full-width shorted wall; and (c), (d) folded wall. (b), (d) show detail expanded from (a), (c).

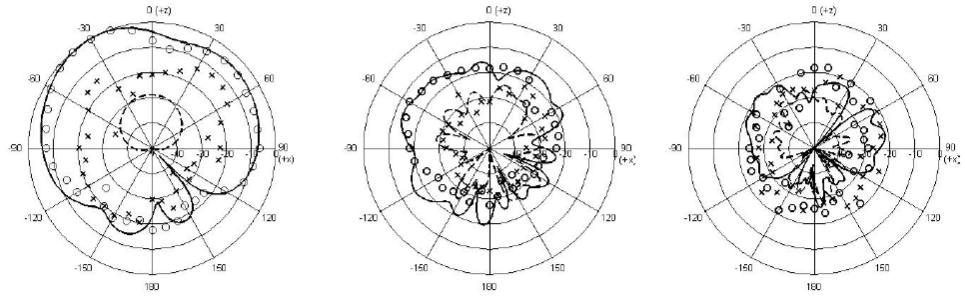

Figure 4: Measured and simulated radiation patterns of the proposed GA-optimised HSA with full-width shorted wall for 2.47 GHz, 4.94 GHz and 7.41 GHz over: z-x plane; ('—' measured E_θ, 'ooo' simulated E_θ, '- - -' measured E_ϕ, 'xxx' simulated E_ϕ).

3. CONCLUSIONS

A novel technique for the design and optimisation of harmonic-suppression patch antennas, applying adaptive surface patch models and genetic algorithms, has been presented. Hardware realisations of three coaxially-fed air-dielectric microstrip patch antennas were used to evaluate and validate the design theory. Comparison of return loss and far field radiation pattern measurements showed good agreement with the predictions. The examples presented confirmed the capability of the proposed method for antenna design using GA and adaptive surface meshing, showing reasonable stability and accuracy in the results.

REFERENCES

1. Elkhazmi, E., N. J. McEwan, and J. Moustafa, "Control of harmonic radiation from an active microstrip patch anrtenna," *Journees Internationale de Nice sur les Antennes*, 313–316, November 1996.
2. Radisic, V., Y. Qian, and T. Itoh, "Class F power amplifier integrated with circular sector microstrip antenna," *IEEE MTT-S Symposium Digest*, 687–690, 1997.
3. Kim, H., K. S. Hwang, K. Chang, and Y. J. Yoon, "Novel slot antennas for harmonic suppression," *IEEE Antennas and Wireless Components Letters*, Vol. 14, No. 6, 286–288, 2004.
4. Sung, Y. J. and Y.-S. Kim, "An improved design of microstrip patch antennas using photonic bandgap structure," *IEEE Transactions on Antennas and Propagation*, Vol. 53, No. 5, 1799–1804, 2005.
5. Radisic, V., S. T. Chew, Y. Qian, and T. Itoh, "High efficiency power amplifier integrated with antenna," *IEEE Microwaves and Guided Wave Letters*, Vol. 7, No. 2, 39–41, February 1997.
6. Sheta, A. F., "A novel H-shaped patch antenna," *Microwave and Optical Technology Letters*, Vol. 29, No. 1, 62–66, April 2001.
7. Chu, Q.-X. and M. Hou, "An H-shaped harmonic suppression active integrated antenna," *International Journal of RF and Microwave Computer-aided Engineering*, Vol. 16, No. 3, 245–249, May 2006.
8. Mangoud, M. A., R. A. Abd-Alhameed, and P. S. Excell, "Optimisation of channel capacity for indoor MIMO systems using genetic algorithm," *Proceedings of the Third International Conference on Internet Technologies and Applications (ITA 09)*, 431–439, Glyndwr University, Wrexham, Wales, UK, 2009.
9. Karamalis, P. D., A. G. Kanatas, and P. Constantinou, "A genetic algorithm applied for optimization of antenna arrays used in mobile radio channel characterization devices," *IEEE Trans. on Intrumentation and Measurements*, Vol. 58, No. 8, 2475–2487, 2009.
10. Carroll, D. L., FORTRAN Genetic Algorithm Driver, Version 1.7, Download from: http://www.staff.uiuc.edu/∼carroll/ga.html, 12/11/98.
11. Abd-Alhameed, R. A., P. S. Excell, and J. Vaul, "Currents induced on wired I.T. Networks by Randomly distributed phones — A computational study," *IEEE Trans. on Electromagnetic Compatibility*, Vol. 48, No. 2, 282–286, May 2006.
12. See, C. H., R. A. Abd-Alhameed, D. Zhou, P. S. Excell, and Y. F. Hu, "A new design of circularly-polarised conical-beam microstrip patch antennas using a genetic algorithm," *Proceedings of the European Conference on Antennas and Propagation: EuCAP 2006*, Session 4PA1, Paper No.100, Nice, France, 2006.
13. Zhou, D., R. A. Abd-Alhameed, and P. S. Excell, "Bandwidth enhancement of balanced folded loop antenna design for mobile handsets using genetic algorithms," *PIERS Online*, Vol. 4, No. 1, 136–139, 2008.
14. Zhou, D., R. A. Abd-Alhameed, C. H. See, P. S. Excell, F. Y. Hu, K. Khalil, and N. J. McEwan, "Quadrifilar helical antenna design for satellite-mobile handsets using genetic algorithms," *Microwave and Optical Technology Letters*, Vol. 51, No. 11, 2668–2671, November 2009.
15. Zhou, D., R. A. Abd-Alhameed, C. H. See, M. S. Bin-Melha, E. T. I. Elferganai, and P. S. Excell, "New antenna designs for wideband harmonic suppression using adaptive meshing and genetic algorithms," *Proceeding of Mosharaka International Conference on Communications, Propagation and Electronics*, Technical Session 1, 5–9, Amman, Jordan, March 5–7, 2010, ISBN: 978-9957-486-06-8.

Two miniaturized printed dual-band spiral antenna designs for satellite communication systems

[1]M.S. Bin-Melha, [1]Chan H. See, [1]Raed A. Abd-Alhameed [1]M. S. Alkambashi, [1]D. Zhou, [1]SMR Jones and [2]PS Excell
[1]Mobile and Satellite Communications Research Centre, University of Bradford, Bradford, UK.
[2]Centre for Applied Internet Research, Glyndwr Wrexham University, UK
m.s.bin-melha@student.bradford.ac.uk r.a.a.abd@bradford.ac.uk
c.h.see2@bradford.ac.uk msaalkha@bradford.ac.uk

Abstract. Two novel reduced-size, printed spiral antennas are proposed for u se in personal communications mobile terminals exploiting the ''big low earth orbit'' (Big-LEO) satellite system (uplink 1.61–1.63 GHz; downlink 2.48–2.5 G Hz). The two proposed antenna give 3.12—6.25% bandwidth at lower resonant mode of 1600MHz, while at the higher resonant mode of 2450MHz a bandwi dth of around 6% is obtained. The experimental and simulated return losses of the proposed antennas show good agreement. The computed and measured gai ns, and axial ratios are presented, showing that the performance of the propose d two antennas meets typical specifications for the intended applications.

Keywords: printed spiral antennas, bandwidth, return losses, axial ratios

1 Introduction

Personal satellite communications systems provide global coverage, especially where there are no nearby terrestrial base stations [1,2]. The majority of systems currently in operation use the 'big low earth orbit' (Big-LEO) satellite system, such as 'Globalstar', which was chosen as a system for detailed study [1]. Handsets of this system require broad-beam radiation patterns with low-cross-polarization, circularly-polarized antennas to get acceptable link margins. These terminals use an uplink band at 1.61-1.6214GHz (L-band) and downlink band at 2.4835-2.5GHz (ISM/S-band).

Satellite mobile communications systems have been available for some years. The systems have experienced some commercial problems, particularly due to the unexpectedly rapid growth of terrestrial systems, but they still have a place in the overall range of wireless communication systems.

The size and appearance of the satellite handset quadrifilar helix antennas and their radomes presents a problem of image and convenience for a public used to the low-profile antennas of terrestrial systems [3-6], whilst the design must achieve specific antenna requirements appropriate for satellite communications.

Reducing the size of the antenna is not easy, since it requires us to have more directive gain than the lowest order (dipole) mode. This causes difficulties if its size is required to be less than about a half wavelength at the operating frequency, due to what is effectively a 'law of physics' for small antennas, the so-called Wheeler limit [7]. Some success in reducing the size of antennas has been achieved by coiling the wire elements, first into helices and later into

spirals [8-13]. Understanding of traditional circular spirals is well advanced, but square designs are likely to fit more conveniently into practical products [8, 9].

Spiral antennas are particularly known for their ability to produce very wide band, almost perfectly circularly-polarized radiation over their full coverage region. As a result of this polarization characteristic and the ability to produce a broad zenith-directed pattern, spiral antennas are popular for use in satellite mobile communication handsets.

In this paper, the achieveable size of the Quadrifilar Square Spiral Antenna (QSSA) discussed in [8- 10] was significantly reduced by a new design of Dual-Arm Square Spiral Antenna (DASSA) on a thin dielectric substrate. This made the new antenna of a size that would be easily mountable on the top of a handheld terminal for use with a low-earth-orbit (LEO) personal satellite communications network. The present program of work has thus initiated a study of a square version of the dual spiral antenna (DASSA) that should satisfy the following design requirements: (i) hemispherical radiation pattern with elevation coverage from the zenith to a nominal minimum elevation angle (typically 10°and 20°); (ii)circular polarization with an axial ratio better than 5dB within the coverage angle; (iii)operational bandwidth to be covered with one antenna operating by itself, either with a single wide bandwidth or, with the assistance of a simple matching circuit, over the two sub-bands of interest; (iv) the size to be minimized by implementing the DASSA over dielectric substrates of high relative permittivity.

The new compact antenna design for handheld satellite mobile communication is investigated and discussed at L band (1.61-1.6214GHz), ISM S-band (2.4835-2.5GHz) and dual L-S bands. Two different antenna types are presented using two-arm spirals connected at the centre by a small rectangular patch and fed via a stripline from each end. Various stripline widths are studied. The inputs return loss and field patterns show quite reasonable results that satisfy the requirements of the communication strategy. The results in terms of the antenna size and radiation performance are addressed and compared to previous published data.

2 Antenna Design Concept and Geometry

The DASSA is an electrically small antenna providing circular polarization over a broad angular region. The antenna consists of two spirals equally spaced circumferentially (placed at 180° to each other) and fed by equal amplitude signals with 180°-phase difference between feeding sources. The DASSA can also be described as two orthogonal bifilar helix antennas fed in phase quadrature, (where a bifilar is a two-element helix antenna). The two spirals are fed at their ends, so that the feed lines in this case do not cause significant problems from the point of view of mutual coupling effects.

The desirable size for the DASSA will be that of the top of a typical personal handset; however, the initial design was made somewhat larger in order to prove the concept [8]: the work presented here uses a solid dielectric beneath the spirals to reduce the antenna size. All antennas were mounted on a thin dielectric substrate of $\varepsilon_r = 2.55$, $\tan\delta = 0.0018$ and thickness of 1.524 mm. Fig.1 shows the geometry of the two proposed antennas for dual-band (L and ISM/S-band) operation. As can be seen, the two antenna sizes and the striplines width used for L and ISM/S bands are (16×12 mm^2 and 0.25mm) and (12.5×8.4mm^2 and 0.75mm) respectively. These two designs will give a variety of choices for antenna designer to further investigate the required antenna performance. Moreover, from the antenna sizes presented, the antennas can easily be mounted on top of a small area of the handset.

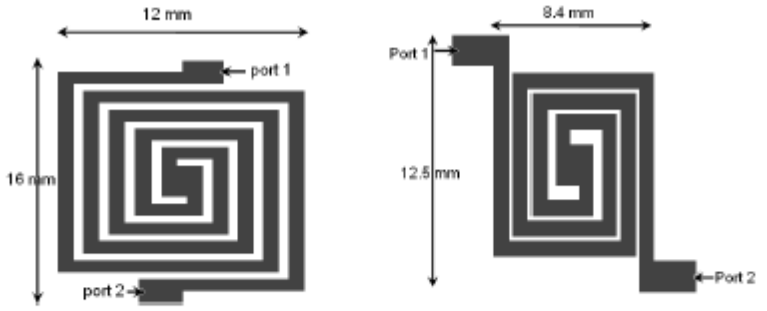

Fig. 1. The geometry of proposed dual-band printed antennas. (Left: Ant1 with stripline width 0.25 mm, Right: Ant2 with stripline width 0.75 mm.)

3 Results and Discussion

The simulated results of all antenna geometries shown in Fig. 1 were carried out using Agilent Advance Design System (ADS) — Momentum 2.5D EM solver [14]. To validate the simulated results, the practical prototypes of the antennas were constructed. Fig.2 and 3 illustrates the computed and experimental results of the two antennas. Two adjacent resonant frequencies in the range of return loss > 10 dB are observed, i.e., 1.61 and 2.485 MHz. 'Ant1' shows the measured impedance bandwidth of 6.25% at 1.6 GHz and 6% at 2.475 GHz whereas the 'Ant2' exhibits narrower bandwidth of 3.15% at 1.6 GHz and 6% at 2.525 GHz. These results confirm that the antennas completely satisfy the desired L frequency band (1.61-1.624 GHz) and ISM/S band (2.4835-2.5GHz) band respectively.

Fig.4 and 5 depicts the axial ratio of the proposed antennas for y-z plane ($\varphi = 90°$). As can be noticed, an axial ratio of less than 3dB over ±45°elevation angle for 'Ant1' whereas it is less than 4 dB over ±40°elevation angle for 'Ant2'. The measured gains for two proposed antenna are shown in Fig.6. The measured gains for both antennas varied between 1.25 and 2.25 dBi over the entire L band; and between 1.4 and 2.75 dBi over the ISM/S band. These results are quite promising and encouraging for practical deployment.

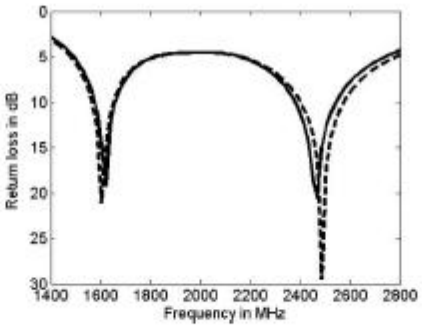

Fig. 2. Return loss of the proposed antenna (Ant1), where '———' simulated, -------- 'measured'

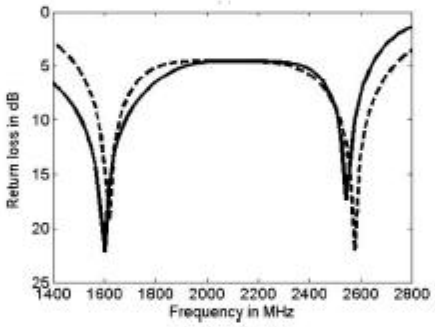

Fig. 3. Return loss of the proposed antenna (Ant2) , where '———' simulated, -------- 'measured'

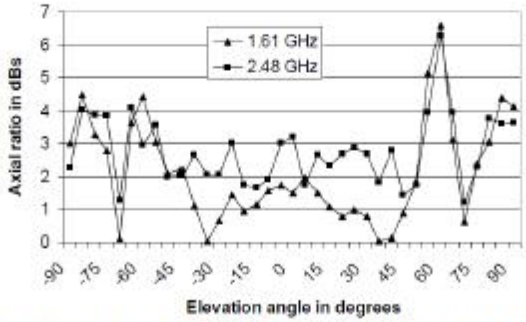

Fig. 4. Measured axial ratios for two operating frequencies versus elevation angle at φ = 90° for antenna (Ant1)

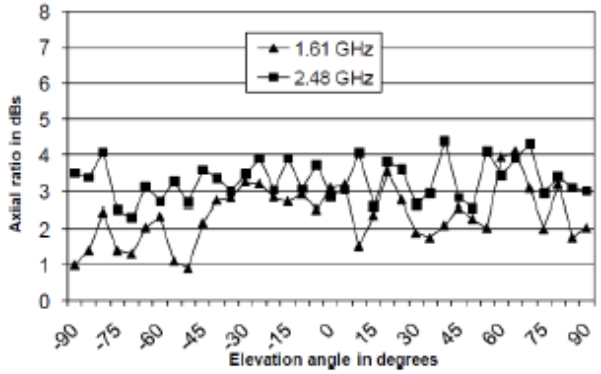

Fig. 5. Measured axial ratios for two operating frequencies versus elevation angle at $\varphi = 90°$ for antenna (Ant2)

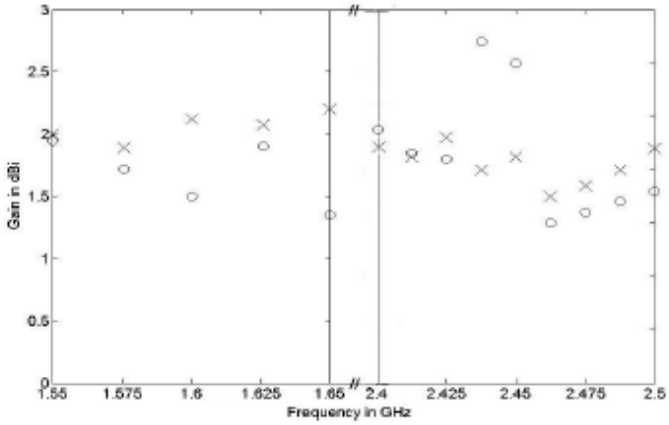

Fig. 6. Measured broadsight gains of the proposed dual-band antennas. (where xxxx is for Ant1 and ooo is for Ant2).

4 Conclusion

A new technique was discussed that reduced the antenna size for satellite-mobile handsets. Different stripline widths were introduced to achieve the frequency response and radiation performance required for Big LEO satellite mobile communications. Two different antenna geometries have been presented. The new designs were found to be very compact compared

with four-square spirals on the same dielectric substrate described in previous studies. The larger antenna achieves a 6% impedance bandwidth in both bands, whilst the more compact design is limited to 3.15% in the lower band. The results in terms of the return loss are extremely promising and the field radiations are acceptable for both bands of interest, almost covering a ±45° range of elevation angles.

References

1. Dietrich, F.J., Metzen, P. & Monte, P., 'The globalstar cellular satellite system', IEEE Trans. Antennas and Propagation, Vol. 46. No. 6, pp. 935-942 (1998)
2. Evans, J.V., 'Satellite systems for personal communications', IEEE Antennas and Propagation Magazine, Vol. 39, No. 3, pp.7-20 (1997)
3. S.M. Daddish, R.A. Abd-Alhameed, and P.S. Excell: 'New Designs for Dual Band Antennas for Satellite-Mobile Communications Handsets', Applied Computational Electromagnetics Society Journal, Vol. 15, No. 3, pp. 248-258 (2000)
4. Agius, A.A., Leach, S.M., Suvannapattana, P. & Saunders, A.R., 'Effects of the human head on the radiation pattern performance of the quadrifilar helix antenna', IEEE Int. Symp. On Antennas and Propagation, 1999, Vol. 2, pp. 1114-1117 (1999)
5. Suvannapattana, P., Agius, A.A. & Saunders, S.R., 'Methods for minimizing quadrifilar helix antenna interactions with the human head', IEE Seminar on Electromagnetic Assessment and Antenna Design Relating to Health Implications of Mobile Phones, IEE Pub. No. 1999/043, pp. 11/1-11/4 (1999)
6. Ermutlu, M.E., 'Modified quadrifilar helix antennas for mobile satellite communication', IEEE Conf. on Antennas and Propagation for Wireless Communications, pp. 141-144 (1999)
7. H.A. Wheeler: 'Fundamental Limitations of Small Antennas', Proc. IRE, Vol. 35, pp. 1479-1484 (1947)
8. K.Khalil, R.A. Abd-Alhameed and P.S. Excell, 'Dual–band quadrifilar square spiral antenna for satellite-mobile handsets' IEE International Conference on Antennas and Propagation, Exeter, Vol. 1, pp. 186-189 (2003)
9. D.Zhou, R. A. Abd-Alhameed, C.H. See, P.S Excell, Y.F.Hu and etc, "Quadrifilar Helical Antenna Design for Satellite-Mobile Handsets Using Genetic Algorithms", *Microwave and Optical Technology Letters*, Vol.51, No.11, pp.2668-2671 (2009)
10. R. A. Abd-Alhameed, D.Zhou, C.H.See and P.S Excell, "Design of Dual-Band Quadrifilar Spiral Antennas For Satellite-Mobile Handsets", *Microwave and Optical Technology Letters*, Vol.52, pp.987-990 (2010)
11. K. Alazhari, R.A. Abd-Alhameed, P.S. Excell and K. Khalil, 'New designs for single and dual band quadrifilar spiral antennas (QSA) for satellite-mobile handsets', IEE International Conference in Antennas and Propagation, Manchester, Vol. 2, pp. 750-753 (2001)
12. H. Nakano, S. Okuzawa, K. Ohishi, H. Mimaki and J. Yamauchi, 'A Curl Antenna', IEEE Transactions on Antennas and Propagation, Vol. 41, No.11, pp. 1570-1575 (1993)
13. J. S. Colburn and Y. Rahmat-Samii, 'Quadrifilar-Curl Antenna for the Big-LEO Mobile Satellite Service System', IEEE Antennas and Propagation Society International Symposium Digest, Vol. 2, pp. 1088-1091 (1996)
14. Momentum- 2.5D EM Simulator, Agilent Advance Design Systems, available: http://www.home.agilent.com/agilent/

Harmonic Rejection Triangle Patch Antenna

M. S. Bin-Melha[1], R. A. Abd-Alhameed[1], C. H. See[1], M. Usman[2], I. T. E. Elfergani[1], and J. M. Noras[1]

[1]Mobile and Satellite Communications Research Centre, University of Bradford, Bradford, UK
[2]Department of Electrical Engineering, University of Hai'l, KSA

Abstract— A triangular patch harmonic-rejecting antenna at 0.7 GHz is proposed. Simulated results obtained using HFSS software show that a triangular antenna with shorting pin feed, and of compact size, exhibits high reflection coefficients at the second and third harmonics (−0.12 dB at 1.4 GHz and −0.16 dB at 2.1 GHz) respectively.

1. INTRODUCTION

Patch antennas, based on printed circuit technology, are flat radiating structures on top of ground-plane-backed substrates, and have the advantages of being compact antennas with low manufacturing cost and high reliability. However, there are difficulties in practice in achieving high bandwidth and efficiency. Nevertheless, improvements in the properties of suitable dielectric materials and in design techniques have led to an enormous growth in popularity of microstrip patch antennas, and there are now a large number of commercial applications. Many shapes of patches are possible, with varying applications, but the most popular are rectangular, circular or thin strips [1].

Patch antennas are typically light in weight, low in cost, and widely used in communications. On the downside, they suffer from excess harmonic radiation. Fortunately, many methods have been developed for suppression of these harmonics. One effective approach to suppress harmonics in microstrip patch antennas (MPA) is to use electromagnetic band gap structures (EBG) [2–5].

In Ref. [1], periodic slots are etched in the ground plane of a MPA, which behave as EBG structures. Higher order harmonics fall in the stop band of the EBG and are suppressed. Another approach is to use defected ground structures (DGS) on microstrip feed lines. Up to third order harmonic rejection was reported combining DGS and EBG structure [4]. However, a problem for the EBG structure is backside radiation due to the etched slots just beneath the radiating patch [2–4]. The radiation pattern differs significantly from that of a single MPA. Recently, another approach is reported which used a 1-D Photonic Band Gap (1-D PBG) structure with a DGS on the feed line for impedance matching and harmonic rejection [5]. Up to second harmonic rejection was reported.

Additionally, a method involving a low-pass filter composed of a circular head dumbbell shaped DGS structure and a circular head shunt open microstrip stub on the feed line was able to suppress up to the fourth harmonic effectively [6]. Finally, second and third harmonics have been eliminated with a microstrip patch antenna with a proximity coupled feeding line by adjusting the length of feed line and introducing one resonant cell [7].

A triangular patch antenna with shorting pin used for suppressing the harmonics is proposed in this paper. This work is very similar to [8], but its performance has been optimized to serve its application.

2. ANTENNA DESIGN CONCEPT

The geometry of the proposed antenna is shown in Fig. 1. This triangular patch is designed on a FR4 substrate of thickness 1.6 mm and relative permittivity of 4.4, mounted over the ground plane. The sizes of the printed antenna patch and the ground plane are $90 \times 25\,\text{mm}^2$ and $135 \times 65\,\text{mm}^2$ respectively. The co-axial or probe feed technique is adopted on this antenna so that the feed point can be placed at any place in the patch to match its 50 ohm input impedance.

3. RESULT AND DISCUSSIONS

Figure 2 shows the simulated reflection coefficient of the proposed antenna. As can be seen, the antenna is designed to operate at 700 MHz and its corresponding second and third harmonics, at 1.4 GHz and 2.1 GHz, were eliminated. By adjusting the location of shorting pin good impedance matching can be easily obtained at the fundamental frequency. As can be seen, the suppression of

the harmonics does not produce any harmful effects on the impedance matching at the fundamental frequency. The simulations were carried out using the HFSS simulator [9].

To overcome the spurious radiation problem, it is necessary to control the input impedance of the antenna and create a reactive termination at harmonic frequencies. The input impedance of the proposed antenna was investigated over a wide frequency band as shown in Fig. 3. The input impedance of this antenna at the fundamental operating frequency and its first two harmonics shows that almost perfect matching to 50 ohm was attained at the fundamental frequency, while fairly small resistive impedances at harmonic frequencies were observed.

Figures 4 and 5 show the corresponding harmonic current distributions on the patch. The position of the shorting pin is optimally set adjacent to a point of maximum voltage, which corresponds to a point of minimum current distribution on the patch.

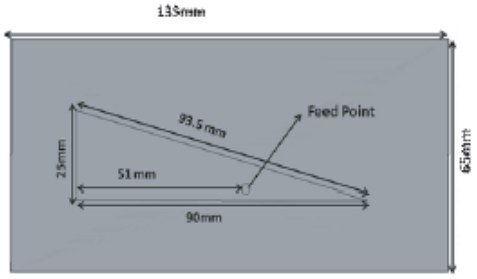

Figure 1: Basic geometry of the proposed antenna.

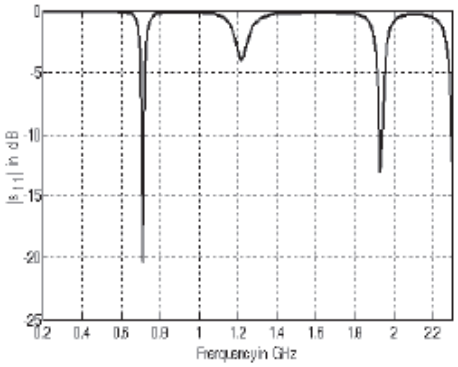

Figure 2: Reflection coefficient of the antenna, and its harmonics.

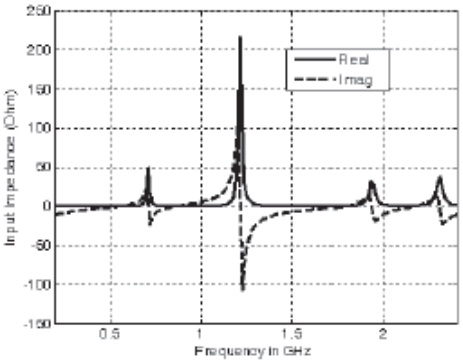

Figure 3: The input impedance of the proposed patch antenna.

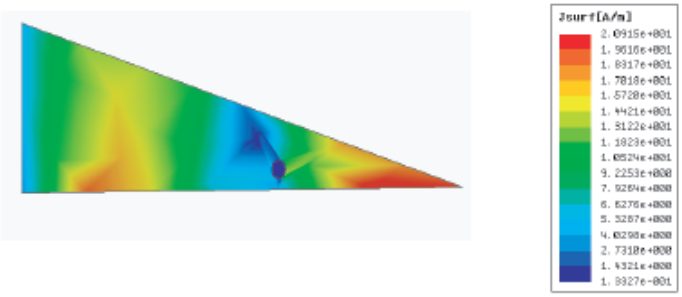

Figure 4: Current distribution on the antenna at the second harmonic frequency.

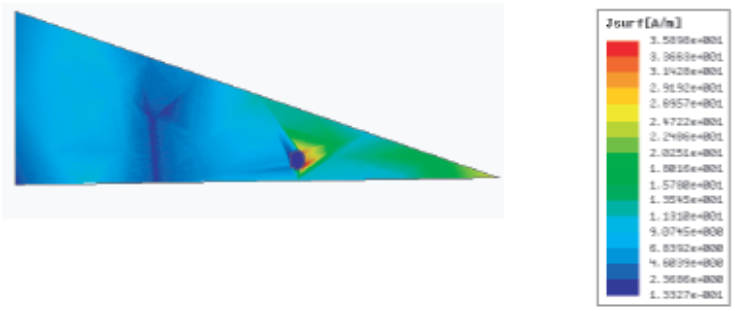

Figure 5: Current distribution on the patch at the third harmonic frequency.

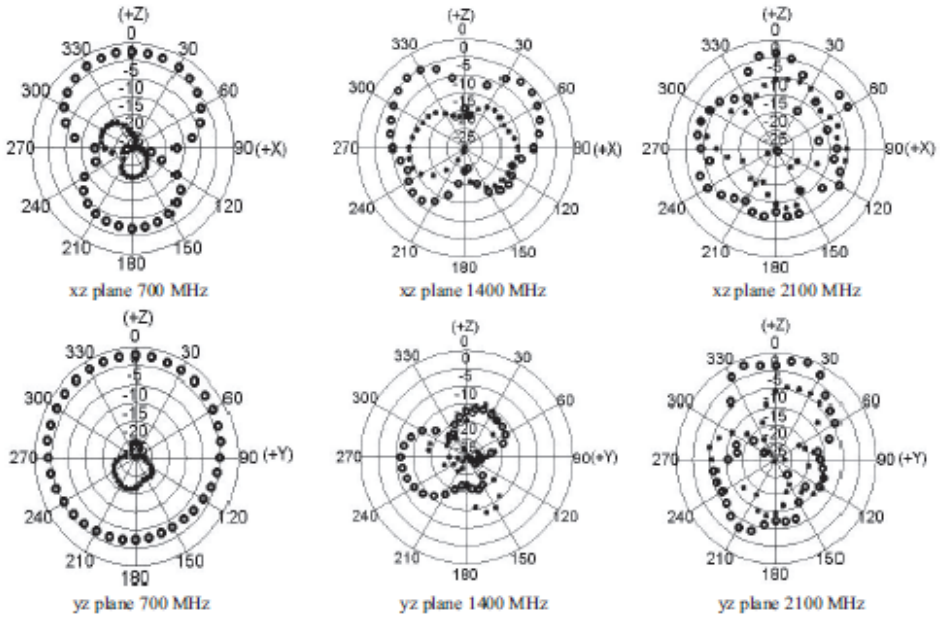

Figure 6: Radiation patterns of antenna design at fundamental, second and third harmonic frequencies. 'ooo': Simulated co-polar, '***': Simulated cross-polar.

The radiation patterns in the xz and yz planes for the antenna shown in Fig. 1 is presented in Fig. 6, at the fundamental, second and third harmonic frequencies. The results confirm viable levels of suppression of harmonics. In other words, these results show that the radiation patterns at the harmonic frequency are acceptably suppressed.

4. CONCLUSION

In this paper, a shorting pin technique for designing a triangular patch with suppression characteristics over harmonic frequency bands has been proposed and investigated. The reflection coefficient was about -0.12 dB at the second harmonic and -0.16 dB at the third harmonic. According to the results obtained, this antenna with its simple harmonic suppression structures is quite effective. Therefore, the proposed antenna can be suitable for active integrated antenna.

REFERENCES

1. Saunders, S. R. and A. Aragon-Zavala, *Antenna and Propagation for Wireless Communication Systems*, John Wiley & Sons, England, 2007.

2. Horri, Y. and M. Tsutsumi, "Harmonic control by photonic bandgap on microstrip patch antenna," *IEEE Microwave Guided Wave Lett.*, Vol. 9, 13–15, 1999.
3. Sung, Y. J., M. Kim, and Y. S. Kim, "Harmonics reduction with defected ground structure for a microstrip patch antenna," *IEEE Antennas Wireless Propag. Lett.*, Vol. 2, 111–113, 2003.
4. Liu, H., Z. Li, X. Sun, and J. Mao, "Harmonic suppression with photonic bandgap and defected ground structure for a microstrip patch antenna," *IEEE Microwave Wireless Compon. Lett.*, Vol. 1, 55–565, 2005.
5. Sung, Y. J. and Y.-S. Kim, "An improved design of microstrip patch antennas using photonic bandgap structure," *IEEE Trans. Antennas Propag.*, Vol. 53, 1799–1804, 2005.
6. Mandal, M. K., P. Mondal, S. Sanyal, and A. Chakrabarty, "An improved design of harmonic suppression for microstrip patch antennas," *Microwave and Optical Technology Letters*, Vol. 49, No. 1, 103–105, January 2007.
7. Luis, I.-S., J.-L. Vázquez-Roy, and E. Rajo-Iglesias, "Proximity coupled microstrip patch antenna with reduced harmonic radiation," *IEEE Transactions on Antennas and Propagation*, Vol. 57, No. 1, 27–32, January 2009.
8. Olaimat, M. M. and N. I. Dib, "A study of 15°–75°–90° angles triangular patch antenna," *Progress In Electromagnetics Research Letters*, Vol. 21, 1–9, 2011.
9. *Ansoft High Frequency Structure Simulator v10 Uses Guide*, CA, USA.

www.ietdl.org

Published in IET Microwaves, Antennas & Propagation
Received on 31st May 2010
Revised on 11th March 2011
doi: 10.1049/iet-map.2010.0218

In Special Section on Selected Papers from Mosharaka International Conference on Communications, Propagation and Electronics (MIC-CPE2010)

ISSN 1751-8725

New antenna designs for wideband harmonic suppression using adaptive surface meshing and genetic algorithms

D. Zhou[1] *R.A. Abd-Alhameed*[2] *C.H. See*[2] *M.S. Bin-Melha*[2] *Z.B. Zainal-Abdin*[2] *P.S. Excell*[3]

[1]*Surrey Space Centre, University of Surrey, Guildford, UK*
[2]*Mobile and Satellite Communications Research Centre, University of Bradford, Bradford, UK*
[3]*Centre for Applied Internet Research, Glyndwr University, Wrexham, UK*
E-mail: r.a.a.abd@bradford.ac.uk

Abstract: A novel design strategy for microstrip harmonic-suppression antennas is presented. The computational method is based on an integral equation solver using adaptive surface meshing driven by a genetic algorithm (GA). Three examples are illustrated, all involving design of coaxially-fed air-dielectric patch antennas incorporating shorting and folded walls. The characteristics of the antennas in terms of the impedance responses and far-field radiation patterns are discussed theoretically and experimentally. The performances of all of the GA-optimised antennas were shown to be excellent and the examples presented show the capability of the proposed method in antenna design using GA.

1 Introduction

Active transmitting antennas often suffer from significant non-linearity; the driving transistor drain (or collector) produces time-harmonic currents which feed directly into the radiator, resulting in unwanted radiated power [1]. In active antenna design these unwanted harmonic currents can be attenuated (or substantially eliminated) using the radiator itself, in which case the active circuit does not require any additional complexity for harmonic tuning, thus contributing to the desired compactness of the design.

Harmonic-suppression antennas (HSAs) are used to suppress power radiation at harmonic frequencies from active integrated antennas. An antenna that presents a good impedance match at the fundamental design frequency (f_o) and maximised reflection at harmonic frequencies is said to be a HSA. In addition, the input impedance of any HSA design has to have minimised resistance at the harmonic frequencies and hence will be largely reactive [2]. Several techniques have been proposed to control such harmonics, such as shorting pins, slots or photonic bandgap structures [3, 4]. In [5], a modified rectangular patch antenna with a series of shorting pins added to the patch centre line was applied to shape the radiated second harmonic from the active amplifying-type antenna, in order to increase the transmitter efficiency. Unfortunately, the proposed design does not provide suppression for the third harmonic. A circular sector patch antenna with 120° cut out was investigated and proved to provide additional harmonic suppression for the third harmonic, also claiming a further enhancement in the transmitter efficiency [2]. Further, an H-shaped patch antenna was designed and applied in oscillator-type active integrated antennas for the purpose of eliminating the unwanted harmonic radiation [6, 7].

Generally, most of the published designs for modified patch HSA have been based on a specific reference antenna, suggesting that the proposed techniques for rejecting harmonic radiation have specific constraints imposed onto them. For example, in [8] a microstrip-line fed slot antenna was developed for harmonic suppression without using a reference antenna. This was achieved with a rather complex geometry for 5 GHz operation. This process does not usefully generalise, so that if a new operating frequency is required, then the whole structure must be redesigned. Thus, there exists a clear motivation to develop a coherent design strategy for microstrip HSA in active integrated applications. In this paper we adopt a computational technique using adaptive surface meshing driven by a genetic algorithm (GA).

2 GA and adaptive meshing program

An approach using the GA in co-operation with an electromagnetic simulator has been introduced for antenna design and has become increasingly popular recently [9]. For example, GA has been employed to design wire antennas [10, 11] and microstrip antennas [12]. Other uses have also been developed, such as wideband antenna designs based on the fundamental requirement for near-field imaging tools which are needed for microwave breast cancer detection: this was reported as having used GA as the main optimisation tool [13]. Another application applied

to beam-control of an antenna array was also derived through the use of a GA, based on adjusting the required reactance values to obtain the optimum solution [14]. In addition, GA can enhance antenna designs for multiple input multiple output (MIMO) systems, which dramatically increase channel capacity in wireless communication systems [15–18]. The GA-optimised MIMO antenna designs provide substantial size reduction, reduced power consumption [17] and cost minimisation [16] in such systems.

The benefit of applying GA methods is that they provide fast, accurate and reliable solutions for antenna structures. A GA driver [19], written in Fortran, was adopted in this work in conjunction with the authors' Fortran source code [20], which was used to evaluate the randomly generated antenna samples. Several antenna designs, derived using GA in previous work by the authors [21–23], have shown the GA method to be an efficient optimisation tool that can be used to search and find rapid solutions for complex antenna design geometries.

An adaptive meshing program was also written in Fortran by the present authors and added as a subroutine to the GA driver, with the primary objective of simulating air-dielectric planar microstrip patch antenna designs: this used a surface patch model in co-operation with a GA. In addition to microstrip patch designs, the program can support the design of any three-dimensional (3D) antenna geometry structure, including moderate amounts of dielectric materials. The present work is an extended version of preliminary work reported in [24].

An antenna under GA optimisation needs to be defined by a number of parameters that can define its configuration. For the electromagnetic surface patch model used, the antenna geometry is adaptively divided into optimum numbers of trilateral and quadrilateral polygons, each polygon node being specified by its x, y and z co-ordinates, subject to the defined antenna parameters. These polygonal surfaces are then optimally subdivided into a set of rectangular and triangular surface patches, constrained to be small compared with the operating wavelength, and then the basis functions are adaptively generated over these patches using a designated algorithm as shown in Fig. 1.

The design of coaxially-fed air-dielectric microstrip harmonic-rejecting patch antennas for 2.4 GHz was investigated, enforcing suppression of the first two harmonic frequencies, using a GA. The designs included patch antennas with a shorted wall, as first presented in [24] and an extended work on a new design with a folded wall is also presented in this paper.

3 Simulation and results

Simple coaxially-fed air-dielectric patch antennas with shorted and folded walls, mounted on an infinite ground plane and operating at 2.4 GHz, were selected for this study as simple examples to demonstrate acceptable harmonic suppression [5]. The proposed outline antenna designs are shown in Fig. 2. The designs include a full-width shorted wall, a truncated shorted wall and a folded wall; each individual antenna configuration model is modelled using surface patch meshing, as Fig. 2 illustrates. The full-width shorted patch is subdivided into four trilaterals and two quadrilaterals, including the conducting shorted wall, as illustrated in Figs. 2*a* and *b*. This design required six parameters to be defined. The second design was subdivided into seven trilaterals to model the surface patch and one quadrilateral to represent the truncated conducting wall, as illustrated in Figs. 2*c* and *d*. This model was implemented using seven GA input parameters. The last design example is similar to the first, but uses a modified folded wall, as shown in Figs. 2*e* and *f*, in which the total surface area was subdivided into four trilaterals and three quadrilaterals. The fold in the wall means that it is no longer electrically connected to the ground plane, although the folded portion will provide strong capacitive coupling to ground. In this model eight GA parameters were considered.

Table 1 presents the GA input parameters in which the possible range of values is shown for all three examples considered. For this optimisation process, real-valued GA chromosomes were used. It should also be noted that the fundamental, first and second-harmonic frequencies were considered within the GA cost function. The randomly generated antenna configurations were evaluated for maximum fitness using the following cost function

$$F = \left[1 + w_1\left|\frac{Z(f_o) - 50}{50}\right| + \sum_{i=2}^{n} w_i\left\{|\Gamma(if_o) - 1| + \frac{R(if_o)}{50}\right\}\right]^{-1} \quad (1)$$

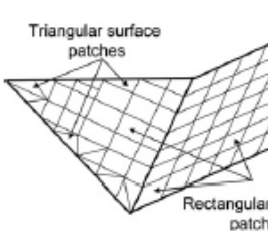

Fig. 1 *Adaptive surface patch meshing used for antenna modelling*

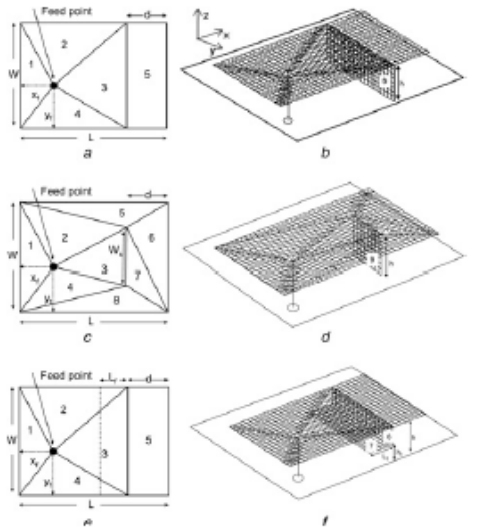

Fig. 2 *Proposed antenna models*
a and *b* Full-width shorted wall
c and *d* Truncated shorted wall
e and *f* Folded wall
a, *c* and *e*: Top view
b, *d* and *f*: 3D view of surface patch meshing

Table 1 Summary of GA input parameters, antenna variables and best solutions for the proposed designs, including shorted and folded walls

GA parameters	HSA parameters Parameters (m)	Fully shorted Optimal (m)	Truncated shorted Optimal (m)	Folded wall Optimal (m)
	antenna length (L) (0.03–0.06)	0.03950	0.03350	0.04540
no. of population size = 4	antenna width (W) (0.02–0.06)	0.03305	0.03820	0.03006
no. of parameters: 6 (Fig. 1*a*), 7 (Fig. 1*c*), 8 (Fig. 1*e*)	shorting or folded wall position (d) (0.002–0.03)	0.00972	0.00986	0.00748
probability of mutation = 0.02	antenna height (h) (0.003–0.01)	0.0079	0.00336	0.00989
maximum generation = 500	feeding point at x-axis (X_f) (0.004–0.02)	0.00723	0.01685	0.00571
no. of possibilities = 32 768	feeding point at y-axis (Y_f) (0.004–0.02)	0.01752	0.01923	0.01392
	variable shorting wall width (W_a) (0.001–0.03)	—	0.02474	—
	extended folded wall length (L_f) (0.005–0.015)	—	—	0.01327
	extended folded wall height (h_f) (0.001–0.0035)	—	—	0.00159

where F is the fitness of the cost function; $n = 3$; W_1, W_2 and W_3 are the weight coefficients of the cost function and they were optimally found to be 0.6, 0.4 and 0.4 after a few trials. The objective is to maximise the fitness F. This implies that very good impedance matching at the fundamental frequency and maximised reflection with minimised resistance at the harmonic frequencies would be desired to achieve a good HSA design solution. For this optimisation procedure, real-valued GA chromosomes were used to investigate the existence of the fundamental and first two harmonic frequencies.

For validation, prototypes of the GA-optimised HSAs of the three models shown in Fig. 2 were designed and tested. Copper sheet with thickness of 0.5 mm was used for the patch antenna, shorted/folded wall and the ground plane. The ground plane size was set to 140 mm × 140 mm; this relatively large size being chosen in order to attenuate the effect of the edges of the finite ground plane. The return losses were validated and the measured results compared with the calculations are shown in Fig. 3. As can be seen, the results for rejection levels of second and third harmonics were quite encouraging and no other resonances or ripples were found over the harmonic frequency bands.

It was found that the full-width shorted-wall prototype antenna was resonant at 2.47 GHz and presented quite a wide bandwidth of around 500 MHz. The reflection coefficient

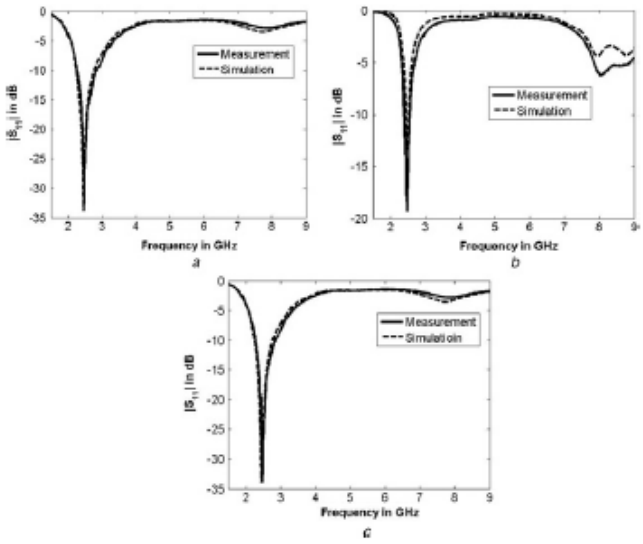

Fig. 3 *Performance of the measured and calculated return losses of the GA-optimised HSAs*
a Full-width shorted wall
b Truncated shorted wall
c Folded wall

IET Microw. Antennas Propag., 2011, Vol. 5, Iss. 9, pp. 1054–1061
doi: 10.1049/iet-map.2010.0218

levels at the second and third harmonic frequencies were found to be 1.71 and 2.45 dB, respectively. These results are quite acceptable, as compared with HSAs published in the open literature [25]. It is notable that the measured resonant frequency of the prototype antenna shows good agreement with the prediction. The second prototype antenna was resonant at 2.48 GHz and presented a narrower bandwidth (around 150 MHz), compared to the first design. This is mainly because the height of this antenna is much lower (about 3.36 mm) than the first design (7.9 mm), correlating with previous experience that has shown that the antenna height has a most important influence on bandwidth enhancement of microstrip patch antennas. The third prototype exhibited approximately 380 MHz bandwidth, centred at a 2.45 GHz resonance frequency. The rejection levels of the second and third harmonics were about 1.5 and 1.9 dB, respectively. It should be noted that the suppression performance at third harmonic frequency for the second prototype antenna could be limited due to the degraded return loss response around 8 GHz, whereas its suppression performance is superior to other two designs at the second harmonic frequency.

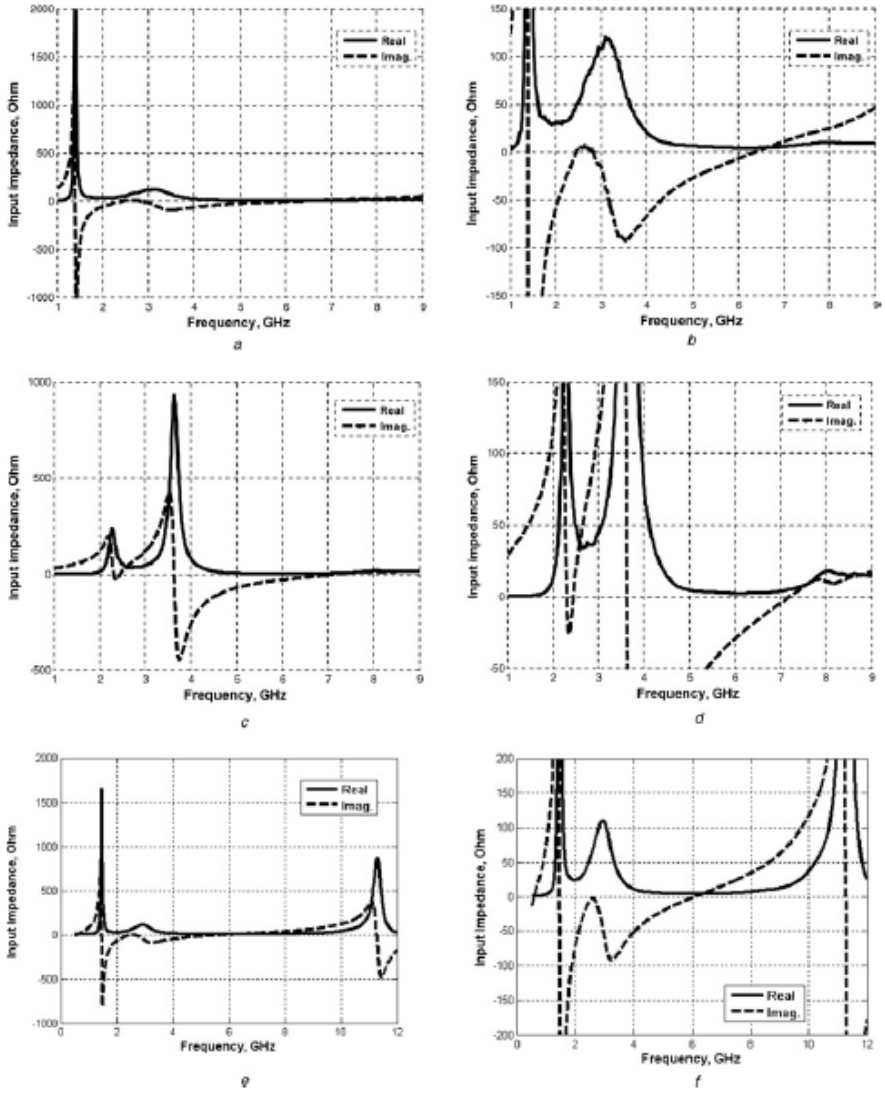

Fig. 4 *Overall measured input impedance of the patch antennas*
a and *b* Full-width shorted wall
c and *d* truncated shorted wall
e and *f* Folded wall
b, *d* and *f* Show detail expanded from *a*, *c* and *e*

Table 2 Performance of antenna input impedance at the fundamental and first two harmonics for the three antennas shown in Fig. 2

Full-width shorted wall			Truncated shorted wall			Folded wall		
Frequency, GHz	Antenna input impedance, Ω		Frequency, GHz	Antenna input impedance, Ω		Frequency, GHz	Antenna input impedance (Ω)	
	Real	Imaginary						
f_o: 2.47	49.87	−0.587	f_o: 2.48	52.75	7.828	f_o: 2.45	49.33	−11.88
$2f_o$: 4.94	6.283	−28.917	$2f_o$: 4.96	4.254	−73.672	$2f_o$: 4.90	5.021	−24.81
$3f_o$: 7.41	6.839	17.64	$3f_o$: 7.44	5.332	15.545	$3f_o$: 7.35	4.606	20.07

The input impedances of the prototype antennas were also measured over a wide frequency band, as shown in Fig. 4. The measured input impedance of these antennas at the fundamental operating frequency and its first two harmonics show that almost perfect matching to 50 Ω was attained at the fundamental frequency, while fairly small resistive impedances at the harmonic frequencies were observed, as illustrated in Table 2. This clearly shows that the design objectives were met. The real part of the input impedance of the proposed antenna is almost constant (less than 10 Ω) across the harmonic frequency bands for all prototypes, as observed. This is a very promising characteristic of the design procedure for such harmonic suppression. The antennas were, therefore, capable of achieving rejection of harmonics from the non-linear active devices, even when the operating frequency was slightly varied. This is because the proposed antennas provide the required reactive termination around the harmonic frequencies.

Measurements of the far-field radiation patterns of the prototype antennas were carried out in a far-field anechoic chamber using an elevation-over-azimuth positioner, with the elevation axis coincident with the polar axis ($\theta = 0°$) of the antenna's co-ordinate system. The reference antenna was a broadband horn (EMCO type 3115) positioned at 4 m from the antenna under test. The azimuth drive thus generated cuts at constant φ. The elevation positioner was rotated over θ from $-180°$ to $180°$ in $5°$ increments. Two principal-plane pattern cuts (i.e. the $z-x$ and $z-y$ planes) were taken at the fundamental and second and third harmonic frequencies for each design.

The simulated and measured radiation patterns in the $z-x$ and $z-y$ planes for all prototype antennas shown in Fig. 2 are presented in Figs. 5–7 for the fundamental, second and third harmonic frequencies, respectively. The radiation patterns for all the three proposed antennas are similar for both plane cuts. It should be noted that, like simple patch antennas, the proposed HSA shows a broadside-type radiation pattern with maximum gain at around $-30°$ for the $z-x$ plane, whereas approximately symmetrical radiation patterns with mixed conical and broadside radiation are

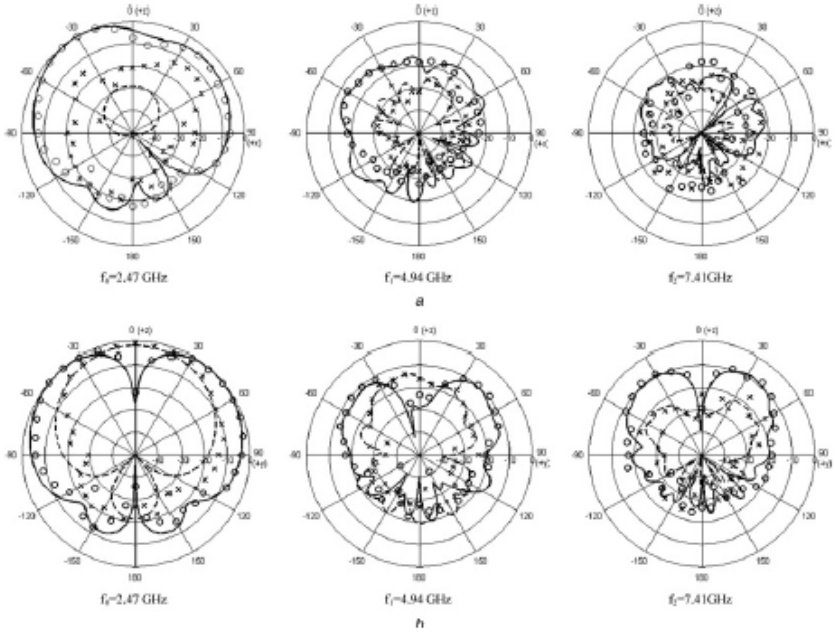

Fig. 5 *Measured and simulated radiation patterns of the proposed GA-optimised HSA with full-width shorted wall for 2.47, 4.94 and 7.41 GHz ('———' measured E_θ, 'o o o' simulated E_θ, '- - - -' measured E_ϕ, 'x x x' simulated E_ϕ)*

a z-x plane
b z-y plane

IET Microw. Antennas Propag., 2011, Vol. 5, Iss. 9, pp. 1054–1061
doi: 10.1049/iet-map.2010.0218

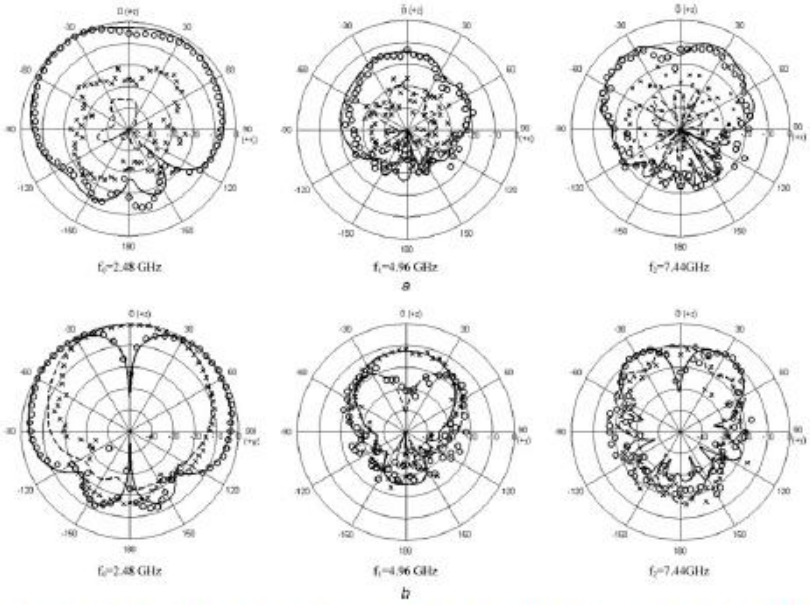

Fig. 6 *Measured and simulated radiation patterns of the proposed GA-optimised HSA with a truncated shorted wall for 2.48, 4.96 and 7.44 GHz ('———' measured E_θ, 'o o o' simulated $E\theta$, '- - - -' measured E_ϕ, 'x x x' simulated E_ϕ)*

a zx plane
b zy plane

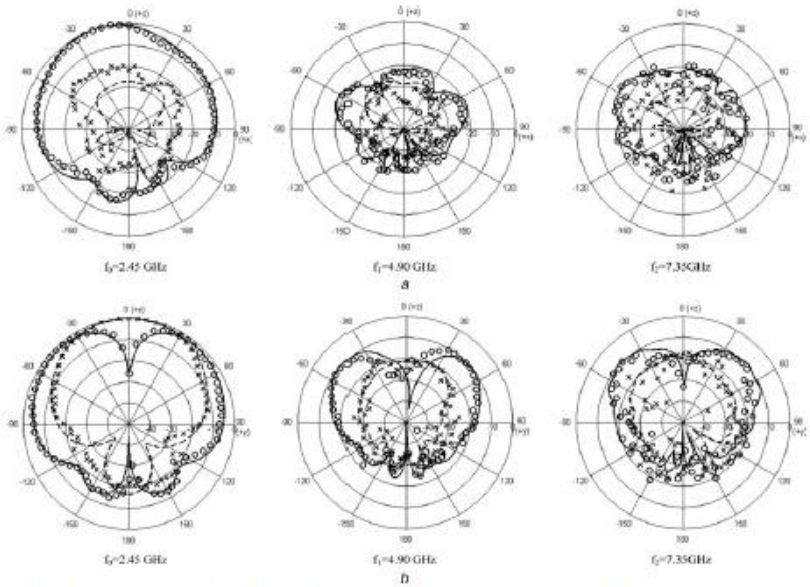

Fig. 7 *Measured and simulated radiation patterns of the proposed GA-optimised HSA with a folded wall for 2.45, 4.90 and 7.35 GHz ('_____' measured E_θ, 'o o o' simulated $E\theta$, '- - - -' measured E_ϕ, 'x x x' simulated E_ϕ)*

a zx plane
b zy plane

Table 3 Simulated and measured gain values at the fundamental frequency for the three antennas shown in Fig. 2

Type of antenna		Full shorted wall		Truncated shorted wall		Folded wall	
Antenna gain, dBi		Measured	Simulated	Measured	Simulated	Measured	Simulated
Frequency, GHz		$f_o = 2.47$		$f_o = 2.47$		$f_o = 2.45$	
$x-z$ plane	H.P.*	−8.35	−24.74	−14.16	−31.58	−13.45	−23.71
	V.P.*	4.14	4.06	3.56	4.37	5.01	5.03
$y-z$ plane	H.P.	1.71	2.29	0.94	1.92	3.11	3.98
	V.P.	0.54	0.16	0.43	1.57	2.04	2.50

*H.P./V.P. indicates the polarisation of the reference Horn antenna; H.P: horizontal polarisation, V.P: vertical polarisation

observed for the $z-y$ plane. These results are in good agreement and confirm a viable level of suppression of second and third harmonic levels. These levels may be summarised as follows: for the fully shorted-wall design the maximum second and third harmonic radiation amplitudes were lower than 13 and 18 dB (respectively) below the fundamental for the $z-x$ plane and 10 and 9 dB below for the $z-y$ plane; similarly for the truncated shorted-wall design they were lower than 12 and 9 dB below for the $z-x$ plane and 11 and 8 dB below for the $z-y$ plane. However, for the folded-wall design the harmonic levels were rather better, at 20 and 16 dB below for the $z-x$ plane and 11 and 10 dB below for the $z-y$ plane. The simulated and measured gain values at the fundamental frequency for the three antennas shown in Fig. 2 are presented in Table 3. The simulated and measured co-polar gain values show reasonable agreement, although the differences in the cross-polar gain values are more significant. The cross-polar results are inherently weaker and hence more susceptible to minor deviations in the practical test implementation.

The designs including patch antennas with shorted and folded walls are described as above and their corresponding results are discussed in terms of return loss, input impedance, radiation patterns and antenna gain, subject to the design criteria for a harmonic-suppression patch antenna. The design goals were met for all three designs, based on the results as presented. The HSA design with a folded wall shows superior harmonic suppression relative to the shorted-wall design. Moreover, it is found that the design of a folded-wall type tends to reach faster convergence than the design of a shorted-wall type when the GA optimisation is performed. This is because the patch with a folded structure provides more freedom in surface geometry compared to the shorted one. Furthermore, the design with a folded patch is also a more attractive candidate in practical application due to its easier fabrication than the shorted-wall type.

4 Conclusions

A novel technique for the design and optimisation of harmonic-suppression patch antennas, applying adaptive surface patch models and GAs, has been presented. Hardware realisations of three coaxially-fed air-dielectric microstrip patch antennas were used to evaluate and validate the design theory. Comparison of return loss and far-field radiation pattern measurements showed good agreement with the predictions. The examples presented confirmed the capability of the proposed method for antenna design using GA and adaptive surface meshing, showing reasonable stability and accuracy in the results.

The antenna designs presented have proved the design concept for HSAs using GA in collaboration with adaptive meshing code. HSAs are attractive for radio-frequency front-end systems of active antennas directly integrated with high efficiency power amplifiers where the antenna functions to suppress undesired harmonic power. However, the current design methodology has some practical limitations since it cannot include dielectric substrates in the design of planar microstrip antennas. For future work, further development of the methodology will address this issue for planar antenna realisation.

5 References

1 Elkhazmi, E., McEwan, N.J., Moustafa, J.: 'Control of harmonic radiation from an active microstrip patch antenna', *Journees Internationale de Nice sur les Antennes*, 1996, pp. 313–316

2 Radisic, V., Qian, Y., Itoh, T.: 'Class F power amplifier integrated with circular sector microstrip antenna'. IEEE MTT-S Symp. Digest, 1997, pp. 687–690

3 Kim, H., Hwang, K.S., Chang, K., Yoon, Y.J.: 'Novel slot antennas for harmonic suppression', *IEEE Antennas Wirel. Compon. Lett.*, 2004, **14**, (6), pp. 286–288

4 Sung, Y.J., Kim, Y.-S.: 'An improved design of microstrip patch antennas using photonic bandgap structure', *IEEE Trans. Antennas Propag.*, 2005, **53**, (5), pp. 1799–1804

5 Radisic, V., Chew, S.T., Qian, Y., Itoh, T.: 'High efficiency power amplifier integrated with antenna', *IEEE Microw. Guided Wave Lett.*, 1997, **7**, (2), pp. 39–41

6 Sheta, A.F.: 'A novel H-shaped patch antenna', *Microw. Opt. Technol. Lett.*, 2001, **29**, (1), pp. 62–66

7 Chu, Q.-X., Hou, M.: 'An H-shaped harmonic suppression active integrated antenna', *Int. J. RF Microw. Comput. Aided Eng.*, 2006, **16**, (3), pp. 245–249

8 Kim, H., Yoon, Y.J.: 'Microstrip-fed slot antennas with suppressed harmonics', *IEEE Trans. Antennas Propag.*, 2005, **53**, (9), pp. 2809–2817

9 Rahmat-Samii, Y., Michielssen, E.: 'Electromagnetic optimization by genetic algorithms' (Wiley, Canada, 1999)

10 Altshuler, E.E., Linden, D.S.: 'Wire-antenna designs using genetic algorithms', *IEEE Antennas Propag. Mag.*, 1997, **39**, pp. 33–43

11 Jones, E.A., Joines, W.T.: 'Design of Yagi-Uda antennas using genetic algorithms', *IEEE Trans. Antennas Propag.*, 1997, **45**, (9), pp. 1386–1392

12 Liu, W.-C.: 'Design of a CPW-fed notched planar monopole antenna for multiband operations using a genetic algorithm', *IEE Proc. Microw. Antennas Propag.*, **152**, (4)2005, pp. 273–277

13 Chung, S.W.J., Abd-Alhameed, R.A., Excell, P.S., See, C.H., Zhou, D., Gardiner, J.G.: 'Resistively loaded wire bow-tie antenna for microwave imaging by means of genetic algorithms'. Int. Multi-Conf. on Engineering and Technological Innovation Proc., Orlando, Florida, USA, 2008, pp. 303–306

14 Abusitta, M.M., Abd-Alhameed, R.A., Zhou, D., See, C.H., Jones, S.M.R., Excell, P.S.: 'New approach for designing beam steering uniform antenna arrays using genetic algorithms'. Loughborough Antennas and Propagation Conf., Loughborough, UK, 2009, pp. 617–620

15 Karamalis, P.D., Skentos, N.D., Kanatas, A.G.: 'Selecting array configurations for MIMO systems: an evolutionary computation approach', *IEEE Trans. Wirel. Commun.*, 2004, **3**, (6), pp. 1994–1998
16 Karamalis, P.D., Skentos, N.D., Kanatas, A.G.: 'Adaptive antenna subarray formation for MIMO systems', *IEEE Trans. Wirel. Commun.*, 2006, **5**, (11), pp. 2977–2982
17 Mangoud, M.A., Abd-Alhameed, R.A., Excell, P.S.: 'Optimisation of channel capacity for indoor MIMO systems using genetic algorithm'. Proc. Third Int. Conf. On Internet Technologies and Applications (ITA 09), Glyndwr University, Wrexham, Wales, UK, 2009, pp. 431–439
18 Karamalis, P.D., Kanatas, A.G., Constantinou, P.: 'A genetic algorithm applied for optimization of antenna arrays used in mobile radio channel characterization devices', *IEEE Trans. Intrum. Meas.*, 2009, **58**, (8), pp. 2475–2487
19 Carroll, D.L.: 'FORTRAN genetic algorithm driver'. Version 1.7, Download from: http://www.staff.uiuc.edu/~carroll/ga.html, 12/11/98
20 Abd-Alhameed, R.A., Excell, P.S., Vaul, J.: 'Currents induced on wired I.T. networks by randomly distributed phones – a computational study', *IEEE Trans. Electromagn. Compat.*, 2006, **48**, (2), pp. 282–286
21 See, C.H., Abd-Alhameed, R.A., Zhou, D., Excell, P.S., Hu, Y.F.: 'A new design of circularly-polarised conical-beam microstrip patch antennas using a genetic algorithm'. Proc. European Conf. On Antennas and Propagation: EuCAP 2006, Session 4PA1, Paper no. 100, Nice, France, 2006
22 Zhou, D., Abd-Alhameed, R.A., Excell, P.S.: 'Bandwidth enhancement of balanced folded loop antenna design for mobile handsets using genetic algorithms', *PIERS Online*, 2008, **4**, (1), pp. 136–139
23 Zhou, D., Abd-Alhameed, R.A., See, C.H., *et al.*: 'Quadrifilar helical antenna design for satellite-mobile handsets using genetic algorithms', *Microw. Opt. Technol. Lett.*, 2009, **51**, (11), pp. 2668–2671
24 Zhou, D., Abd-Alhameed, R.A., See, C.H., Bin-Melha, M.S., Elferganai, E.T.I., Excell, P.S.: 'New antenna designs for wideband harmonic suppression using adaptive meshing and genetic algorithms'. Proc. Mosharaka Int. Conf. On Communications, Propagation and Electronics, Amman, Jordan, 5–7 March 2010, Technical Session 1, pp. 5–9
25 Kwon, S., Lee, B.M., Yoon, Y.J., Song, W.Y., Yook, J.-G.: 'A harmonic suppression antenna for an active integrated antenna', *IEEE Antennas Wirel. Propag. Lett.*, 2003, **13**, (2), pp. 54–56

Progress In Electromagnetics Research C, Vol. 17, 121–130, 2010

HARMONICS MEASUREMENT ON ACTIVE PATCH ANTENNA USING SENSOR PATCHES

D. Zhou

Surrey Space Centre, University of Surrey
Guildford, GU2 7XH, UK

R. A. Abd-Alhameed and C. H. See

Mobile and Satellite Communications Research Centre
University of Bradford, Bradford, BD7 1DP, UK

N. T. Ali

Electronic Engineering, Sharjah Campus
Khalifa University of Science, Technology & Research (KUSTAR)
P. O. Box 573, Sharjah, UAE

M. S. Bin-Melha

Mobile and Satellite Communications Research Centre
University of Bradford, Bradford, BD7 1DP, UK

Abstract—Performance of the sensing patch technique for measuring the power accepted at the antenna feed port of active patch antennas has been evaluated at harmonic frequencies. A prototype antenna, including two sensors at appropriate locations, was fabricated and tested at the fundamental and two harmonic frequencies to estimate the power accepted by the antenna, including determination of the sensor calibration factor.

Received 28 September 2010, Accepted 29 October 2010, Scheduled 8 November 2010
Corresponding author: Dawei Zhou (d.zhou@surrey.ac.uk).

1. INTRODUCTION

The active integrated antenna (AIA) has been growing area of research over the recent years, due to its compact size, low weight, low cost, and multiple functionalities. An AIA can generally be considered as an active microwave circuit in which the output or input port is free space instead of conventional 50 Ω interface. In all cases, the antenna is fully (or closely) integrated with the active device to form a subsystem on the same board and can provide certain circuit functions such as resonating, duplexing, filtering as well as radiating, that describes its original role. AIAs are typically classified into three types: amplifying-type, oscillating-type and frequency-conversion-type, according to how the active device acts in the antenna [1–8].

In general, radiated power by the active integrated antenna at the targeted design frequency and its harmonics can be measured using Friis transmission equation in the anechoic chamber [9]. In addition, a simple measurement technique for measuring the power accepted by the active patch antenna, using a sensing patch feeding a network or spectrum analyzer, was first proposed in [10]. The technique eliminates many uncertainties and errors, such as cable losses, effects of the pattern, effects of nearby scatterers, and gain estimation errors, and even makes it unnecessary to operate in the far field. This technique was originally developed for the measurement of amplifying-type active patch antennas at their fundamental design frequency. It was subsequently applied to measurements on oscillating-type antennas [11].

In this paper, the possibility of using this technique to find the power accepted by the antenna at harmonic frequencies is studied. Performance of the sensing patch technique for measuring the power accepted at the antenna feed port of active patch antennas at harmonic frequencies is evaluated using an electromagnetic (EM) simulator Ansoft Designer® [12] in terms of the current distribution. A prototype antenna, including two sensors at appropriate locations around the patch, is fabricated and tested at three designated frequencies to estimate the accepted power by the antenna, including determination of the sensor calibration factor. It is shown, based on experimental results, that the original technique can also be employed to measure the second harmonic power; measurement of the third harmonic power is also possible if another sensing patch is added in an appropriate position.

2. SENSOR SIMULATION AND MEASUREMENT OF HARMONICS

An inset microstrip-fed patch antenna, resonating at 2.44 GHz, was chosen for the test, since this type of antenna is convenient for the design of active oscillator antennas. The important dimensions of this antenna have been illustrated in Fig. 1. The performance of the sensing patch method at 2nd and 3rd harmonic frequencies was evaluated with this antenna. The current distribution on the patch at harmonic frequencies was first studied to find the proper position for the sensing patch. Figs. 2 and 3 show the corresponding harmonic current distributions on the patch. The position of the sensing patch is optimally set adjacent to a point of maximum voltage, which corresponds to a point of minimum current distribution on the patch. Thus the position of the sensing patch can be set next to the middle of the end edge of the patch for the 2nd harmonic and one-third of the way along one side of the patch for the 3rd harmonic. It was also found that the presence of the sensing patch has very little effect (about ± 0.2 dB) on the return loss at the input port of the main patch at the fundamental operating frequency and the first two harmonics as

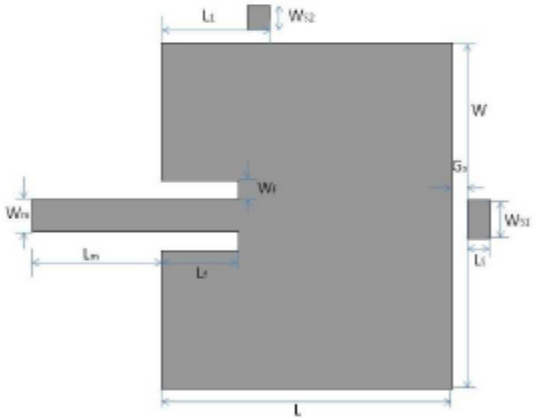

Figure 1. Important dimensions of the patch antenna studied in this paper ($W = 38.15$, $L = 45.96$, $L_1 = 18.32$, $W_m = 4.24$, $L_m = 17$, $W_f = 2.54$, $L_f = 10.02$, $G_s = 2$, $W_{s1} = 5$, $W_{s2} = 3$ and $L_s = 3$; all dimensions in millimetre).

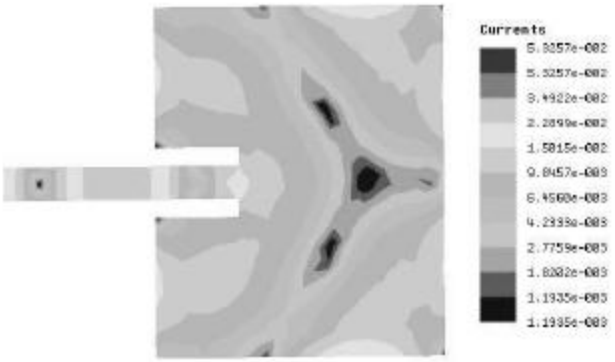

Figure 2. Current distribution on the patch antenna at 2nd harmonic frequency.

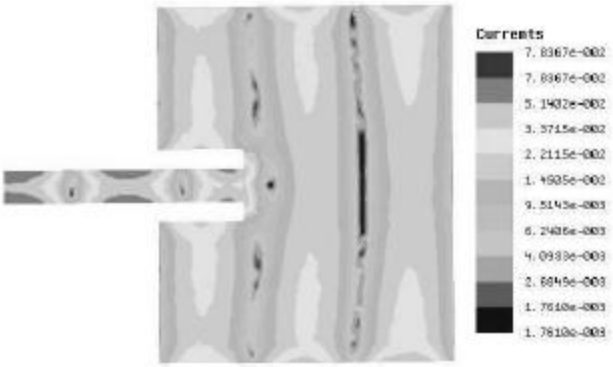

Figure 3. Current distribution on the patch antenna at 3rd harmonic frequency.

shown in Fig. 4.

The antenna with two sensing patches was mounted on 1.524 mm thick Duroid substrate material with relative permittivity of 2.55 and loss tangent of 0.0018. The sizes of the sensing patches used for the 2nd and 3rd harmonic frequencies were 3 mm × 5 mm and 3 mm × 3 mm, respectively. A spacing distance of 2 mm between the sensing patches and the antenna patch (see Fig. 5) was found acceptable for sufficient coupling and had no noticeable effect on the antenna input return loss. It has to be noted that the sensing patch at the 2nd harmonic has the

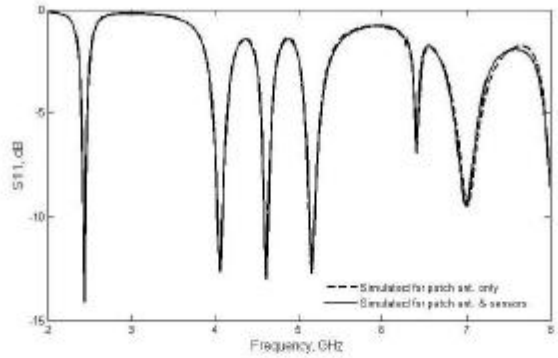

Figure 4. Simulated antenna return loss with and without the sensor patch.

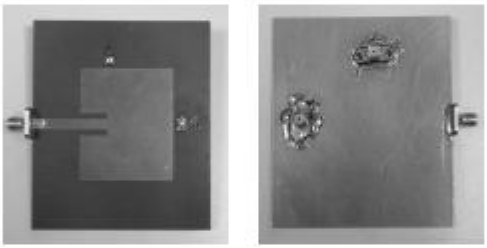

Figure 5. Fabricated antenna showing sensor locations: (left) Top view, (right) Underside.

same location as at the fundamental. The sensing patch was connected to ground via a 50-ohm chip resistor. The inclusion of the 50-ohm resistor creates a relatively well-matched source for the attached cable. A 50-ohm coaxial probe was mounted at the rear of the circuit board and connected to the resistor load: This fed the sensor output to a traceably-calibrated network analyzer.

The sensing patch for the 2nd harmonic was first tested. According to the work presented in [10], the performance of the sensing patch for harmonics can be evaluated using the calibration factor $|S'_{21}|$, which relates the sensor's output power to the power accepted by the radiator from RF circuitry (e.g., a RF power amplifier or oscillator),

as follows:

$$\left|S'_{21}\right|^2 = |S_{21}|^2/(1-\left|S^2_{11}\right|) \quad (1)$$

where $[S] = \begin{bmatrix} S_{11} & S_{12} \\ S_{21} & S_{22} \end{bmatrix}$.

The scattering parameters $[S]$ in Eq. (1) were obtained by measuring two-port S-parameters between the antenna input feed line and the sensor's output from 2 GHz to 8 GHz using a traceably-calibrated network analyzer (HP 8510C). The variations of the measured $[S]$'s extended over the fundamental frequency and the first two harmonics are presented in Fig. 6; the corresponding calibration factor from the measured antenna data was computed using Eq. (1). The measured return loss and computed calibration factors are presented in Table 1 at 2.44, 4.88, and 7.32 GHz, respectively.

In order to evaluate the sensor's calibration factor for harmonics, a 0 dBm RF signal was injected into the main patch from a sweep oscillator HP 8350B at the fundamental and harmonic frequencies. The

Table 1. 2nd harmonic sensor measurement results for the fundamental and harmonics.

Freq (GHz)	S_{11} (dB)	$\|S'_{21}\|^2$ (dB)	L_{cable} (dB)	P_{reading} (dBm)	P_{accepted} (dBm)	P'_{accepted} (dBm)
2.44	−24.86	−23.20	1.33	−25.33	−0.0144	−0.8
4.88	−1.75	−20.42	2.67	−28.5	−4.796	−5.412
7.32	−4.241	−23.45	4	−27	−2.052	0.45

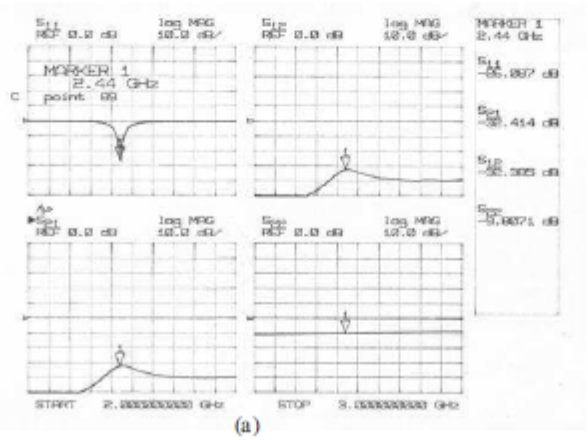

(a)

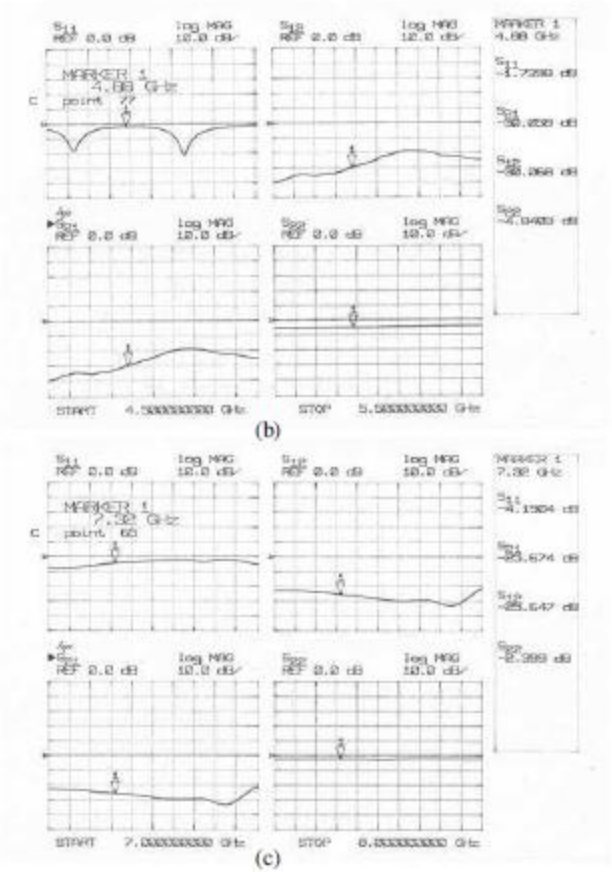

Figure 6. Measured two-port S-parameters between the antenna input port and the sensor's output port at, (a) fundamental frequency, (b) 2nd harmonic frequency, (c) 3rd harmonic frequency.

measurement setup is illustrated in Fig. 7. The Return Loss (R.L.) of the antenna tested was optimized at its fundamental frequency into an impedance of $50\,\Omega$, as shown in Table 1. However, at harmonic frequencies, the input impedance of the antenna was greatly different from $50\,\Omega$. Thus, the power accepted by the antenna (P_{accepted}) is

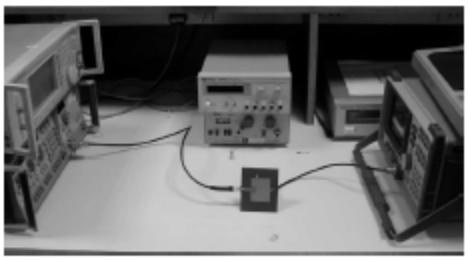

Figure 7. Photograph of measurement setup in this study.

given by:

$$P_{\text{accepted}} = P_{\text{incident}} \left(1 - |\Gamma|^2\right) \tag{2}$$

where Γ is the reflection coefficient at the input of the antenna and $|\Gamma|^2 = P_{\text{reflected}}/P_{\text{incident}}$. $P_{\text{reflected}}$ is the power reflected at the antenna input, and P_{incident} is the power outgoing from the signal generator (in this case, $P_{\text{incident}} = 0\,\text{dBm}$ at all frequencies). The power from the sensor's output (P_{reading}) was observed using a spectrum analyzer (HP 8563A). Care was taken to find the loss in the cable (L_{cable}) before measuring the output power from the sensor. The estimated power accepted by the antenna (P'_{accepted}) can be found as:

$$P'_{\text{accepted}} = P_{\text{reading}} - \left|S'_{21}\right|^2 - L_{\text{cable}} \tag{3}$$

A summary of measured parameters for the 2nd harmonic sensor is presented in Table 1. The technique shows that the power accepted by the antenna at the fundamental and 2nd harmonic frequencies can be achieved using the same sensing patch. As can be seen from Table 1, the accuracy of this technique is around 0.7 dB (i.e., the maximum difference between the P_{accepted} and P'_{accepted} at the fundamental and 2nd harmonic). It should be noted that the power accepted at the 3rd harmonic frequency varies greatly in the measurement and this is because the sensor at this position is weakly coupled to the maximum voltage of the 3rd harmonic.

Similarly, for the 3rd harmonic sensor, the same process was used as with the 2nd harmonic sensor. A summary of measured parameters for the 3rd harmonic sensor is presented in Table 2 at the intended frequencies. It is shown that the technique is still valid within 1 dB accuracy for 3rd harmonic power measurement. In addition, this sensor can also be applied for the 2nd harmonic power measurement, with very good accuracy. This is because the current distribution at

Table 2. 3rd harmonic sensor measurement results for the fundamental and harmonics.

Freq (GHz)	S_{11} (dB)	$\lvert S'_{21}\rvert^2$ (dB)	L_{cable} (dB)	P_{reading} (dBm)	P_{accepted} (dBm)	P'_{accepted} (dBm)
2.44	−26.09	−32.403	1.33	−33	−0.0109	0.733
4.88	−1.74	−25.25	2.6	−33	−4.814	−5.155
7.32	−4.19	−23.59	4	−30.67	−2.084	−3.08

the 2nd harmonic frequency near to the location of the 3rd harmonic sensor is close to minimum, and this can be easily seen from Fig. 3. It is notable that the power accepted at the fundamental frequency varies greatly in the measurements. In addition, care should be taken on means of improving the port impedance matching at the sensor patch port in order to eliminate measurement errors and improve measurement accuracy at fundamental and harmonic levels using this proposed technique. This challenging problem including the antenna operation over a wide frequency band is left to future work.

3. CONCLUSION

The measurement of the power accepted by a microstrip patch antenna, using the sensing patch measurement technique, has been demonstrated at both fundamental and first two harmonic frequencies. The results of the present work were exhibited to be acceptable and agreed with direct measurements. The proposed technique was shown to achieve 0.7 dB and 1 dB relative accuracy for the 2nd and 3rd harmonic measurements respectively.

REFERENCES

1. Kaya, A. and S. Comlekci, "The design and performance analysis of integrated amplifier patch antenna," *Microwave and Optical Technology Letters*, Vol. 50, No. 10, 2732–2736, October 2008.
2. Kim, H. and Y. J. Yoon, "Wideband design of the fully integrated transmitter front-end with high power-added efficiency," *IEEE Transactions on Microwave Theory and Techniques*, Vol. 55, No. 5, 916–924, May 2007.
3. Chou, G.-J. and C.-K. C. Tzuang, "Oscillator-type active-integrated antenna: The leaky-mode approach," *IEEE Transactions on Microwave Theory and Techniques*, Vol. 44, No. 12, 2265–2272, December 1996.

4. Choi, D.-H. and S.-O. Park, "Active integrated antenna using T-shaped microstrip-line-fed slot antenna," *Microwave and Optical Technology Letters*, Vol. 46, No. 6, 538–540, September 2005.
5. Cha, K., S. Kawasaki, and T. Itoh, "Transponder using self-oscillating mixer and active antenna," *IEEE MTT-S Int. Microwave Symp. Digest*, 425–428, 1994.
6. Montiel, C. M., L. Fan, and K. Chang, "A novel active antenna with self-mixing and wideband varactor-tuning capabilities for communication and vehicle identification applications," *IEEE Transactions on Microwave Theory and Techniques*, Vol. 44, No. 12, Part 2, 2421–2430, 1996.
7. Bilotti, F., F. Urbani, and L. Vegni, "Design of an active integrated antenna for a PCMCIA card," *Progress In Electromagnetics Research*, Vol. 61, 253–270, 2006.
8. Yang, S., Q.-Z. Liu, J. Yuan, and S.-G. Zhou, "Fast and optimal design of a k-band transmit-receive active antenna array," *Progress In Electromagnetics Research B*, Vol. 9, 281–299, 2008.
9. Balanis, C. A., *Antenna Theory: Analysis and Design*, 3rd edition, 94–96, John Wiley & Sons Inc., 2005.
10. Elkhazmi, E. A., N. J. McEwan, and N. T. Ali, "A power and efficiency measurement technique for active patch antennas," *IEEE Transactions on Microwave Theory and Techniques*, Vol. 48, No. 5, 868–870, May 2000.
11. Abd-Alhameed, R. A., P. S. Excell, and E. Elkhazmi, "Design of integrated-oscillator active microstrip antenna for 2.45 GHz," *XXVIIth General Assembly of URSI*, Paper No. 1181, Maastricht, August 2002.
12. Ansoft Designer, Version 1.0, Ansoft Corporation, USA.

A Frequency Tunable PIFA Design for Handset Applications

Issa Elfergani[1], Raed Abd-Alhameed[1], M.S. Bin-Melha[1], Chan See[1], Da-Wei Zhou[2], Mark Child[1], and Peter Excell[3]

[1]Mobile & Satellite Communications Research Centre, University of Bradford, Bradford, United Kingdom, BD7 1DP.
[2]Pace PLC, Victoria Road, Saltaire, West Yorkshire.
[3]Centre for Applied Internet Research, Glyndwr University, Wrexham, United Kingdom.
{i.t.e.elfergeni, r.a.a.abd,m.s.bin-mehla,c.h.see2, d.zhou2,m.b.child}@bradford.ac.uk
{p.excell}@glyndwr.ac.uk

Abstract. A frequency tunable planar inverted F antenna (PIFA) is presented for use in the following bands: DCS, PCS, and UMTS. Initially, the tuning was achieved by placing a lumped capacitor, with values in the range of 1.5 to 4 pF, along the slot of the radiator. The final tuning circuit uses a varactor diode, and discrete lumped elements are fully integrated with the antenna. The antenna prototype is tunable over from 1850 MHz to 2200 MHz, with an associated volume of 21×13.5×5 mm^3, making it suitable for potential integration in a commercial handset or mobile user terminal.

Keywords: PIFA, slot antenna, varactor diode.

1 Introduction

Low profile and space efficient antenna designs with suitable bandwidth for use in multi-standard mobile handsets and user terminals continue to pose a major design challenge. Microstrip patch radiators are a common starting point for such applications, but are constrained in both bandwidth and gain. Various techniques have been proposed to improve on both of these criteria, and one of the most common configurations is the planar inverted F antenna (PIFA) [1]. PIFA structures possess omni-directional radiation patterns, and have improved average power where the cross polarisation is relatively large [2]. They are of course, physically small and compact. The most basic PIFA realisation consists of a rectangular planar patch, shorting pins and a ground plane. Dual band operation may be achieved in several ways, but the introduction of a slot is among the most common [3]. However, the use of a slot may not be optimal in design terms as they can only generate narrowband resonances at two or three frequencies on interest, depending on the number and configuration of the perturbations, and resonators. Proper modal identification may also be an issue. A possible workaround, which preserves the same overall electromagnetic geometry, is the introduction of PIN or varactor diodes, the resulting

tuning may have a large dynamic range [4]. Switches may be less desirable as their reactive load may affect the bandwidth of the PIFA; both performance improvement and degradation are both possible [5].

Recent attempts at producing viable multi-standard designs for small antennas have used a variety of techniques including RF switching, MEMS (relay) switching and the use advanced materials [6] [7]. Varactor diodes are an important departure here, as they combine the advantages of a large capacitance ratio, a suitable small size, and DC voltage control over the tuning of the resonant frequency. PIFA structures are eminently suited to this approach, in spite of the relatively narrow operating bandwidth [8]. Since a varactor tuned antenna uses a DC bias, two DC blocking capacitors are typically required. In the PIFA case, the antenna shorting pin is already connected to ground, and one of the DC capacitors can be removed. The final structure is still consistent with the volume constraint of a typical handset chassis.

This paper presents a new tuned PIFA-slot type antenna which covers the operating ranges of DCS, PCS and UMTS. The antenna is designed iteratively using a frequency domain finite element analysis (Ansoft HFSS), and work bench results. The final design optimisation was cross validated using CST Microwave Studio, and a representative prototype was constructed on this basis.

2 The Basic Antenna Geometry

The antenna is placed on the ground plane of dimensions by means of a shorting pin of height of 5 mm and width 2 mm, as shown in Fig. 1. The antenna is fed by means of a vertical plate, of maximum height 4.5 mm and width 2 mm. It is connected to the feeding probe through the slot in the ground plane and the effective substrate is air. The slot has a uniform width of 1mm. The detailed dimensions of the radiator patch are illustrated in Table I. The structure and lumped element parameters were simulated using HFSS. The tuning range was investigated initially through manipulating lumped capacitance parameters in the range [1.5, 4.0] pF.

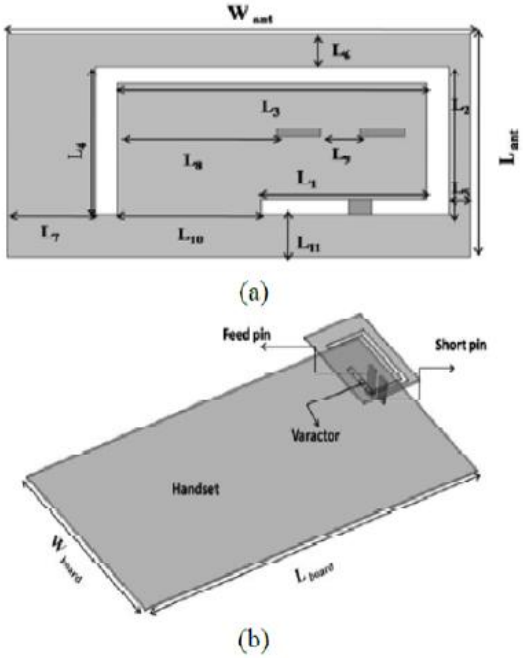

Fig. 1. Basic antenna structure; (a) plan view (b) 3D.

Table I. Detailed Dimensions of Radiator Patch

Parameter	Value/mm	Parameter	Value
L1	7.5	L7	4
L2	9	L8	7.2
L3	14	L9	1.8
L4	9	L10	6.5
L5	1	L11	2.5
L6	2	W_{ant}, L_{ant}	21, 13.5

3 The Impact of the Loading Capacitor

The impact of the loading capacitance on overall antenna performance, including the return loss and radiation pattern needs to be investigated both in simulation, and through performance assessments on the physical prototype. For comparison purposes in simulation, we require a fully characterised reference antenna which omits the

varactor, this structure resonates at 2.36 GHz (see Fig. 2). A loading capacitor with values selected from {1.5, 2, 3, 4} pF is placed over the slot radiator in a fixed location, making the antenna resonate over the range $1.88 \leq f_0 \leq 2.2$ GHz. In the first instance the tuning is investigated via a lumped (ceramic) capacitor, instead of a varactor, therefore the DC bias and circuit parasitic effects are excluded. The effects of lumped capacitors have been tested on the working prototype, without the DC circuit, in order to find out how the loaded capacitors could affect the antenna performance; and the optimal location on the slot 'arm'. The working prototype in Fig. 3 was tested without the bias circuit. The loading capacitor was varied over [1.5, 4.0] pF, which was found to be sufficient to control the antenna response.

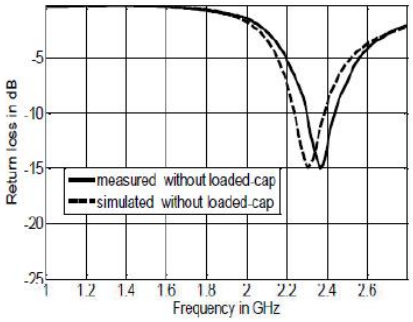

Fig. 2. Return loss of antenna prototype, without loading capacitor present.

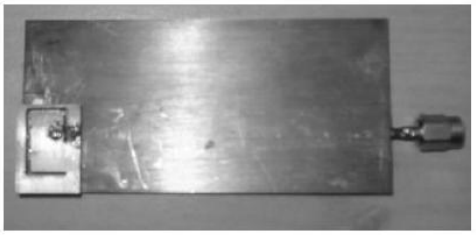

Fig. 3. The prototype (loaded) antenna structure.

4 Results and Discussion

The tuned working prototype relies on the introduction of the slot on the radiator arm, and the placement of a varactor diode over the slot, to achieve the required tuning range. As the capacitance is varied tuning may be demonstrated over the range

$1.88 \leq f_0 \leq 2.2$ GHz. Measurements from a VNA are presented in Fig. 4(c) illustrating this performance for the antenna reflection coefficient. Both the predicted and measured return loss results of this antenna are presented for different values of capacitors (varactor). Fig (4) shows fairly good agreement between simulated and measured results. By increasing the capacitor value from 1.5 to 4 pF the resonant frequency is increased from 1.85 to 2.2 GHz. The simulated gain of the proposed tuned PIFA over the various target frequencies is shown in fig. 5. The simulated radiation patterns are shown in Fig. 6, along with the maximum gain forecast. Two pattern cuts were selected (H-plane, E-plane) for the three operating frequencies, covering the designated composite bandwidth. Corresponding measurements were made for the working prototype, with radiation patterns presented in the xz-plane and yz-plane at 2.1 GHz, 1.95 GHz, and 1.85 GHz.

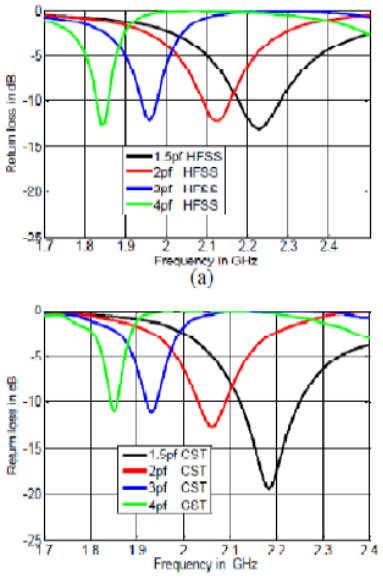

Fig. 4. Input return loss at the input port; (a) HFSS output (b) CST output (c) measured

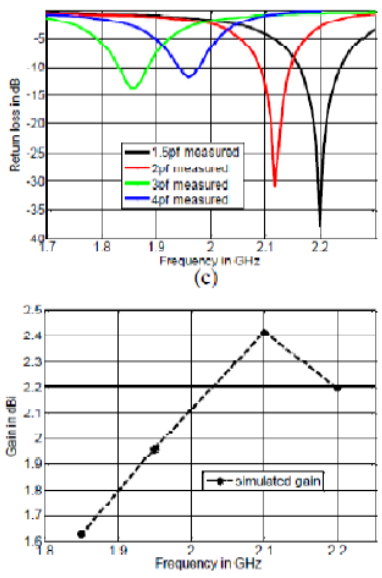

Fig. 5. predicted (HFSS) antenna gain

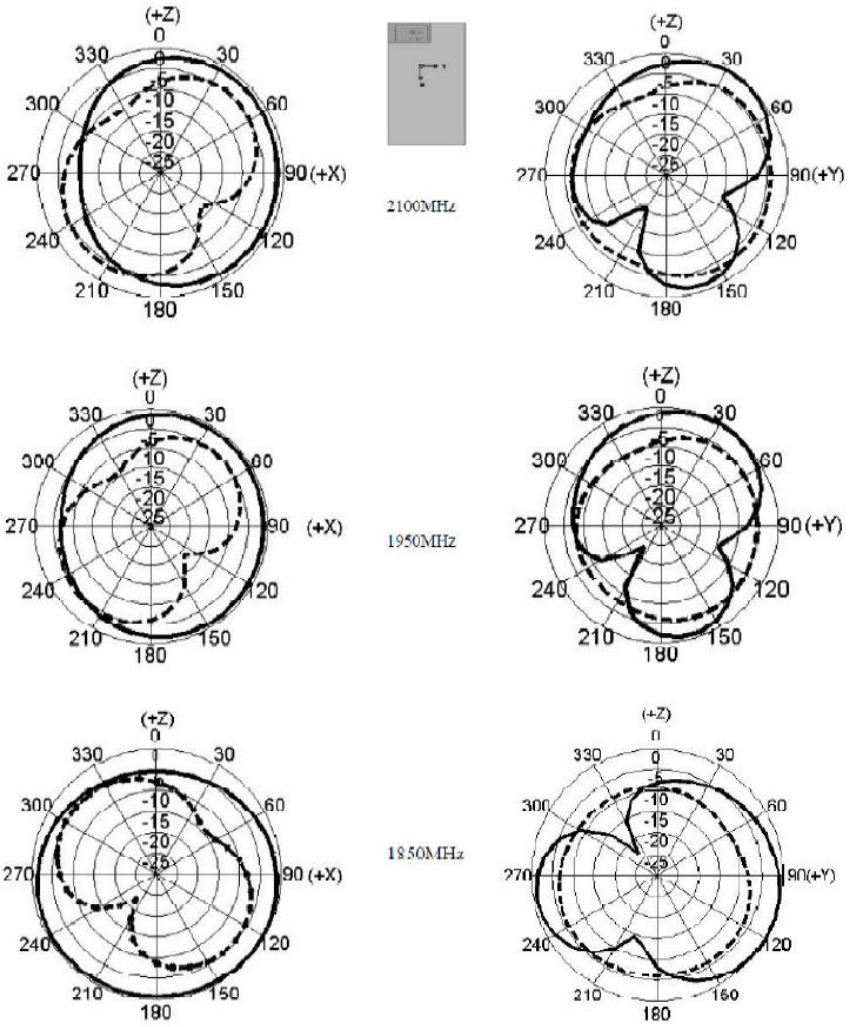

Fig. 6. Simulated radiation field patterns of the antenna for various operating frequencies; left: xz plane, right: yz plane('——': Simulated Co-polar, '------': Simulated Cross-polar).

6 Conclusions

A tuned PIFA prototype has been designed and constructed. This antenna consists of a radiating element, and a tuning circuit. The tuning circuit consists of simple fixed capacitor that is equivalent to varactor diode operation to control the frequency response of the antenna. The antenna has an effective operating band which covers the union of the DCS, PCS and UMTS frequency standards. The simulated and measured reflection coefficients, gains and radiation patterns are consistent, and indicate a potentially good performance, and the physical dimensions are consistent with the volume constraint for a mobile handset. The actual antenna volume is $21 \times 13.5 \times 5$ mm^3. This tuneable PIFA design may be used in other wireless applications.

References

[1] Liu, Z-D, Hall, P.S., and Wake, D., Dual-Frequency Planar Inverted-F, IEEE Transactions on Antennas and Propagation, 45, 10, pp, 1452-1457, Oct. 1997.

[2] Hirazawa, K., Haneishi, M, 'Analysis, design and measurement of small and low profile antennas', ARTECH HOUSE INC, 1992.

[3] Zhang, J-W and Liu, Y., 'A Novel Dual-frequency Planar Inverted-F Antenna,' PIERS Proceedings, Moscow, Russia, August 18-21, pp, 662-665, 2009.

[4] Nguyen, V.-A., Bhatti, R. A., and Park, S.O., 'A simple PIFA-based tunable internal antenna for personal communication handsets,' Antennas and Wireless Propagation Letters, Vol. 7, 130-133, 2008.

[5] Caverly R.H. and Hiller, G., Distortion In Microwave and RF Switches By Reverse Biased Pin Diodes, IEEE, 1989.

[6] Dimitrios, P., Sarabandi, K., and Katehi, L.P.B., "Design of Reconfigurable slot Antennas," IEEE Transactions on Antennas and Propagation, VOL. 53, No. 2, February 2005.

[7] Huff G.H, and Bernhard, J.T., "Integration of Packaged RF MEMS Switches With Radiation Pattern Reconfigurable Square Spiral Microstrip Antennas," IEEE Transactions on Antennas and Propagation. VOL. 54, No. 2, February 2006.

[8] Nader, B. and Sarabandi, K., "Dual-Band Reconfigurable Antenna with a Very Wide Tunability Range," IEEE Transactions on Antennas and Propagation," VOL. 54, No. 2, February 2006.

Design of 2x2 U-shape MIMO slot antennas with EBG material for mobile handset applications

Z.Z. Abidin[1,2], Y.Ma[1], R.A. Abd-Alhameed[1], K.N. Ramli[1,2], D Zhou[3], M.S. Bin-Melha[1], J. M. Noras[1] and R. Halliwell[1]

[1]Mobile and Satellite Communications Research Centre, University of Bradford,
Bradford, West Yorkshire, BD7 2DF, UK

[2]Faculty of Electrical and Electronic Engineering, Universiti Tun Hussein Onn Malaysia,
Parit Raja, Batu Pahat, Johor, Malaysia

[3]Surrey Space Centre, University of Surrey, Guildford, GU2 7XH, UK

Abstract- A compact dual U-shaped slot PIFA antenna with Electromagnetic Bandgap (EBG) material on a relatively low dielectric constant substrate is presented. Periodic structures have found to reduce mutual coupling and decrease the separation of antenna and ground plane. A design with EGB material suitable for a small terminal mobile handset operating at 2.4 GHz was studied. Simulated and measured scattering parameters are compared for U-shaped slot PIFA antenna with and without EBG structures. An evaluation of MIMO antennas is presented, with analysis of the mutual coupling, correlation coefficient, total active reflection coefficient (TARC), channel capacity and capacity loss. The proposed antenna meets the requirements for practical application within a mobile handset.

1. INTRODUCTION

The potential for MIMO antenna systems to improve reliability and enhance channel capacity in wireless mobile communications has generated great interest [1]. A major consideration in MIMO antenna design is to reduce correlation between the multiple elements, and in particular the mutual coupling, electromagnetic interactions that exist between multiple elements, is significant, because at the receiver end this could largely determine the performance of the system. Lower mutual coupling can result in higher antenna efficiencies and lower correlation coefficients. The effect of mutual coupling on capacity of MIMO wireless channels is studied in [2]. Spatial diversity is strongly affected by mutual coupling and correlation. For minimal coupling, it has been shown in [3], than the separation between multiple antenna elements should be at least 0.5 λ. A 2 x2 MIMO meander planar inverted-F antenna (PIFA) at 2.6 GHz is reported in [4] to obtain a mutual coupling of -15 dB, with a separation between two antenna elements of 0.23 λ. Authors in [5] introduced a U-shaped slot patch antenna operating at 2.6 GHz for mobile handset applications, with isolation of -20 dB achieved by pattern diversity and a capacity loss of 0.2bits/s/Hz.

EBG structures have the ability to act like perfect magnetic conductors (PMC), so that the distance between the antenna and ground plane can be smaller than λ/4. This can be compared to perfect electric conductors (PEC) where a distance of λ/4 is essential so that the reflected wave interferes constructively with the emitted one [6]. When the height of the antennas to the ground plane is reduced, mutual coupling can be expected to be decreased [7, 8].

This paper presents a compact dual U-shaped slot PIFA antenna with EBG material on a relatively low dielectric constant substrate, operating at 2.4 GHz and suitable for for compact mobile handsets. S-parameters for U-shaped slot PIFA antennas with and without EBG materials are compared. In addition, the MIMO antennas are analysed in terms of their mutual coupling, correlation coefficient, total active reflection coefficient (TARC), channel capacity and capacity loss.

2. MIMO

2.1Basic theoretical concepts

2.1.1 Total active reflection coefficient (TARC)

TARC is defined as the ratio of the square root of total reflected power divided by the square root of total incident power. The TARC for a 2 x 2 antenna array can be directly calculated from the scattering matrix elements as follows [5]

$$TARC = \sqrt{(|\ (s_{11} + s_{12}e^{j\theta})^2 + |\ (s_{21} + s_{22}e^{j\theta})^2)}/\sqrt{2} \quad (1)$$

where θ represents the phase from 0 to 2π.

2.1.2 Correlation coefficient

Previous work shows that the correlation coefficient, ρ, of a 2 x 2 antenna system can also be determined using S-parameters [9]

$$\rho = \frac{S_{11}^{*}S_{12} + S_{21}^{*}S_{22}{}^{2}}{(1 - S_{11}{}^{2} - S_{21}{}^{2})(1 - S_{22}|^{2} - S_{12}{}^{2})} \quad (2)$$

2.1.3 Channel Capacity

Based on the channel transfer matrix, H, the Shannon capacity, C, for the MIMO system channel is [1]

$$C = log_2\left(det\left(I + \frac{SNR}{M} HH^{\dagger}\right)\right)$$

(3)

where $H^{\dagger}$ is the Hermitian of the matrix H, M is is the number of receivers and SNR is the estimated channel signal-to-noise ratio.

2.1.4 Capacity Loss

In case of high SNR, the capacity loss is given by [10]

$$C(loss) = -log_2 det(\Psi^R) \quad (4)$$

where Ψ^R is the receiving antenna correlation matrix.

3. Design of 2 × 2 U-shaped slot PIFA antenna integrated with EBG material

The basic geometrical configuration and dimensions of the PIFA with the U-shape slot structure is shown in Figure 1. The design frequency in this study is 2.4 GHz, and the antenna assembly is mounted on a 0.36 λ × 0.68 λ ground plane. The antennas are constructed from 0.5 mm thick plate, with a maximum area of 0.12 λ × 0.12 λ. The antenna is shorted to the ground plane by a metallic strip and fed by a standard 50 Ω SMA connector. The antennas are mounted on FR4 substrate with relative permittivity of 4.5, and loss tangent of 0.002 at 2.4 GHz. The substrate thickness is 1.6 mm, and the distance between two antenna elements is 0.24 λ.

Surface waves play a dominant role in the mutual coupling between the antenna array elements. Since the EBG structure has the ability to suppress surface waves, an EBG structure [11] is implemented with the antennas as shown in Figure 1. The EBG unit cell is shown in detail in Fig. 1 (v), with the dimensions of a = 9.7 mm, b = 0.2 mm, c = 4.0 mm, g = 0.2 mm, and w = 0.2 mm. In [7], the reduction in height between the PIFAs and the EBG material is shown to

mitigate the effects of mutual coupling, and thus improves the antenna efficiency. Therefore, the height of the antennas in this study has been reduced to 2 mm, with other dimensions of the antenna unchanged.

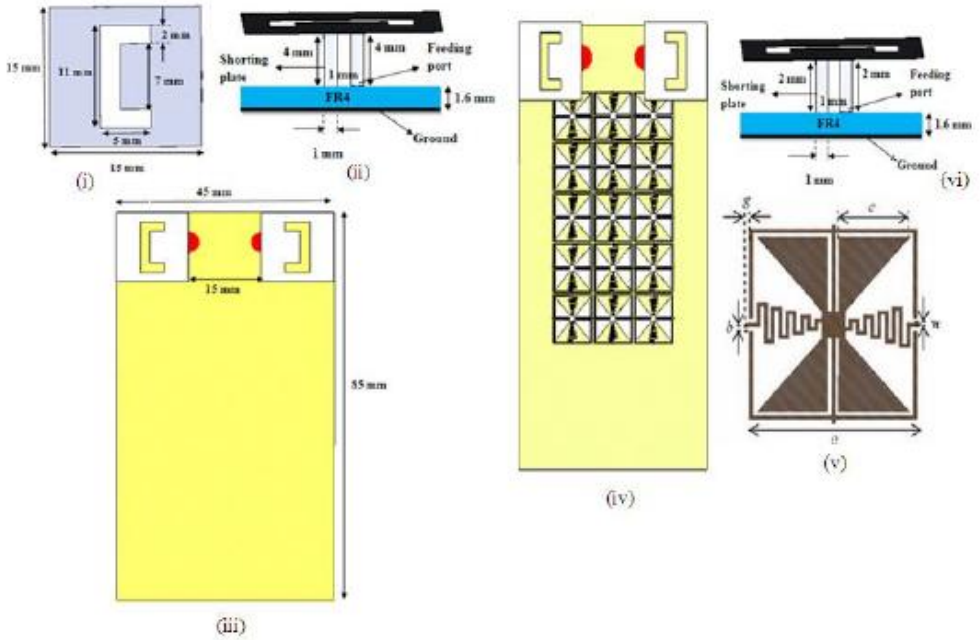

Figure 1 Geometries and dimensions: U-shape antenna (i) top view, (ii) side view, (iii) 2-D schematic; U-shape antenna with EBG (iv) 2-D schematic, (v) EBG unit cell, (vi) side view

4. SIMULATED AND MEASURED PERFORMANCE

Figure 2 and Figure 3 show the simulated and measured s-parameters output for PIFAs without and with EBG material respectively. Measurements show that the predictions for return loss and mutual coupling for both PIFAs are quite accurate with impedance bandwidth approximately 11.2% for both designs. Apparent discrepancies are believed to be due to minor inconsistencies in prototyping. It can be seen that an improved isolation of -6 dB is achievable against the PIFAs without EBG as shown in Figure 4. Next, to show the performance of the MIMO system, the correlation coefficient, TARC, capacity loss and capacity are presented in Table 1. This shows that the PIFAs with EBG material have lower loss of capacity, and better performance for TARC and correlation coefficient compared to PIFAs without EBG. The channel capacity of PIFAs with and without EBG is 5.62 bits/s/Hz and 5.64 bits/s/Hz at 2.4 GHz, respectively, as depicted in Figure 5.

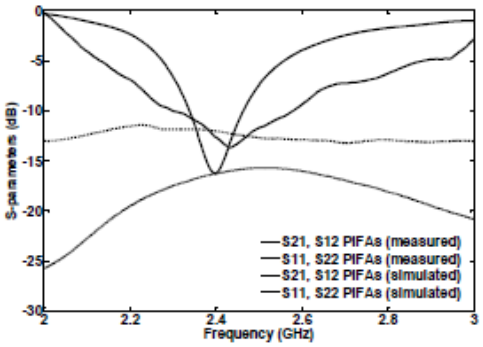

Figure 2 Comparative plot of s-parameters output for simulated and measured results for PIFAs without EBG

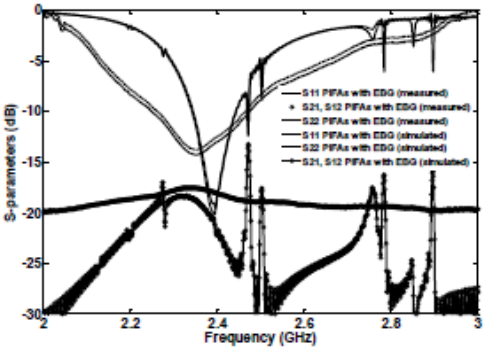

Figure 3 Comparative plot of s-parameters output for simulated and measured results for PIFAs with EBG

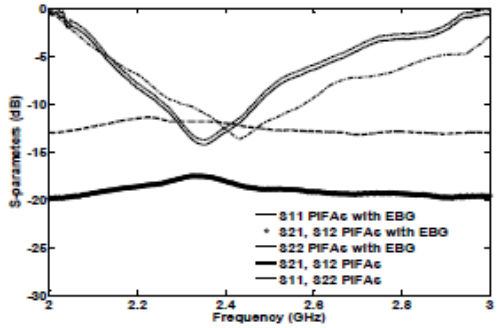

Figure 4 Measured s-parameters of PIFAs with and without EBG

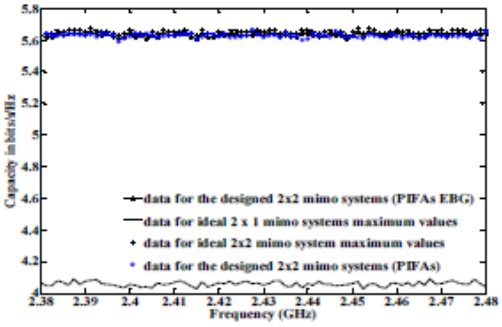

Figure 5 Measured capacity of PIFAs with and without EBG

Table 1 Measured results for correlation coefficient, TARC and capacity loss at 2.4 GHz

	PIFAs	PIFAs with EBG
Correlation Coefficient (dB)	-43.99	-49.53
TARC (dB)	-5.65	-7.17
Capacity Loss (bits/s/Hz)	0.45	0.43

4. CONCLUSIONS

Isolation improvement using an EBG structure on 2 × 2 U-shape slot patch traditional PIFA antennas for 2.4 GHz WLAN operation in mobile application has been verified. The proposed antenna can be effectively implemented on a thinner profile FR4 substrate with a low cost and is thus particularly suitable for compact mobile handsets. The use of EBG material plays an important role in reducing the mutual coupling between dual antenna elements at 2.4 GHz. The proposed antenna design was mounted on a reasonable ground size of 0.36 λ × 0.68 λ in which 3×5 EBG unit cells are used, has achieved a good isolation of 6 dB at 2.4 GHz. Further, the correlation coefficient, TARC, capacity and capacity loss have been analysed for PIFA with and without EBG. It has been shown that the proposed antenna has met the requirements for practical application in mobile handsets.

REFERENCES

1. G. J. Foschini and M. J. Gans, "On limits of wireless communications in a fading environment when using multiple antennas", *Wireless Pers. Commun.*, Vol. 6, No. 3, 311-335, 1998.
2. J. Thaysen and Kaj. B. Jakobsen, "Wireless System: Design considerations for low antenna correlation and mutual coupling reduction in multi antenna terminals", *Euro. Trans. Telecomms.,* 319-326, 2007.
3. W. L. Stutzman and G. A. Thiele, *Antenna Theory and Design*, 2nd edition, Wiley, New York, 1998.
4. W. Qiong, P. Dirk, Z. Hui and W. Klaus, "Diversity performance of an optimized meander PIFA array for MIMO handsets", *Inst. Elect. Eng. Proc.*
5. Chae, S. H., S.-K. Oh, and S.-O. Park, "Analysis of mutual coupling, correlations, and TARC in WiBro MIMO array antenna", *IEEE Antennas and Wireless Propagation Letters*, Vol. 6, 122-125, 2007.
6. D. Sievenpiper, "High Impedance Electromagnetic Surfaces", Ph.D. Dissertation, Department of Electrical Engineering, University of California, Los Angeles, 1999.
7. Z. Z. Abidin, R. A. Abd-Alhameed, N. J. McEwan, and M. B. Child, " Analysis of the effect of EBG on the mutual coupling for two-PIFA assembly*", Loughborough Antennas & Propagation Conference*, 2010.
8. Y. Zhao, Y. Hao, and C. G Parini, "Radiation properties of PIFA on electromagnetic bandgap substrates", *Microwave and Optical Technology Letters*, vo. 44, 21-24, 2005.
9. S. Blanch, J. Romeu, and I. Corbella, "Exact representation of antenna system diversity performance from input parameter description", *Electron. Lett.,* vol. 39, 705–707, May 2003.
10. H. Shin, and J. H. Lee, "Capacity of multiple-antenna fading channels: spatial fading correlation, double scattering, and keyhole", *IEEE Trans. Inform. Theory*, vol. 49, 2636-2647, 2003.
11. Z. Z. Abidin, R.A.Abd-Alhameed, N. J. McEwan, S. M. R. Jones, K. N. Ramli, and A. G. Alhaddad, "Design and Analysis of UC-EBG on Mutual Coupling Reduction", *Loughborough Antennas & Propagation Conference,* 693-696, 2009.

Proceedings of

Mosharaka International Conference on Communications, Propagation, and Electronics

(MIC-CPE 2010)

5-7 March 2010

Amman - Jordan

Organized by

MOSHARAKA FOR RESEARCHES AND STUDIES

Conference General Chairman

MOHAMMAD M. BANAT, JORDAN UNIVERSITY OF SCIENCE AND TECHNOLOGY, JORDAN

Conference Organizer

JASER MAHASNEH, MOSHARAKA FOR RESEARCHES AND STUDIES, JORDAN

Proceedings Editor

JASER MAHASNEH, MOSHARAKA FOR RESEARCHES AND STUDIES, JORDAN

ISBN: 978 - 9957- 486 - 10 - 5

New Dual-Band Balanced Handset Antenna for WLAN Application

A.G. Alhaddad [#1], R.A. Abd-Alhameed[#2], D. Zhou[#3], I.T.E. Elfergani[#4], C.H. See [#5], P.S. Excell[*6] and M.S. Bin-Melha[#7]

[#] *Mobile and Satellite Communications Research Centre*
University of Bradford, Bradford, UK
[1]a.g.alhaddad@bradford.ac.uk, [2]r.a.a.abd@bradford.ac.uk
[3]d.zhou2@bradford.ac.uk
[4]i.t.e.elfergani@bradford.ac.uk
[5]c.h.see2@bradford.ac.uk
[7]m.s.binmelha@bradford.ac.uk

[*] *Centre for Applied Internet Research, Glyndwr University, Wrexham, UK*
[6]p.excell@glyndwr.ac.uk

Abstract— **In this paper, a dual band balanced-antenna for mobile handset applications, covering the 2.4 GHz and the entire 5 GHz WLAN frequency bands, is investigated and discussed. The antenna is a thin-strip planar dipole with folded structure and a dual arm on each monopole. The performance of the proposed antenna was analysed and optimised against the two targeted frequency bands. For validation, the antenna prototype was fabricated and tested. The performance of this balanced antenna was verified and characterised in terms of the antenna return loss, radiation pattern, power gain and surface current distribution of the proposed antenna. The predicted and measured results show fairly good agreement and the results also confirm good impedance bandwidth characteristics with excellent dual-band operation.**

I. INTRODUCTION

Wireless communication has been characterized of the new modern move to make the mobile handsets small and light as possible; without compromising functionality. To miniaturize in line with consumer needs and aspiration and retain multiband functionality, mobile handsets development must be characterized by making all physical components as small as physically possible. The key concerns considered here on the design of antenna systems for small handsets relates to keeping the antenna performance unchanged or improved, even though the antenna size becomes small and reduces the degradation of antenna performance caused by the operator's adjacent effect [1]. A balanced structure is a genuine choice to avoid the aforementioned degradation of the antenna performance when held by users [2] since balanced currents only flow on the antenna element in this type of antenna, thus dramatically reducing the effect of current flow on the ground plane. As a result, balanced antennas should have good efficiency and more important to maintain their performance when in use adjacent to the human body [3]. In recent years, several novel mobile antennas designed with the balanced technique have demonstrated the enhanced stability of antenna performance, compared to the unbalanced type, when the handset is approximately placed next to the human head and/or hand [4-8].

A built-in planar metal plate antenna for mobile handsets with balanced operation is presented in this paper. The antenna was designed by folding a thin strip planar dipole with extra arm on each monopole. The antenna features balanced operation, is to reduce the current flow on the conducting surface of the handset body. The antenna design model intends to cover 2.4 GHz (2.4-2.4835 GHz) and the 5 GHz (5.15-5.35 GHz & 5.650–5.925 GHz) WLAN applications.

In short, this paper presents and investigates a new design of a built-in dual-frequency balanced antenna for WLAN and short range wireless communications. The characteristics of this balanced folded dipole antenna with a novel dual-arm structure for mobile handsets are analysed, including calculating the return loss and the radiation patterns for comparisons.

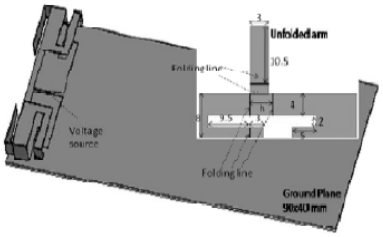

Fig. 1 Balanced mobile antenna configuration studied.

II. ANTENNA DESIGN CONCEPT

The proposed dual-band balanced mobile antenna was achieved to generate another resonant frequency by using a two tier process. Firstly, it was started by folding the monopole arm and having a slot inside each monopole with a cut on the bottom side, as shown Figure 1. Secondly, an additional thin-strip arm was inserted into each arm of the planar dipole. This folded element of the proposed antenna

was designed to operate at 2.4 GHz with a single arm to generate the second resonant frequency for 5 GHz frequency band [9]. In order to achieve a low-profile folded (i.e lower h) balanced antenna, while maintain the sufficient impedance bandwidth required at the two WLAN bands, a long slot is introduced on the each folded arm of the dipole antenna. In this way, the equivalent wavelength of the surface current at 2.4 GHz is increased, compared to the case without the long slot. As a result, the folded antenna height (h) can be reduced by 50% and the low-profile design is therefore realised.

The dimensions of the antenna geometry were found comparable to the practical handset sizes. Parametric study has been carried out to optimize the impedance matching bandwidth for the proposed antenna in order to achieve the required impedance matching covering the frequencies bands of interested at 2.4 GHz and 5 GHz bands for WLAN and. The antenna height (h) was considered to be one of the most sensitive parameters to control the impedance bandwidth of the proposed antenna for meeting the design goals.

The parameter h was varied from 2 to 5mm with 1mm each step. The optimum value of h was found to be 4 mm as shown in Fig. 2. By modifying the length and location of the additional arm of the proposed antenna, it was able to let the antenna covers the required two frequency bands at acceptable return loss ≤ -10 dB (see Fig. 2).

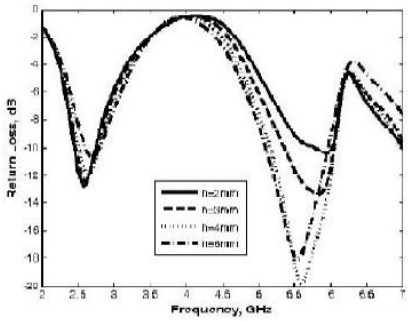

Fig. 2 Variation of the parameter h on the effect of the return loss.

The optimal antenna configuration studied in terms of return loss, radiation patterns and power gain was achieved and the important parameters are illustrated in Fig. 1, where all presented dimensions are in millimetres. The proposed antenna features of the compact design used, has the size dimensions of (l × w × h) of 38 × 10 × 4 mm. The length and location of the additional arm, including other parameters of the proposed antenna, were adjusted and further optimised to ensure that the design entirely covered the required two frequency bands at suitable working return loss ≤ -10 dB.

III. SIMULATION AND MEASUREMENT RESULTS

For the hardware realisation, copper sheet with 0.15 mm thickness was used for fabricating the proposed balanced antenna (see Fig. 4). For a balanced antenna (e.g. dipole) system, a balun is usually required as a support feeding network, to provide a balanced feed from an unbalanced source. A commercially hybrid junction from ET Industries [10] that operates from 2 to 12 GHz has been utilized in this work. Moreover, an S-Parameter method for measuring input impedance for the balanced antennas [11] was also adopted in order to verify the impedance of the proposed antenna. In this case, balanced antennas are considered as two-port devices and the S-Parameters can be obtained from a well-calibrated Network Analyzer. Subsequently, a simple formula is employed to derive the differential input impedance of the balanced antenna. Fig. 5 presents the measured return loss in two different methods compared with the simulations, in which a good agreement between the simulated and measured return loss (i.e. simulated (ant) and measured (ant) and measured (ant and balun)) was observed. This result verified the actual impedance response of the proposed antenna.

Fig. 4 Photograph of prototype of the proposed balanced antenna design.

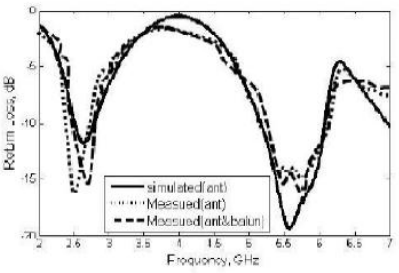

Fig. 5 Comparison of simulated and measured return loss.

Measurements of the radiation patterns of the prototype were carried out in a far-field anechoic chamber. Two pattern cuts were taken for three WLAN operating frequencies that

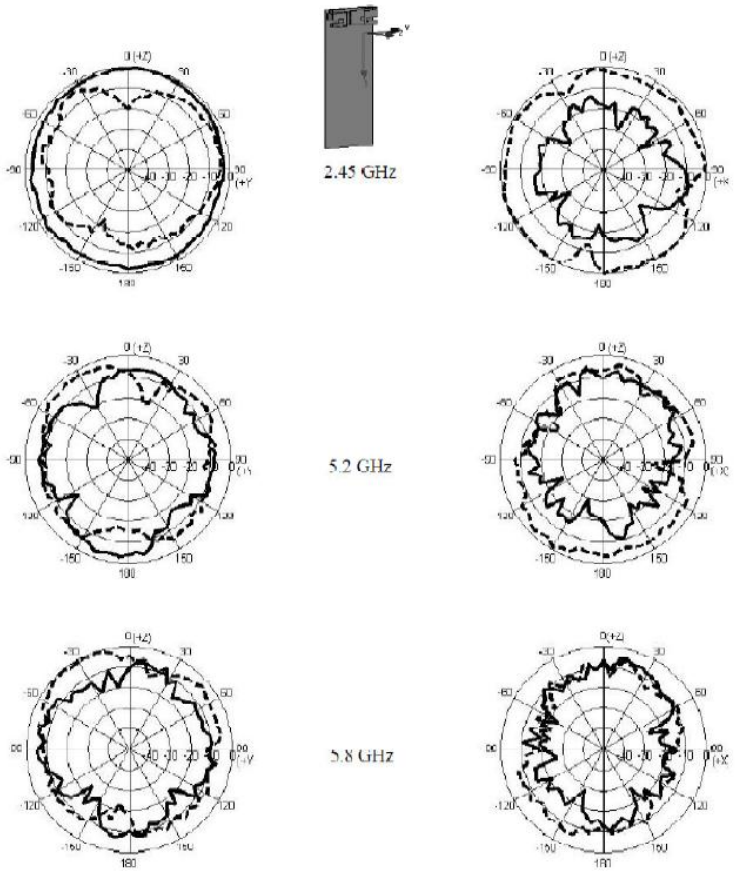

Fig. 6 Radiation patterns of the proposed antenna for 2.45 GHz, 5.2 GHz and 5.8 GHz at: (left) xz plane; (right) yz plane, where ' ' measured E_θ and '- - -' measured E_ϕ.

cover the designated whole bandwidth in this study. The radiation patterns in the xz plane and yz plane for the balanced antenna at 2.45 GHz, 5.2 GHz and 5.8 GHz were measured, as presented in Fig. 6. The measured patterns at the lower band have shown asymmetrical radiation, which is mainly due to the asymmetrical antenna structure in fabrication and imbalanced outputs from the balun device.

Measured broadside antenna power gain for the frequencies across the 2.4 GHz, 5.2 GHz and 5.8 GHz WLAN bands were also investigated. It is notable that the insertion loss of the feeding network was subsequently compensated for each measured power gain over all bands. It was found that the maximum measured antenna gain at lower and upper WLAN bands were 4 dBi, 6 dBi and 5.6 dBi at the selected frequencies, respectively.

In addition, current distribution on the mobile phone ground plane was analyzed using the EM simulator at three specific frequencies (including 2.4 GHz, 5.2 GHz and 5.8 GHz) of the frequency bands studied in this work and presented in Fig. 7. As can be seen in Fig. 7, it was observed that most of the current induced on the ground plane were high in the area beneath the antenna and minimum current distribution appeared on the rest of the ground plane, as theoretically expected. This proves the model advantage of using a balanced antenna designs for future mobile handsets.

which indicates that the proposed handset antenna design will be insensitive to the hand loading effect.

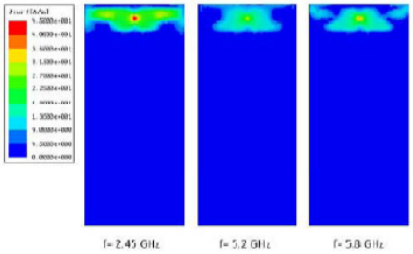

Fig. 7 Surface current distributions for the proposed balanced antenna at 2.4 GHz, 5.2 GHz and 5.8 GHz, respectively.

IV. Conclusions

A very-low-profile dual-band balanced handset antenna with novel structure for mobile devices operated over 2.4 GHz and the whole 5 GHz WLAN bands has been presented. The proposed antenna model was simulated and tested to verify the design concept. The characteristics of designed balanced antenna was analysed in terms of antenna return loss, radiation pattern and power gain. The simulated and measured results over the two frequency bands considered show a good agreement, which leads that the proposed design can be recommended as a promising candidate mobile-antenna solution for WLAN applications.

References

[1] H. Morishita, H. Furuuchi and K. Fujimoto, "Performance of balance-fed antenna system for handsets in vicinity of a human head or hand", IEE Proc.-Microw. Antennas Propag., Vol. 149, No. 2, pp. 85-91, April 2002.

[2] R.A. Abd-Alhameed, P.S. Excell, K. Khalil, R. Alias and J. Mustafa, "SAR and radiation performance of balanced and unbalanced mobile antennas using a hybrid formulation", IEE Proceedings-Science, Measurement and Technology special issue on Computational Electromagnetics, vol. 151, No. 6, pp. 410-414, November 2004.

[3] D. Zhou, R.A. Abd-Alhameed and P.S. Excell, "Wideband balanced folded dipole antenna for mobile handsets", In proceedings of The European Conference on Antennas and Propagation: EuCAP 2007, Paper no. MoPA.012, Edinburgh, UK, 11-16 November 2007.

[4] H. Morishita, S. Hayashida, J. Ito and K. Fujimoto, "Analysis of built-in antenna for handset using human (head,hand,finger) model", Electronics and communications in Japan, Part 1, Vol. 86, No. 9, pp. 35-45, 2003.

[5] S. Kingsley, "Advances in handset antenna design", RF Design, pp. 16-22, May 2005.

[6] B.S. Collins, S.P. Kingsley, J.M. Ide, S.A. Saario, R.W. Schlub and S.G. O'Keefe, "A Multi-band hybrid balanced antenna", IEEE 2006 International Workshop on Antenna Technology: small antennas, novel metamaterials, White Plains, New York, pp.100-103, March 6-8, 2006.

[7] D Zhou, RA Abd-Alhameed, CH See, AG Alhaddad and PS Excell, "New mobile balanced mobile antenna with wide bandwidth performance", In proceeding of the European Conference on Antennas and Propagation: EuCAP 2009, pp. 549-552, March 23-27, Berlin, Germany, 2009.

[8] J.J. Arenas, J. Anguera and C. Puente, "Balanced and single-ended handset antennas: free space and human loading comparison", Microwave and optical technology letter, vol. 51, no. 9, pp. 2248-2254, September 2009.

[9] D Zhou, RA Abd-Alhameed, CH See, SWJ Chung, AG Alhaddad and PS Excell, "Dual-frequency balanced mobile antenna for WLAN and short range communication systems", In proceeding of Progress In Electromagnetics Research Symposium, pp. 1277 – 1280, March 23-27, Beijing, China, 2009.

[10] ET industries, USA, http://www.etiworld.com/.

[11] R. Meys and F. Janssens, "Measuring the impedance of balanced antennas by an S-Parameter method", IEEE antennas and propagation magazine, vol. 40, no. 6, pp. 62-65, December 1998.

A MODIFIED PRINTED MONOPOLE ANTENNA FOR ULTRA-WIDEBAND APPLICATIONS

S. Adnan, R. A. Abd-Alhameed, S.M.R. Jones, H. I. Hraga, M. S. Bin-Melha and E. A. Elkhazmi

Mobile and Satellite Communications Research Centre University of Bradford, Bradford, West Yorkshire, BD7 1DP, UK
sadnan@bradford.ac.uk
S.M.R.Jones@bradford.ac.uk
Mobile and Satellite Communications Research Centre University of Bradford, Bradford, West Yorkshire, BD7 1DP, UK
r.a.a.abd@bradford.ac.uk

Abstract-- **In this paper, a planer printed monopole antenna for Ultra Wide Bandwidth (UWB) applications is presented and discussed. To obtain the required wide response, the base of the monopole is tapered in five steps to match the width of the feeding line as it emerges from the ground plane. A parametric study is carried out for various antenna parameters using the HFSS software tools. The influence of variations and the optimum value of these parameters for UWB response are discussed. The antenna is fed via a microstrip line matched at 50Ω impedance. The simulated and measured results are presented and they show reasonable agreement over the whole UWB frequency band 3.1 to 10.6 GHz.**

I. INTRODUCTION

Ultra-wideband (UWB) is a technology in which information is transmitted in the form of very narrow pulses or other spread-spectrum transmissions. It is applicable to short-range, low power density communications for which the allocated band ranges from 3.1GHz to 10.6 GHz [1]. The technology has gained a lot of popularity among researchers and the wireless industry due to the numerous advantages of UWB services and applications, such as their low cost, low energy, capability to provide high channel capacity over a short range whilst co-existing with more traditional narrower-band services. The global interest in UWB is increasing rapidly into numerous applications such as medical imaging, indoor positioning, sensor applications and wireless communication for which a compact and cheap UWB antennas are required.

The antenna is an important part of the communication system since it has great impact on the performance, complexity and size. However, the antenna design procedure for UWB applications is a very challenging task because of the dufficulty of achieving the required impedance match, high radiation efficiency and uniform radiation pattern over such a wide bandwidth. UWB monopole antennas are planar structures [2-4] which require a ground plane, creating problems for integration with an integrated circuit. This drawback limits its practical application. However, one of the serious limitations of conventional microstrip antennas is their narrow bandwidth, which is normally only a few percent of the centre frequency. Therefore, printed planer monopole antennas may provide the best candidate for this application for its low cost, light weight and easy fabrication. Planar monopole antennas of various configurations have been proposed and offer different attractive feature [5-14].

In this paper the design process for an ultra-wideband printed monopole antenna is described and an optimised design is proposed. The antenna geometry consists of a conducting plate in a form of triangular and rectangular pieces. The starting width of the antenna base was gradually increased in five steps starting from the feeding strip width to the total width of the monopole. The radiating patch is fed by a 50Ω microstrip line. The steps and a partial ground are introduced to enhance the impedance bandwidth while the antenna size is reduced.

II ANTENNA GEOMETRY AND DESIGN

Figure 1 and Table I show the detailed geometry and specified lengths of the proposed antenna as printed on the FR4 substrate with dimensions 30 mm x 30 mm. The antenna is designed and optimised using Ansoft High Frequency Structure Simulator (HFSS) [15] based on the Finite Element Method (FEM). The antenna is optimised to operate over 3GHz to 14GHz band. The length and the width of the steps and the size of the ground along with other parameter of the antenna are optimised to cover the UWB bandwidth. The parametric study helped to optimise the antenna performance before the antenna was built and tested experimentally. Different parameters of the antenna are optimised for maximizing the bandwidth. To check the influence of these parameters on the Impedance bandwidth each parameter is varied whilst the remaining parameters remain fixed.

Figure 2(a) illustrates the simulated return loss for different numbers of steps while the other antenna parameters remain fixed. As can be seen that the -10dB return loss bandwidth of the antenna varies remarkably by increasing the number of steps. The antenna covers an extremely wide frequency range from 3GHz to 14GHz by introducing five taper steps.

The operating bandwidth with and without employing the taper steps are shown in Figure 2(b). It is clearly shown that -10dB bandwidth is critically dependent on the introduction of the taper steps. The other parameter that undergoes parametric study is the width of the ground plane. It can be noticed in Figure 2(c) that the antenna operating bandwidth increases greatly by reducing the length of the ground plane. The maximum bandwidth of the antenna is achieved by reducing the length of the ground to 8mm as shown in Figure 2(c).

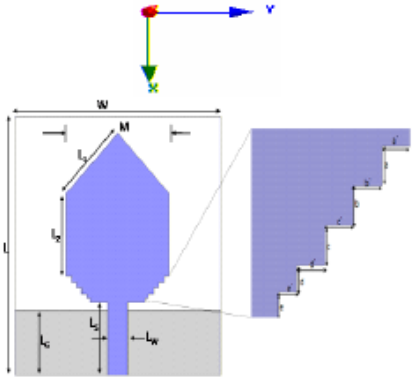

Figure 1: Antenna Geometry with ground plane

Table I: Detail parameter of the antenna

W	30 mm
L	30 mm
M	15 mm
L_1	10.5 mm
L_2	10.25 mm
L_S	9 mm
LW	3 mm
L_G	8 mm
a`=a=b`=b=c`=c=d`=d	0.75 mm
e`=e	0.5 mm

Figure 3 shows the variations the antenna impedance versus the operating frequency for the optimum achievable antenna performance. Throughout the antenna bandwidth the real part varies very closely to 50Ω, whereas the imaginary part is not far from zero

III RESULT AND DISCUSSION

Using the optimised dimensions, the proposed antenna was manufactured and their characteristics were tested using an HP 8510C network analyzer. The experimental results show reasonable agreement with the simulated ones, as shown in Figure 4. A bandwidth from 3GHz to 14GHz defined by a return loss ≥ 10dB shows clearly that the antenna is a good candidate for the UWB application assigned by FCC.

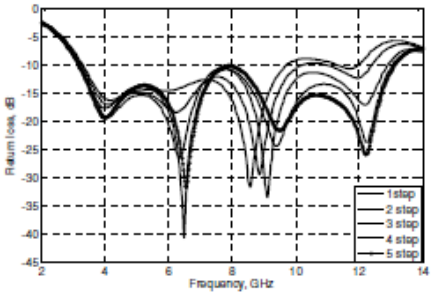

Figure: 2(a). Return loss for the different number of steps

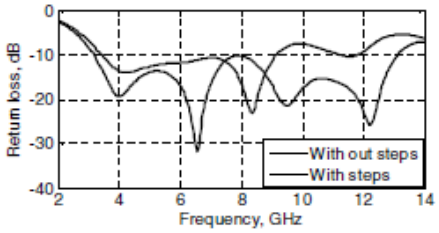

Figure: 2(b). Return loss with and without taper steps

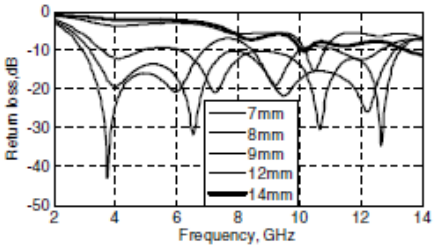

Figure: 2(c). Return loss for the different length of the ground plane

The measured and the simulated normalised radiation patterns of the co and cross-polar component in the x-z and y-z planes at three selected frequencies (e.g., 4GHz, 7.5GHz and 10GHz) are shown in Figure 5 and 6 respectively. The x-z radiation pattern is omnidirectional at low frequencies but still retains good omnidirectionality at higher frequencies (7.5GHz and 10GHz). The y-z has a donut shape at 4GHz and then starts to form humps, getting more directional at higher frequencies. In

summary, there were quite good agreement found between the measured and simulated results for both planes considered.

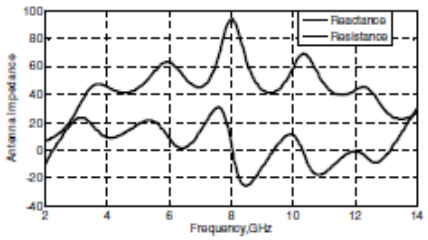

Figure: 3. Antenna impedance versus frequency

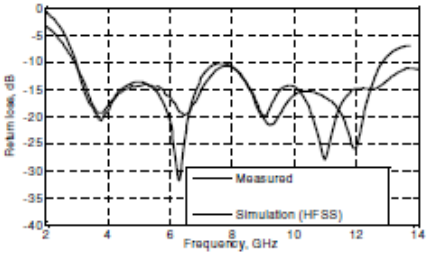

Figure: 4. Measured and simulated return losses

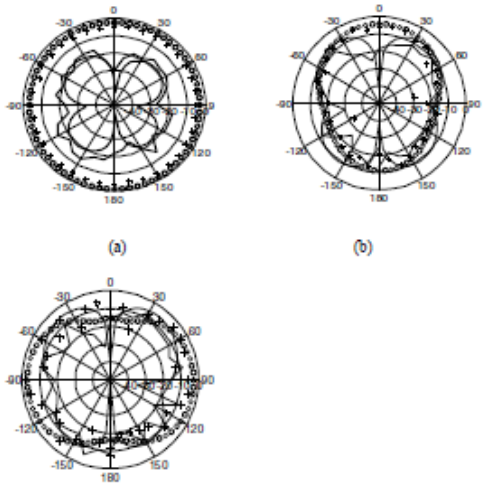

Figure: 5. Radiation patterns for x-z plane of the proposed antenna at (a) 4 GHz, (b) 7.5 GHz, (c)10 GHz (+++measured co, ooo simulated co, ------- measured cross and ..... simulated cross).

The simulated 3D radiation pattern of the proposed antenna at 4, 7.5 and 10GHz are shown in Figure 7. The radiation pattern is similar to the dipole at the first resonance i.e. 4GHz. At the second and third resonances the radiation pattern is like a pinched donut. The antenna shows reasonable power gain of 4.2, 5 and 5.6 dBi at 4, 7.5 and 12 GHz respectively. The simulated surface current distributions of the printed monopole antenna at different resonances are shown in Figure 8. Minimum induced currents have been confirmed on the finite ground except the small surface area surrounding the feeding line.

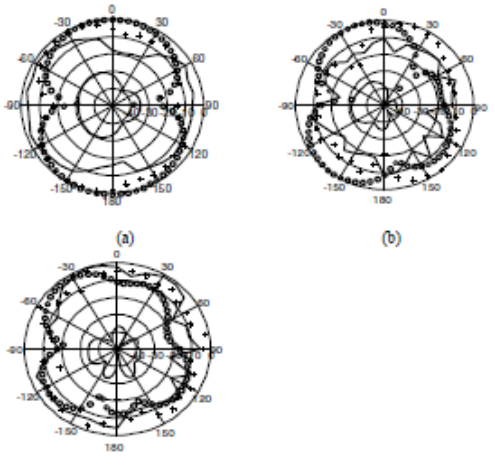

Figure: 6. Radiation patterns for y-z plane of the proposed antenna at (a) 4 GHz, (b) 7.5 GHz, (c)10 GHz (+++measured co, ooo simulated co, ------- measured cross and ..... simulated cross).

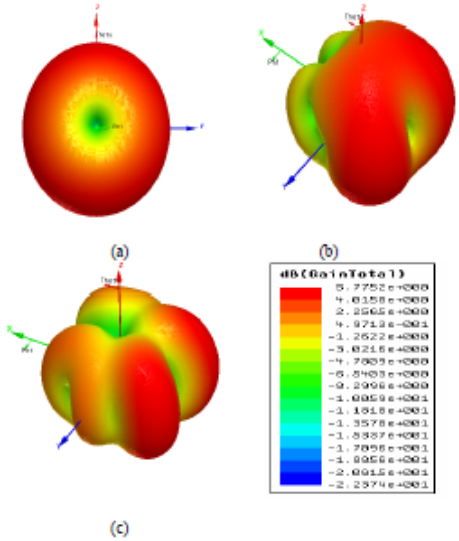

Figure: 7. 3D Radiation plots at (a) 4GHz, (b) 7.5GHz, (c) 12GHz

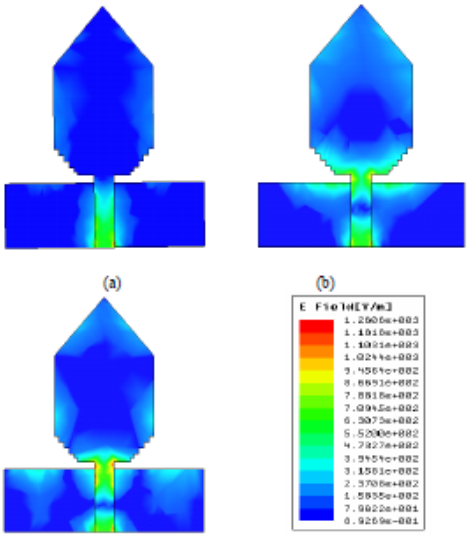

Figure: 8. Current distribution plots at (a) 4GHz, (b) 7.5GHz, (c) 10GHz

IV CONCLUSION

A compact printed monopole antenna for UWB applications has been presented. The surface taper steps proposed between the feeding microstrip line and the antenna base has improved the impedance bandwidth. Parametric studies of various parameters were carried out to synthesise and maximize the operating bandwidth. The simulated and measured results showed good agreement in which the antenna covers a maximum bandwidth from 3 to 14 GHz.

ACKNOWLEDGEMENT

The authors would like to thanks Mr A Leach for his help in the fabrication and measurement of the antenna.

REFRENCES

[1] First Report and Order (FCC 02-48), Action by the Commission "New public safety applications and broadband internet access among uses envisioned by FCC authorization of ultra-wideband technology," February 14, 2002 February, 2002.

[2] G.R. Aiello, G.D Rogerson, "Ultra-wideband Wireless System," *IEEE Microwave Magazine*, pp. 36-47, June, 2003.

[3] B. Allen, M. Dohler, E.E Okon, W.Q. Malik, A.K. Brown, D.J. Edwards, *Ultra-wideband Antennas and Propagation for Communication, Radar and Imaging*: John Wiley &Sons, 2007.

[4] D.M. Pozar, *Microwave Engineering*: John Wiley & Sons Inc, 2005.

[5] J. Jung, K. Seol, W. Choi and J. Choi, "Wideband monopole antenna for various mobile communication applications," *Ellectronics Letters*, vol. 41, pp. 1313-1314, 24th November 2005.

[6] I. Hossain, S. Noghanian , S. Pistorius "A diamond shaped small planar ultra wide band (UWB) antenna for microwave Imaging Purpose" in *Antennas and Propagation Society International Symposium, 2007 IEEE*, 2007, pp. 5713-5716.

[7] Yen-Liang Kuo, Kin-Lu Wong, "Printed Double-T Monopole Antenna for 2.4/5.2 GHz Dual-Band WLAN Operations," *IEEE Transactions on Antennas and Propagation on Antennas and propagation*, vol. 51, pp. 2187-2191, September 2003.

[8] Kyungho Chung, Jaemoung Kim and Jaehoon Choi, "Wideband Microstrip-Fed Monopole Antenna Having Frequency Band-Notch Function," *IEEE Microwave and Wireless Components Letters*, vol. 15, pp. 766-768, November 2005.

[9] Young Jun Cho, Ki Hak Kim, Soon Ho Hwang and Seong-Ook Park, "A Minia-ture UWB Planar Monopole Antenna with 5GHz Band-Rejection Filter," in *35th European Microwave Conference*,. Paris, France, October 2005, pp. 1911-1914.

[10] Horng-Dean Chen, Hong-Twu Chen, "A CPW-Fed Dual-Frequency Monopole Antenna," *IEEE Transactions on Antennas and Propagation*, vol. 52, pp. 978-982, April 2004.

[11] J.-Y. Jan, and T.-M. Kuo, "CPW-fed wideband planar monopole antenna for oper-ations in DCS, PCS, 3G, and Bluetooth bands," *Ellectronics Letters*, vol. 41, pp. 991-993, 1st September 2005.

[12] Y. Kim , and D.-H. Kwon, "CPW-fed planar ultra wideband antenna having a frequency band notch function," *Electronics Letters*, vol. 40, pp. 403-405, 1st April 2004.

[13] Wei Wang, S. S. Zhong and Sheng-Bing Chen, "A Novel Wideband Coplanar-Fed Monopole Antenna," *Microwave and Optical Technology Letters*, vol. 43, pp. 50-52, October 5 2004.

[14] Seong H. Lee, Jong K. Park and Jung N. Lee, "A Novel CPW-Fed Ultra-Wideband Antenna Design," *Microwave and Optical Technology Letters*, vol. 44, pp. 393-396, March 5 2005,.

[15] Ansoft High Frequency Structure Simulator corporation, V 11, 2007.